FINAL REPORT OF RESULTS

September 26, 2019

ADVANCED LOW-COST INTERMETALLIC COATINGS FOR MOLTEN SALT PUMP IMPELLER

PREPARED FOR:

Department of Energy
Grant Award Number DE-SC0017722

Research period 10/01/2017-03/31/2019

PREPARED BY:

ATC President, Jeff Henry, PI
ATC Chief Metallurgist, Dr. Joe Zhou, co-PI
Applied Thermal Coatings
200 Compress Street
Chattanooga, Tennessee 37405

Program Participants:

Jeff Henry, Metallurgical Engineering Consultant	15%
Joe Zhou, Metallurgical Engineering Consultant	13%
Leo Antony, Metallurgical Engineering Consultant	12%
Keith Linebarger, Technical Project Specialist	16.5%
Randy Price, Special Projects Manager	7%
Chris Moyer, Heat Treat Specialist	1%
Earl Babb, Welding Specialist	.5%
Dakota Price, Heat Treat Assistant	1%
Jesse Cross, Director of Operations	3%
Trudie Denton, Business Administration	2%
Dr Ramana Reddy, University of Alabama	8.5%

There were no unexpended funds at the end of the final budget period.

There have been no papers published as a result of this project.

Applied Thermal Coatings
200 Compress Street
Chattanooga, TN 37405
Telephone: 423-267-0647
Fax: 423-267-0637
Email: jhenry@atc-tn.com

INDEX

Introduction	pages 4-5
Project Overview	pages 5-11
Coating Development	pages 11-21
Conclusions and Recommendations	pages 21-55
Appendix	pages 56-85

Applied Thermal Coatings
200 Compress Street
Chattanooga, TN 37405
Telephone: 423-267-0647
Fax: 423-267-0637
Email: jhenry@atc-tn.com

September 26, 2019

FINAL REPORT of RESULTS:

Subject: Advanced Low-Cost Intermetallic Coatings for Molten Salt Pump Impeller
DOE Project Number

1.0 INTRODUCTION

The use of solar energy to produce steam for the generation of electricity is an established technology, with multiple designs for concentrating solar power (CSP) steam generators available commercially and a number of such units currently operating. As part of the effort to improve the overall efficiency of this technology, designers have developed thermal energy storage (TES) mechanisms that employ molten salt to capture a portion of the solar energy available during the day-time hours and make that energy available for steam generation during periods when the sun's energy is not available.

In current TES systems, nitrate salts are used extensively as the medium of energy exchange. However, due to the chemical instability of these salts at temperatures above 600ºC, they are not being considered for use in the next more efficient generation of CSP plants, in which the energy exchange fluids will be required to operate in the range 600ºC to 800ºC. At these higher temperatures, molten chloride salts, such as KCl-$MgCl_2$, are viewed as promising alternatives to the nitrate salts, but, of course, these chloride-based salts are highly corrosive to the engineering alloys commonly used in the construction of pressure vessels, heat exchangers, pumps and piping at high temperatures. Hence, a solution to the problem of material degradation is essential if the next generation of CSP plants is to be commercially viable (Ref 1).

In order to effectively address the problem of molten chloride salt corrosion at high temperatures (≥ 750ºC) and thereby to reduce the cost of molten salt tanks and related apparatus, various options have been considered, with one of the most promising being an innovative coatings system developed and applied onto low alloy ferritic or austenitic stainless material. Development of such a coating system would reduce the capital costs of thermal energy storage (TES) and increase the overall efficiency of the concentrating solar power (CSP) system.

Although high strength nickel base alloys are well suited for many high temperature applications, they have significant limitations when exposed to molten chloride salt

Applied Thermal Coatings
200 Compress Street
Chattanooga, TN 37405
Telephone: 423-267-0647
Fax: 423-267-0637
Email: jhenry@atc-tn.com

conditions and they are very expensive. Monolithic materials such as the austenitic stainless steels (e.g., SS310 and SS347) and the more common nickel base alloys (e.g., IN625 and IN800H) have exhibited high corrosion rates in molten chloride salt environments (Ref1). Molten salt corrosion of IN625 in salts containing chlorides showed a catastrophic corrosion rate of 1.111”/year at 800ºC (Ref1). Hence, an innovative coatings solution to mitigate molten chloride salt corrosion is needed.

Of the many coating techniques available in the market, no one technique appears to be capable of producing effective protection from molten salt corrosion at a relatively low cost. There are thermal spray coating techniques, in particular the twin wire-arc technology, that are attractive when considering the coating of large molten salt tanks because the coatings application rate is high, the overall application cost is low and repairs to the coating can readily be made either in the shop or in the field. However, the twin wire arc coating materials currently available in the market have certain inherent limitations, including porosity and mechanical bonding to the substrate, which limit their effectiveness in providing protection against molten chloride salt corrosion at high temperatures. What is required is an approach that combines the economy and versatility of thermal spray wire-arc technology with the superior resistance of advanced alloys to effectively combat molten chloride salt corrosion at elevated temperatures.

Applied Thermal Coatings, Inc. (ATC) has investigated an innovative coatings technology to produce dual layer cermet/ceramic coatings that will be dense and impervious to any corrosive molten salts/fluids, thereby resisting the effects of molten salt corrosion. Development of coatings using this technology will make it possible to fabricate the molten salt systems using a relatively low-cost base material, which will reduce the overall cost of the power generating system and enhance the commercial viability of solar power.

2.0 PROJECT OVERVIEW

Of the coating technologies available for the production of a cost-effective method of protection from the effects of high-temperature chloride attack, there are two that offer specific advantages for the CSP/TES application, particularly when used in a way that effectively complements the strengths of each coating method. The first of these is electroless nickel plating, through which a nickel-rich layer is produced on the surface of a component through chemical reduction. The second coating technology is aluminizing, in which aluminum is diffused into the surface of a component and, depending on the composition of the substrate, aluminides are formed. A brief discussion of each process as it was used for this project is provided below.

2.1 Electroless Nickel Plating

In electroless nickel plating a nickel-rich alloy is deposited on a substrate that

Applied Thermal Coatings
200 Compress Street
Chattanooga, TN 37405
Telephone: 423-267-0647
Fax: 423-267-0637
Email: jhenry@atc-tn.com

is immersed in an aqueous solution without the use of electric current. It differs, therefore, from electro-plating, in which an external source of direct current is required to reduce nickel ions in the electrolyte to promote deposition of nickel metal onto the substrate. In electroless nickel plating the reduction of the nickel ions in solution occurs through a chemical process. The most common reducing agent used is sodium hypophosphite. Alternatives are sodium borohydride and dimethylamine borane, but they are used much less frequently (Ref 2).

A schematic of the electroless nickel plating process is presented in Figure 1 below. The plating bath typically contains a source of metal ions, a reducing agent, a complexing agent, a stabilizer, a buffering agent and a wetting agent, with the critical process parameters being temperature and ph. Each parameter/component function is briefly summarized in Table 1 (Ref 3). The electroless nickel coating process has gained wide acceptance in the market due to the coating's excellent corrosion and wear resistance properties (Ref 2).

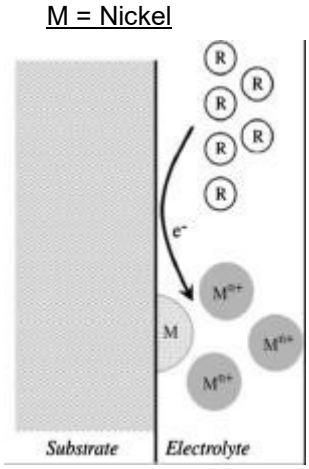

Figure 1. Schematic of electroless plating process. Electroless deposition with reducing agent R as the source of electrons (Ref 3).

General categories of electroless nickel coatings are listed in Figure 2. Electroless plating can be used to deposit a broad range of engineering metals, including nickel, copper, gold, silver, palladium and cobalt. The industrial use of electroless nickel plating, especially the nickel/phosphorus alloy, has grown steadily during the last decade due to the favorable properties coating, including uniformity of thickness, hardness, corrosion resistance and magnetic response. (Ref 2).

Table 1. Components and parameters of bath and their functions (Ref 3)

Component/Parameter	Function
Metal ions	Source of metal
Reducing agents	Supply electrons to reduce the metal ions
Complexers	Prevent excess of free metal ions concentration
Accelerators	Accelerate the reducing agent and increase the deposition
Stabilizers	Stabilize the bath from decomposition by shielding catalytically active depositions
pH regulators	pH adjustment
Temperature	Energy for deposition

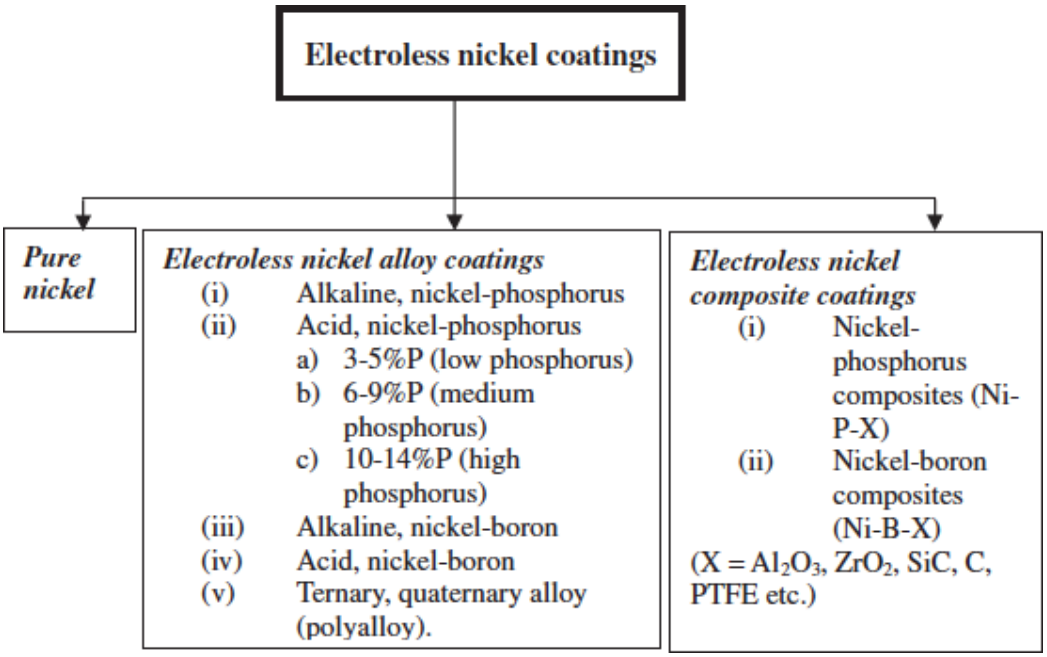

Figure 2. General categories of electroless nickel coatings (Ref 3)

2.2 Diffusion of Aluminum Through Pack Cementation

a) Pack cementation is a method of surface protection that for many years has been used for the *in situ* chemical vapor deposition (CVD) of elements with

specific favorable characteristics onto and then into the surface of low-cost substrates to produce corrosion, erosion, and wear-resistant behavior. There are four necessary components in the process: a) the substrate or parts to be altered; b) the master alloy (i.e. a powder of the element or elements to be deposited on the surface of the parts, such as Cr, Al, Si, B etc.; c) a halide salt activator or energizer (e.g. NaCl, NaF, NH_4C1, etc.); and, d) a relatively inert filler powder (e.g. Al_2O_3, SiO_2, or SiC). The master alloy powder, the halide salt activator, and the inert filler are mixed thoroughly and the parts to be processed are covered with the mixed powder in a sealed retort. The retort size and shape can be scaled to the size and shape of the parts to be coated. The packed and sealed retort is heated to an elevated temperature that is a function of the element, or elements to be diffused and is held for a time sufficient to produce an enriched layer of the desired thickness. At the high processing temperatures required for diffusion, the metallic in the master alloy powder reacts with the halide salt activators to form volatile metal halides, which then disperse as a gas through the pack, where they deposit on the component surfaces and diffuse into the substrate. The processing time and temperature are selected so that adequate halide vapor pressures are generated and solid-state diffusion occurs to the required depth (Ref 4).

When aluminum is the element to be diffused, the following reactions take place (Ref 5):

Decomposition of NH4Cl

NH_4Cl (s) = NH_3 (g) + HCl (g)

Formation of volatile aluminum halides

6HCl (g) + 2Al (pack) = $2AlCl_3$ (g) + $3H_2$ (g)
$AlCl_3$ (g) + 2Al (pack) = 3AlCl (g)

Deposition of aluminum onto steel (substrate) surface

2AlCl (g) + 3Fe (substrate) = 2Al-Fe(alloy) + $FeCl_2$ (g)
(displacement reaction)

$3FeCl_2$(g) + 5Al (pack)= 3Al-Fe(alloy) + 2AlCl3 (g)
(displacement reaction)

3AlCl (g) + 2Fe (substrate) = $AlCl_3$ (g) + 2Al-Fe (alloy)
(disproportionation reaction)

Applied Thermal Coatings
200 Compress Street
Chattanooga, TN 37405
Telephone: 423-267-0647
Fax: 423-267-0637
Email: jhenry@atc-tn.com

$2AlCl(g) + 2Fe(substrate) = 2Al\text{-}Fe(alloy) + Cl_2(g)$
(decomposition reaction)

$2AlCl(g) + H_2(g) + 2Fe(substrate) = 2Al\text{-}Fe(alloy) + 2HCl(g)$
(reduction reaction)

Various metal aluminide coatings produced through the aluminizing process have been employed successfully in the Energy, Aerospace and Marine industries. For the CSP/TES application, nickel aluminide coatings are of particular interest because of their high temperature strength and superior corrosion resistance. Successful applications have included, a) furnace fixtures, b) turbochargers, c) hydro-turbines, c) pump components, and e) manufacturing tooling (Ref 6).

Applied Thermal Coatings
200 Compress Street
Chattanooga, TN 37405
Telephone: 423-267-0647
Fax: 423-267-0637
Email: jhenry@atc-tn.com

2.3 Technical Approach

The objective of this project has been to demonstrate the feasibility of a low-cost coating for the protection of pump impellers used for the inductive transport of molten salts. Initial interest focused on an inter-metallic nickel aluminide coating and subsequently, for economic reasons, consideration also was given to a coating composed of iron aluminides. Applying such coatings to low alloy or austenitic stainless-steel substrates will provide the superior resistance to molten chloride salt corrosion and blade tip erosion that normally can be achieved only through the use of more highly alloyed – and, therefore, more expensive - nickel-base materials and it will do so at a substantially lower cost.

The coating systems evaluated were designed to take advantage either of the combined strengths of the electroless nickel plating process and the aluminizing process to produce a nickel-aluminide intermetallic coating or to rely solely on the aluminizing process to produce, in conjunction with iron from the substrate, a protective layer consisting of iron aluminides.

With respect to the nickel aluminide protection, this has been achieved by first depositing a layer of nickel-rich alloy onto an austenitic stainless substrate using the electroless nickel plating process and then aluminizing the nickel-coated surface to produce the nickel aluminide coating. With respect to the iron aluminide protection, this has been achieved by aluminizing bare austenitic stainless steel. Testing has supported the conclusion that the developed coatings will resist attack by molten chloride salts at high temperatures (550°C to 750°C) and have sufficient hardness to resist blade tip erosion.

2.4 Processing Approach

The steps taken to develop either a low-cost intermetallic nickel aluminide coating using electroless nickel plating and aluminizing or a low-cost iron aluminide coating using aluminizing only, and to demonstrate the quality of the coatings and their effectiveness against molten chloride salt corrosion and erosion at high temperatures (≤ 750ºC) have been as follows:

1. Design of the optimum electroless nickel plating and aluminizing mixtures using advanced thermodynamic analysis.
2. Development of processing parameters for the electroless nickel plating and aluminizing processes, to be used either together or separately.
3. Production of specimens coated using the designated electroless nickel plating process.

Applied Thermal Coatings
200 Compress Street
Chattanooga, TN 37405
Telephone: 423-267-0647
Fax: 423-267-0637
Email: jhenry@atc-tn.com

4. Production of samples with intermetallic nickel aluminide coating or iron aluminide coating.
5. Investigation of the performance of the intermetallic nickel aluminide coating and the iron aluminide coating when subjected to molten chloride salts corrosion at high temperatures (≥ 750ºC).
6. Metallurgical characterization of the microstructure of the coatings, both prior to and after exposure to molten salt environments at elevated temperatures.

Descriptions for each of these steps are provided below.

3.0 COATING DEVELOPMENT

3.1 Thermodynamic Basis for Coating Design

Thermodynamic calculations were performed using the computer program "HSC Chemistry", which is based on the Gibbs energy minimization method, to determine the target composition of feed stock materials in order to produce an intermetallic nickel aluminide coating with the desired level of resistance to molten salt corrosion and blade tip erosion.

For the first set of calculations the input values were the compositions of the electroless nickel coating and the aluminizing composite powder mixture, with specific proportions of each (i.e., the recipe) designated for a given "run" – i.e., a cycle of controlled heating of the electroless nickel coating embedded in a specific aluminizing composite powder mixture. Using these values, the program calculated the amount of nickel aluminide produced at equilibrium for each unique set of input values based on the Gibbs free energy minimization method. Results of the calculations for the eleven different "recipes" are shown in Figures 3.1 to 3.13.

The results of the calculations were compared to identify those "recipes" that would be likely to produce the greatest amount of nickel aluminide, and on a preliminary basis three of the "recipes" were selected for a final review to determine their suitability for evaluation under simulated service conditions in the TES. The three "recipes" selected for the final review were "B", "D" and "Y", and with respect to final composition of the nickel aluminide protection, these three "recipes" were considered to be roughly comparable.

In response to requests from the DOE for preliminary information that could be used to support a second phase of the development effort to

achieve the objectives of this program, the preliminary review of the three recipes was expedited to identify the “recipe” that would combine relative ease of processing with achievement of a desirable nickel aluminide composition. Preliminary processing tests were conducted and it was decided based on the results of those tests to focus future processing efforts on the “B” recipe.

The formulation for the production of an iron aluminide coating was more straightforward, since ATC has had extensive experience in processing components to produce iron aluminide coatings and has developed an optimized set of processing parameters for that purpose.

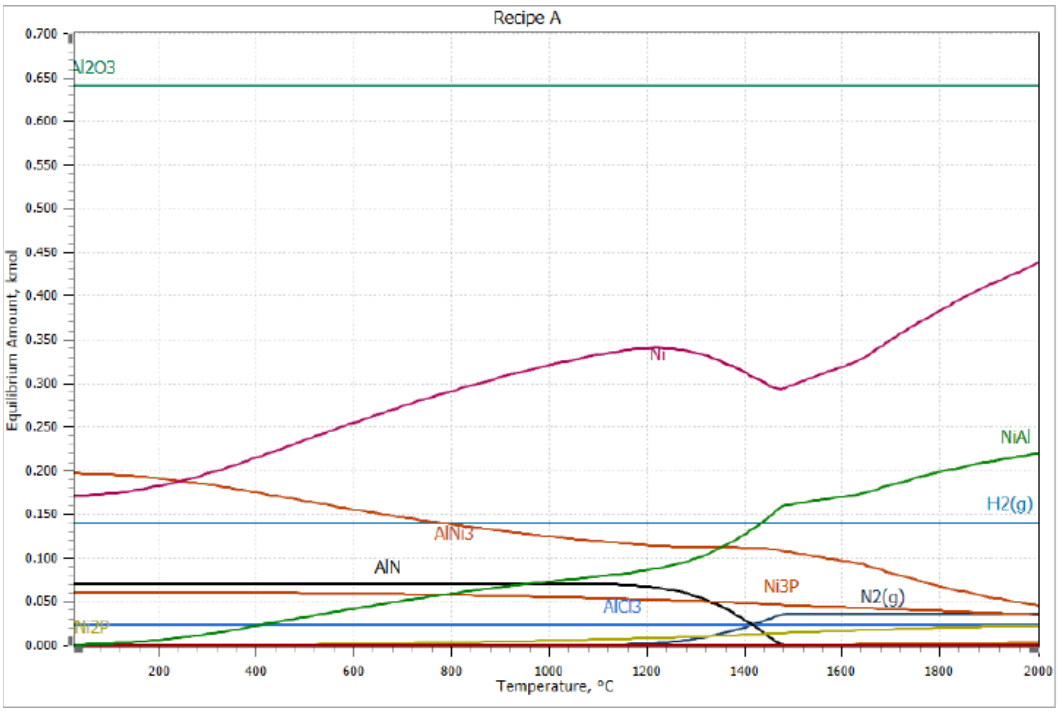

Pack Powder Composition:

Al: 10 Wt.%
NH_4Cl: 5 Wt.%
Al_2O_3: 85 Wt.%

Figure 3.1 Equilibrium Composition Results for Recipe A are shown.

Applied Thermal Coatings
200 Compress Street
Chattanooga, TN 37405
Telephone: 423-267-0647
Fax: 423-267-0637
Email: jhenry@atc-tn.com

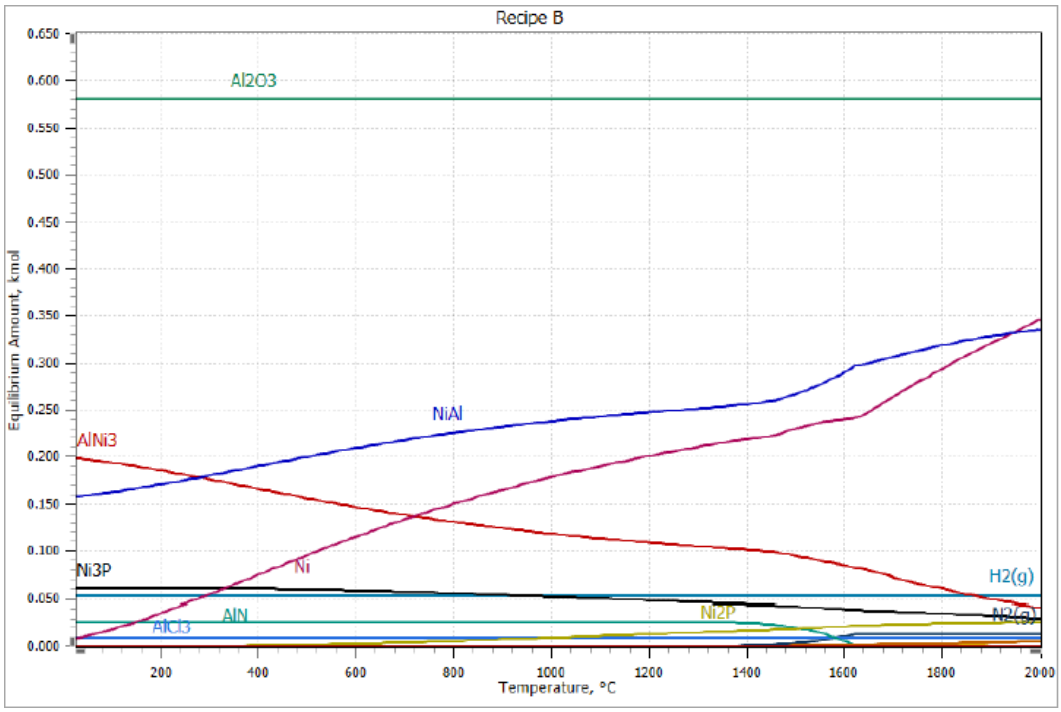

Pack Powder Composition:

Al: 15 Wt.%
NH_4Cl: 2 Wt.%
Al_2O_3: 83 Wt.%

Figure 3.2 Equilibrium Composition Results for Recipe B are shown.

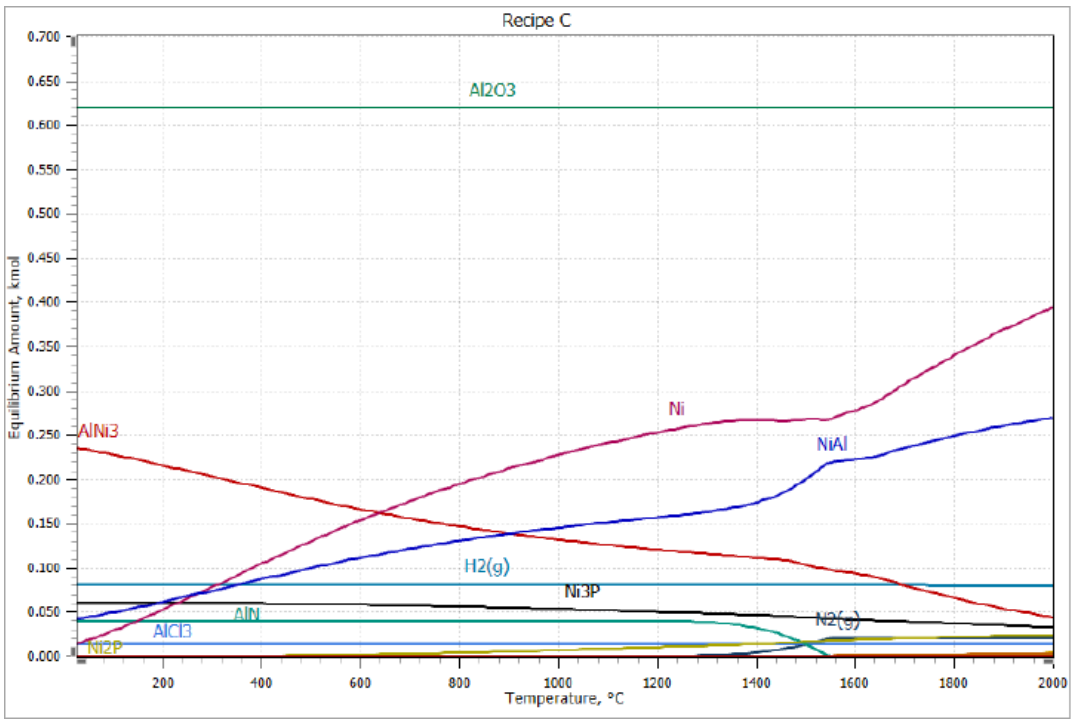

Pack Powder Composition:

Al: 12 Wt.%
NH_4Cl: 3 Wt.%
Al_2O_3: 85 Wt.%

Figure 3.3 Equilibrium Composition Results for Recipe C are shown.

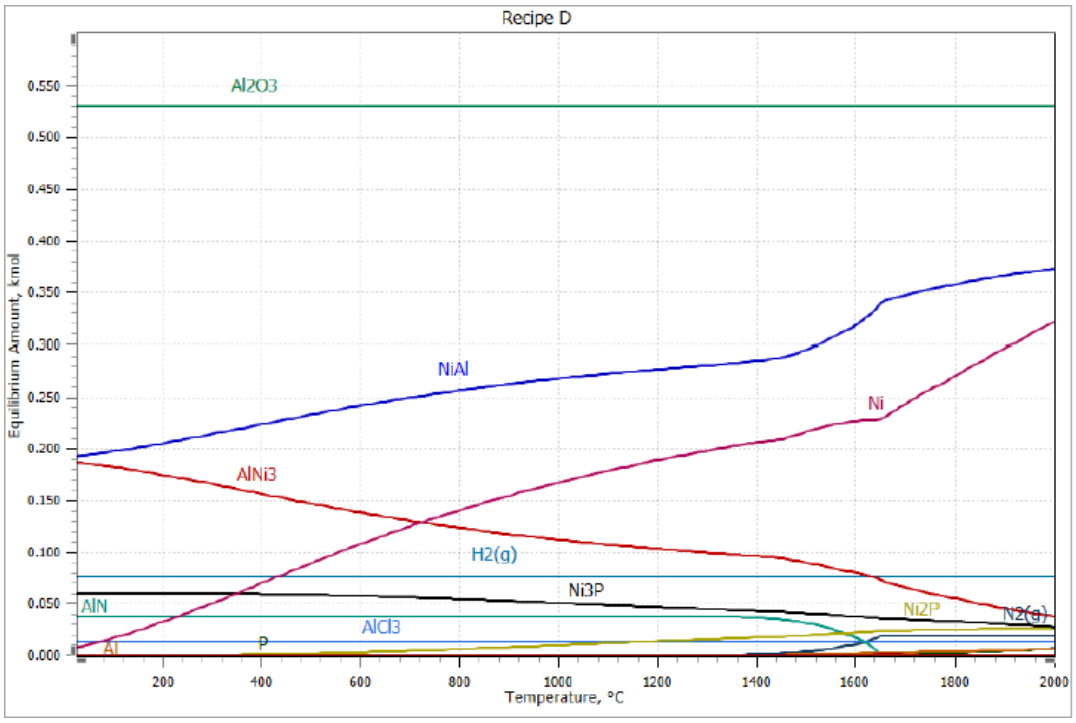

Pack Powder Composition:

Al: 17 Wt.%
NH_4Cl: 3 Wt.%
Al_2O_3: 80 Wt.%

Figure 3.4 Equilibrium Composition Results for Recipe D are shown.

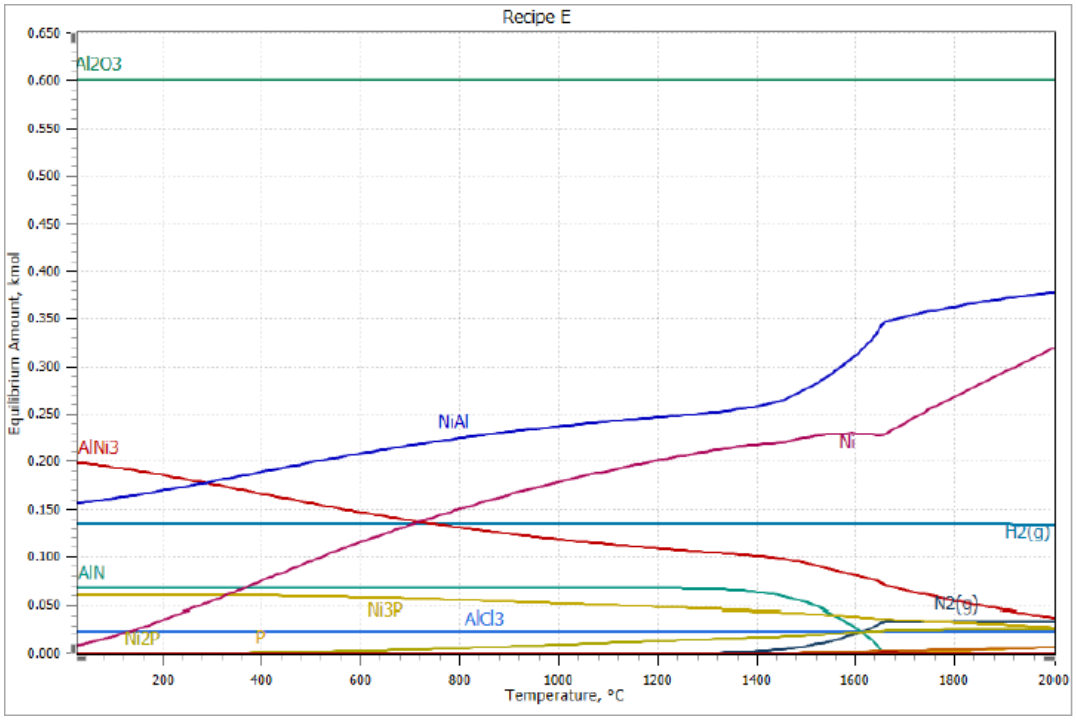

Pack Powder Composition:

Al: 12 Wt.%
NH_4Cl: 5 Wt.%
Al_2O_3: 83 Wt.%

Figure 3.5 Equilibrium Composition Results for Recipe E are shown.

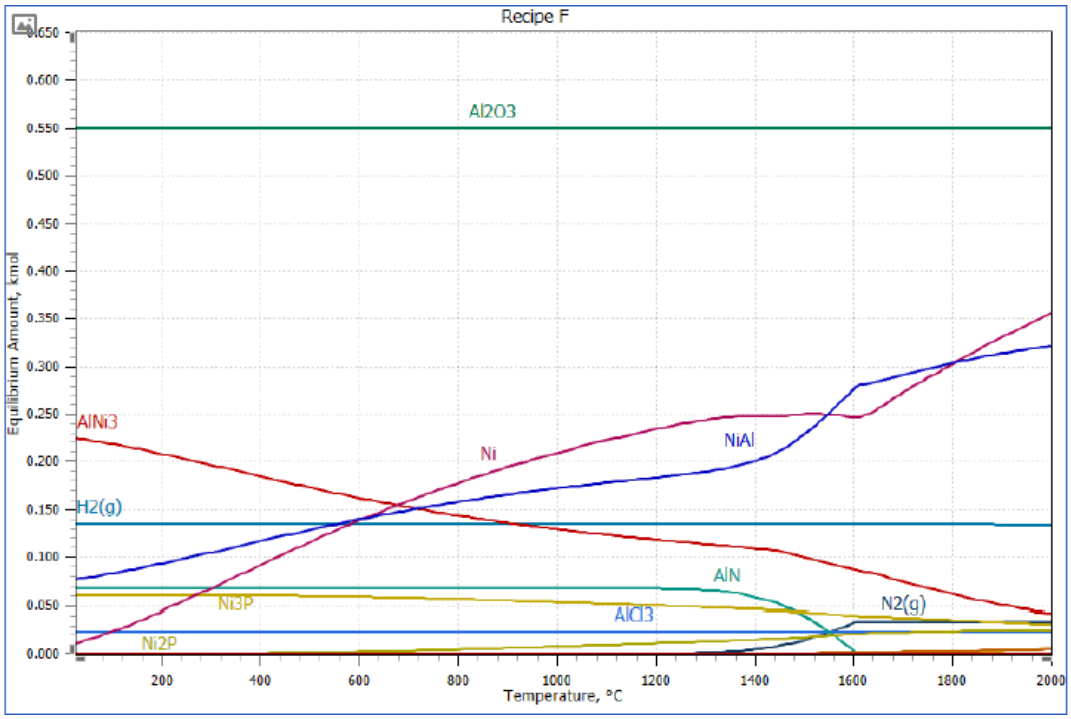

Pack Powder Composition:

Al: 15 Wt.%
NH_4Cl: 5 Wt.%
Al_2O_3: 80 Wt.%

Figure 3.6 Equilibrium Composition Results for Recipe F are shown.

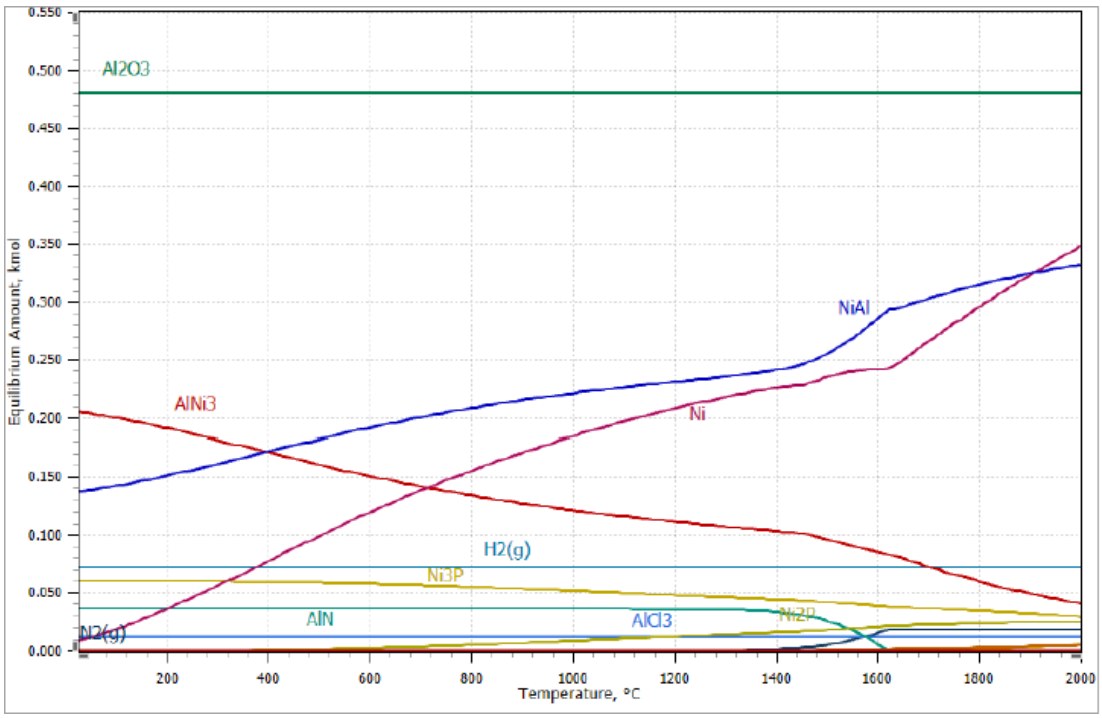

Pack Powder Composition:

Al: 20 Wt.%
NH_4Cl: 3 Wt.%
Al_2O_3: 77 Wt.%

Figure 3.7 Equilibrium Composition Results for Recipe G are shown.

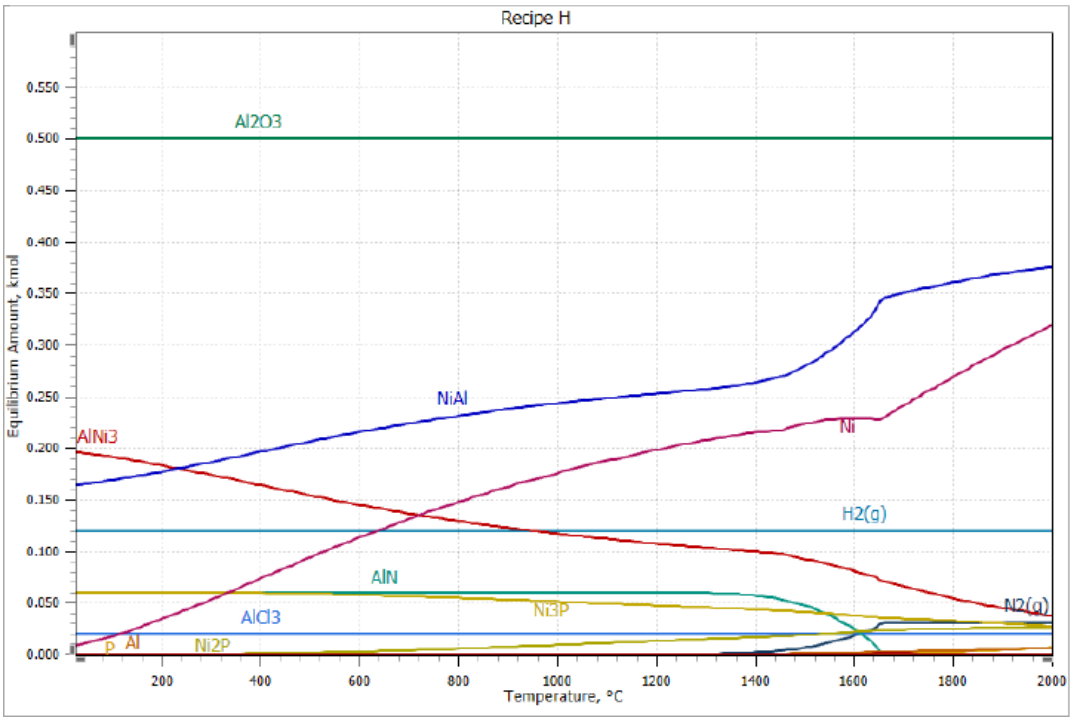

Pack Powder Composition:

Al: 18 Wt.%
NH_4Cl: 5 Wt.%
Al_2O_3: 77 Wt.%

Figure 3.8 Equilibrium Composition Results for Recipe H are shown.

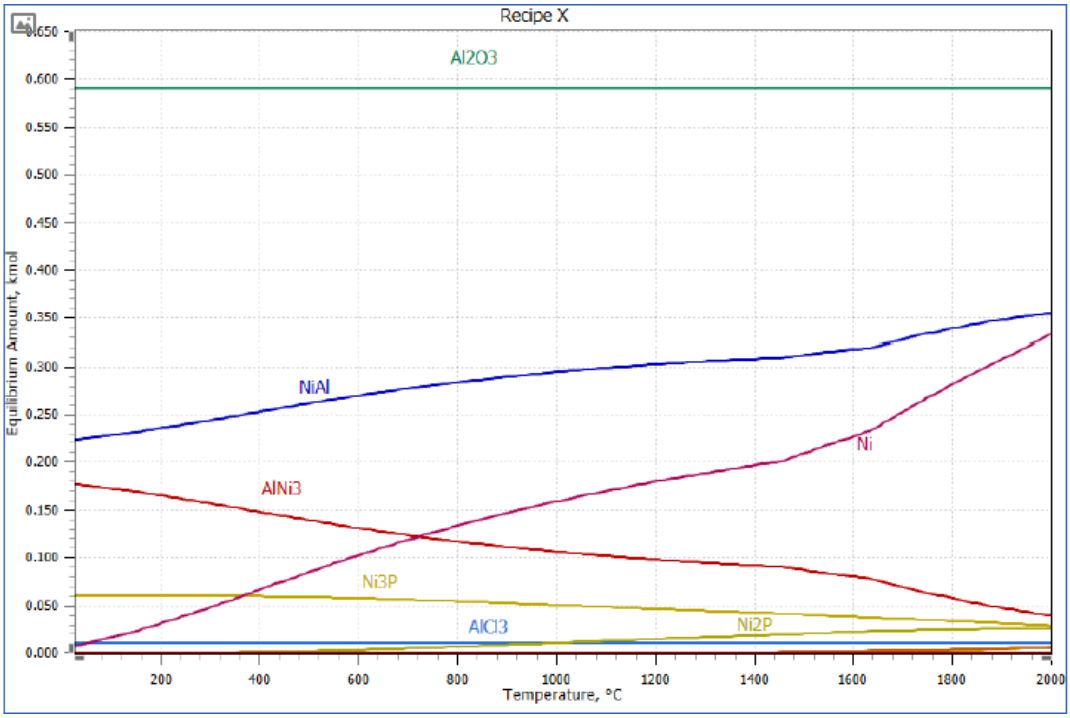

Pack Powder Composition:

Al: 15 Wt.%
$AlCl_3$: 2 Wt.%
Al_2O_3: 83 Wt.%

Figure 3.9 Equilibrium Composition Results for Recipe X are shown.

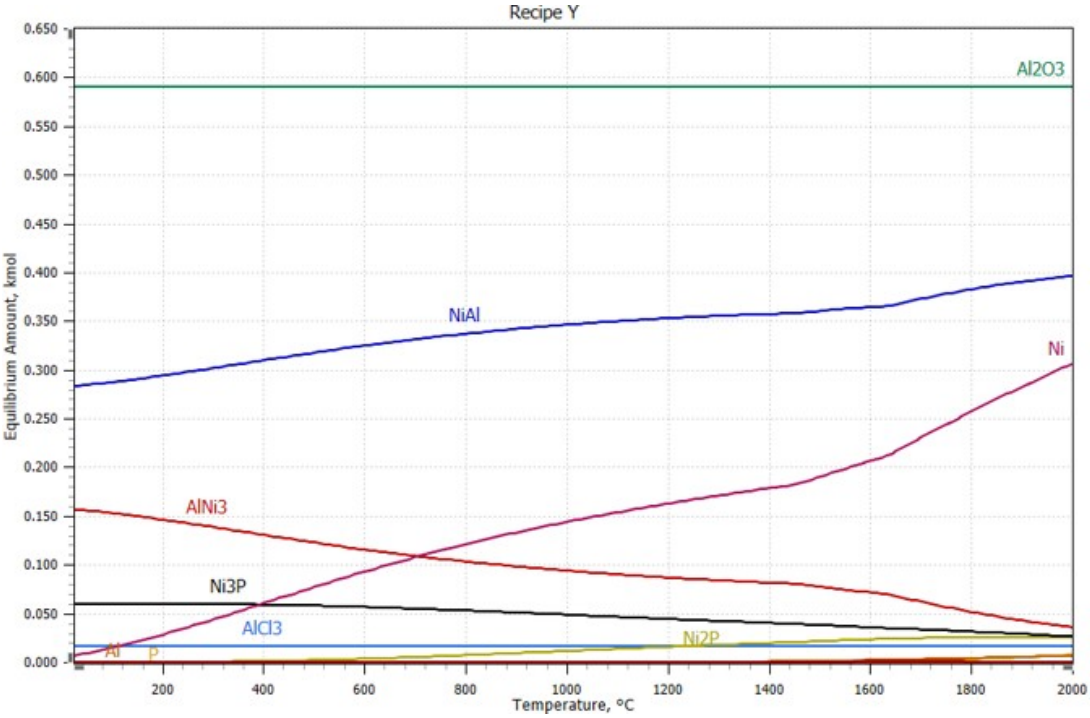

Pack Powder Composition:

Al: 17 Wt.%
$AlCl_3$: 3 Wt.%
Al_2O_3: 80 Wt.%

Figure 3.10 Equilibrium Composition Results for Recipe Y are shown.

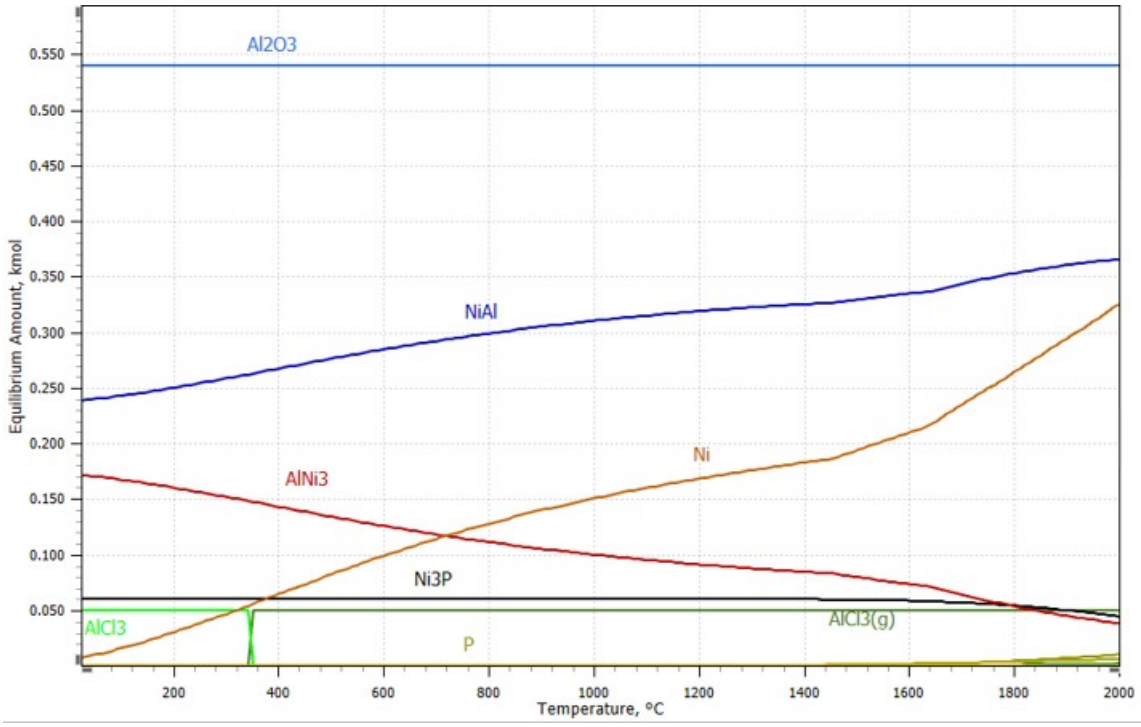

Pack Powder Composition:

Al: 15 Wt.%
$AlCl_3$: 10 Wt.%
Al_2O_3: 75 Wt.%

Figure 3.11 Equilibrium Composition Results for Recipe Z are shown.

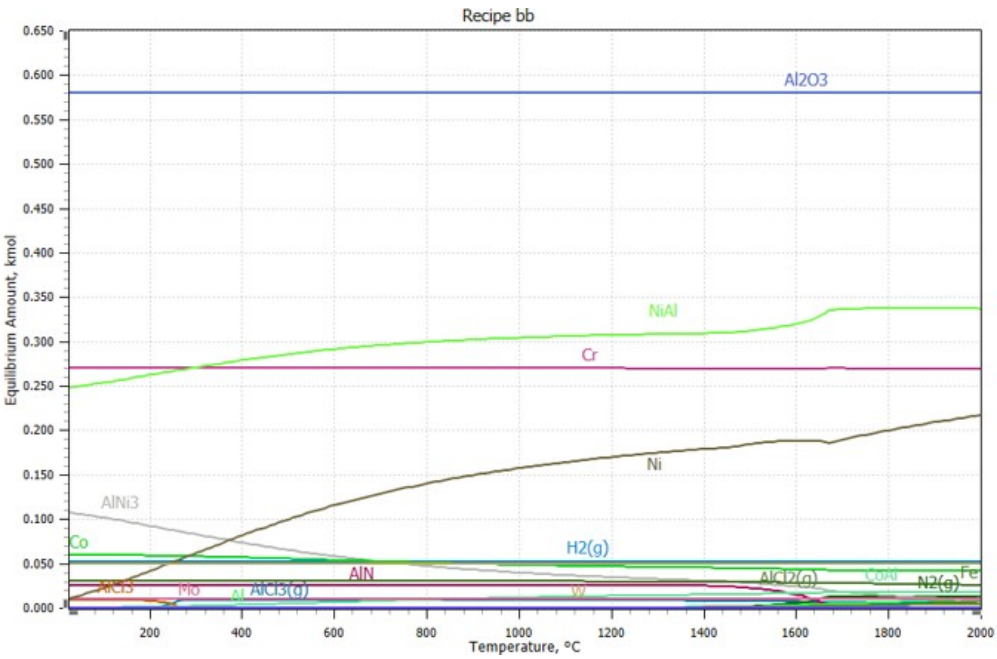

Pack Powder Composition:

Al: 15 Wt.%
NH_4Cl: 2 Wt.%
Al_2O_3: 83 Wt.%

Recipe B and Recipe BB are same with respect to pack powder composition. Difference is the substrate material instead of EN it is directly on nickel base material

Figure 3.12 Equilibrium Composition Results for Recipe bb are shown.

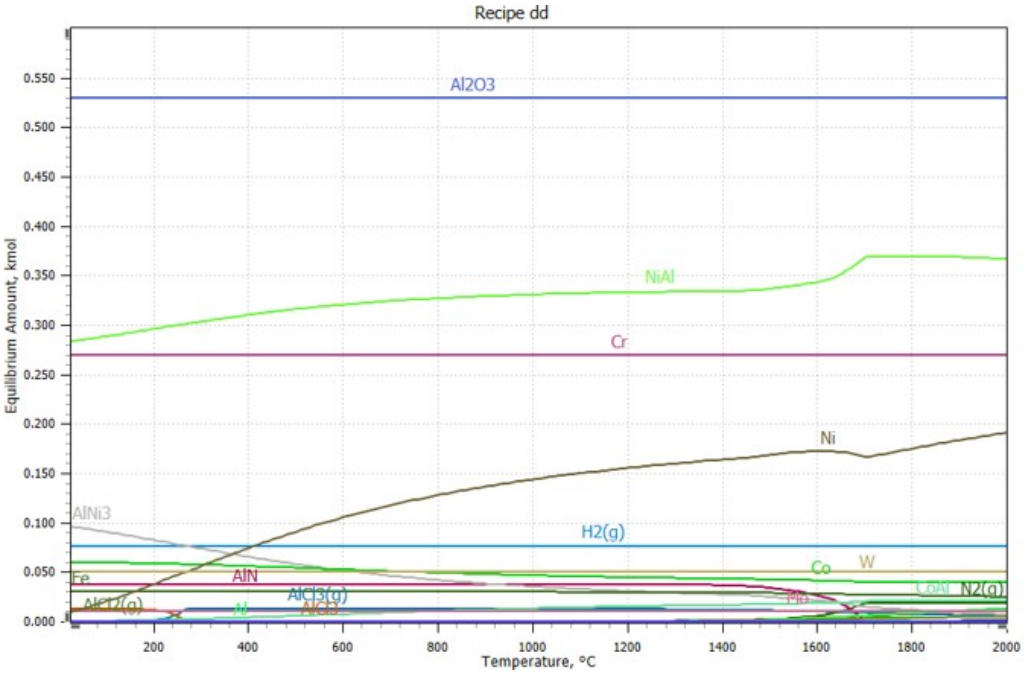

Pack Powder Composition:

Al: 17 Wt.%
NH_4Cl: 3 Wt.%
Al_2O_3: 80 Wt.%

Recipe D and Recipe DD are same with respect to pack powder composition. Difference is the substrate material instead of EN it is directly on nickel base material

Figure 3.13 Equilibrium Composition Results for Recipe dd are shown.

3.2 Coupon Design

Two different sample types or coupons were prepared for the testing phase of the project. One type was a 3" long full circumference tube section, examples of which are shown in Figure 4, 5 and 6, and the other was a ½" X ½" X 1/8" square coupon machined either from round or flat bar, examples of which are documented in Figure 6. Typical profiles of the coupons prior to nickel plating are recorded in Figures 12, 13 and 14.

The total number of each type of coupon produced is indicated in Table 1, as well as what processing was performed on each coupon. Note that ultimately it was decided to conduct all tests in the simulated molten salt environment using the square coupons due to the limitations of the testing equipment.

3.3 Electroless Nickel Plating

As the initial step in the creation of coupons for testing in the simulated molten salt environment, a number of the square coupons were prepared for plating using the low-phosphorus electroless nickel process. For this purpose, samples of four different materials were plated. The materials evaluated included: (1) AISI 1018, a low carbon steel supplied as flat bar; (2) Grade 91, a 9%Cr1%MoVNbN medium alloy steel supplied as tubing; (3) TP347H, a 18%Cr8%NiNb austenitic stainless steel supplied as both round bar and tubing; and (4) Alloy 230, a nickel-base alloy with nominally 22%Cr14%W2%MoCo supplied as round bar. The appearance of the nickel plating as it was applied to coupons of the 1018 material, the T91 material, the TP347H material is documented in the micrographs presented in Figures 7, 8, 10 and 11. An EDS (Energy Dispersive Spectrometry) scan of the nickel plating applied to the 1018 material, which was consistent with the composition observed on the nickel plating on all of the samples, regardless of substrate material type, is presented in Figure 9.

The purpose in the initial evaluation of the four different substrate materials was to determine the influence of base metal chemistry on the composition and structure of the nickel aluminide layer produced using the target aluminizing "recipe". Following a series of screening processing tests, the decision was made to use the TP347H austenitic stainless material exclusively for the production of all test samples for the corrosion testing based on the combined benefits of good elevated temperature strength and the material's relative receptivity to the diffusion of aluminum. For the TP347H material a total of fifty-six square coupons were nickel plated.

Applied Thermal Coatings
200 Compress Street
Chattanooga, TN 37405
Telephone: 423-267-0647
Fax: 423-267-0637
Email: jhenry@atc-tn.com

3.4 Aluminizing

A group of the nickel-plated square coupons together with a group of bare square coupons were prepared for aluminizing. Two different master alloy formulations were used in the production of test samples, one consisting of 15% aluminum powder by weight, 2% ammonium chloride powder by weight and 83% alumina powder (Formulation A) by weight and the other consisting of 3% aluminum powder by weight, 3% ammonium chloride powder by weight and 94% alumina powder by weight (Formulation B). For Formulation A two different processing temperatures and hold times were used, one at 1472°F for 8 hours and one at 1292°F for 4 hours. For Formulation B the processing temperature was 1700°F for a hold time of 10 hours.

Typical results of the aluminizing tests for the different processing parameters used are documented in Figures 15 through 22. The information contained in these figures includes documentation of the "typical" microstructure of the coating produced using different process parameters (Figures 15, 18 and 20), the through-thickness composition of the coatings as determined by EDS (Figures 16, 21 and 22), and the through-thickness hardness of the coatings as determined by hardness measurements made using a microhardness tester with a 1kg test load (Figures 17 and 19).

3.5 Results of Processing Steps

Evaluation of the coupons that had been aluminized with and without the nickel coating and reflecting the three different aluminizing procedures provided information that led to the following conclusions:

a. For the coupons that had been nickel coated, the best aluminizing results were achieved using Formulation A with a processing temperature of 1292°F and a hold time at temperature of 4 hours.

b. For the coupons that had not been nickel coated, the best aluminizing results were achieved using Formation B with a processing temperature of 1700°F and a hold time at temperature of 10 hours.

3.6 Results of Testing in Simulated Molten Salt Environment

Three sets of square coupons were prepared for testing: one set represented TP347H material that had been nickel plated and then aluminized to produce a coating rich in nickel aluminides; the second set represented TP347H material that had been aluminized only to produce a coating rich in iron aluminides; and the third set represented uncoated TP347H material.

These samples were used to conduct a series of tests in the simulated molten salt environment that were designed to assess the relative ability of the nickel

Applied Thermal Coatings
200 Compress Street
Chattanooga, TN 37405
Telephone: 423-267-0647
Fax: 423-267-0637
Email: jhenry@atc-tn.com

aluminide and iron aluminide coatings to provide protection from the effects of the molten salt environment. The manner in which the testing was conducted for each test series and the results of the tests in each test series are discussed in detail in the three research reports which are attached as Appendices 1, 2 and 3. As a supplement to the information provided in the three reports, selected documentation of the condition of the tested specimens following exposure to the test conditions is presented in Figures 23 through 34 of this report.

4.0 CONCLUSIONS AND RECOMMENDATIONS

4.1 Conclusions

Based on the information obtained from the testing in a simulated molten salt environment of coupons representing two different coating methods, one of which produced a coating rich in nickel aluminides the other of which produced a coating rich in iron aluminides, the following conclusions have been drawn:

a. In the longer-term tests, both coating types provided enhanced protection from the simulated molten salt environment when compared to bare TP347H material.

b. The coating rich in nickel aluminides provided superior resistance to the simulated molten salt environment when compared with the coating rich in iron aluminides at all times and temperatures tested. The improvement in resistance of the nickel aluminide rich coating to the simulated molten salt environment was at least 5X that of the resistance of the iron aluminide rich coating.

4.2 Recommendations

The following recommendations are made based on the results of the tests conducted during this project:

a. Additional processing tests should be carried out to determine if the structure of the nickel aluminide coating can be improved to minimize the likelihood of separation of the outer nickel aluminide rich layer from the underlying nickel phosphorus layer.
b. Tests that expose coupons of an “optimized” nickel aluminide coating to the simulated molten salt environment while cycling temperature should be carried out to determine if the improved performance of the nickel

aluminide coating is maintained under the conditions of thermal cycling that would be anticipated in actual service in a solar boiler.

Applied Thermal Coatings
200 Compress Street
Chattanooga, TN 37405
Telephone: 423-267-0647
Fax: 423-267-0637
Email: jhenry@atc-tn.com

As-Received

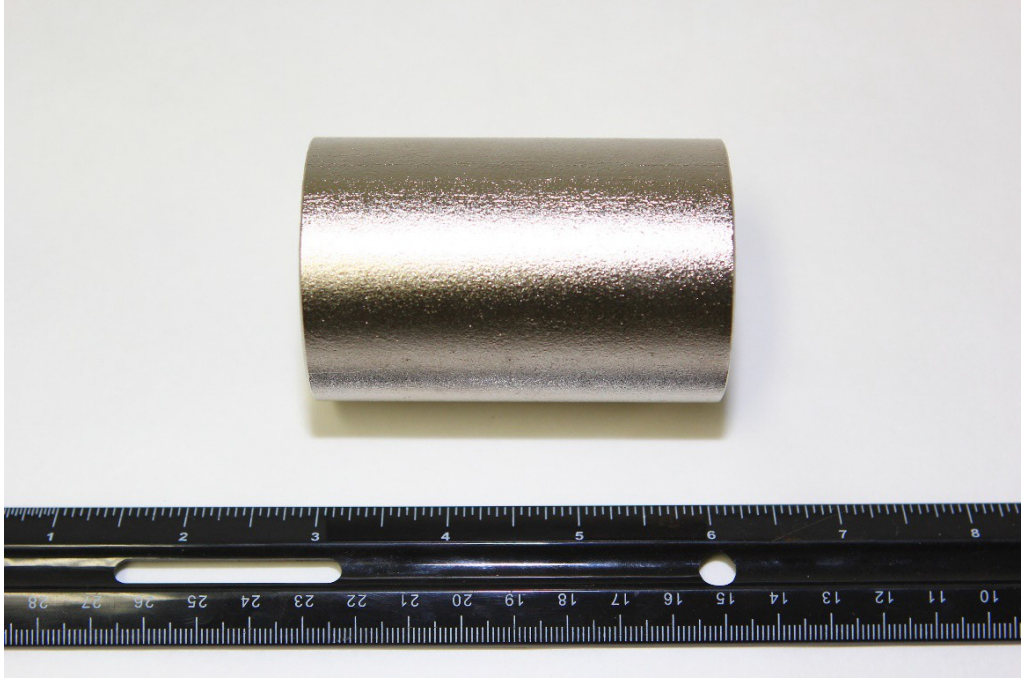

After Nickel Plating

Figure 4. Tubular coupon for TP347H material, as-received and after nickel plating

As Received

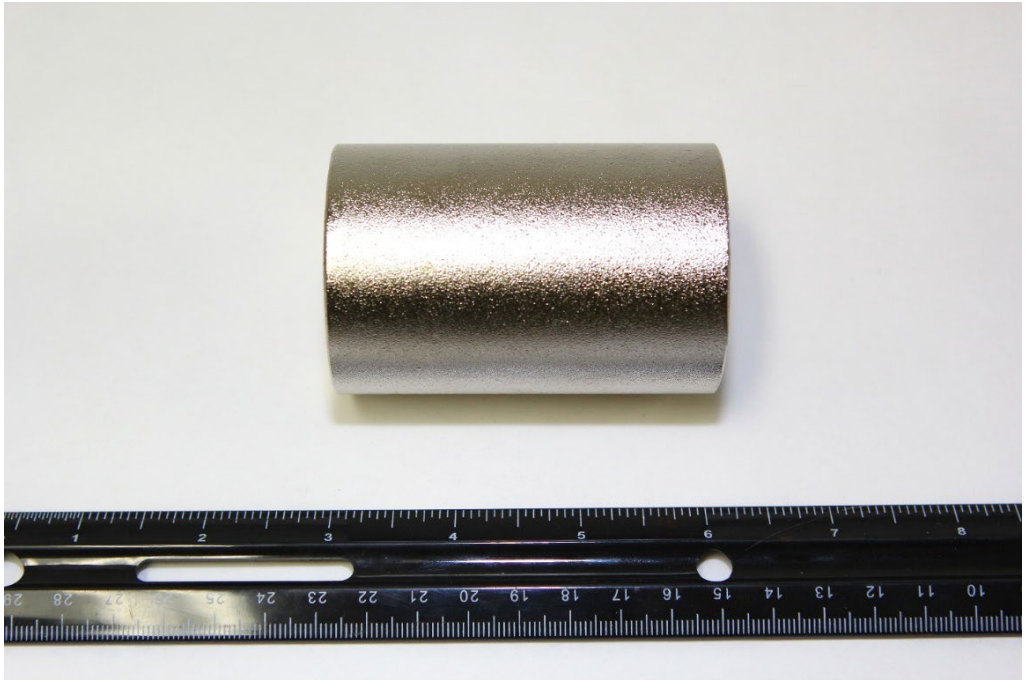

After Nickel Plating

Figure 5. Tubular coupon for T91 material, as-received and after nickel plating

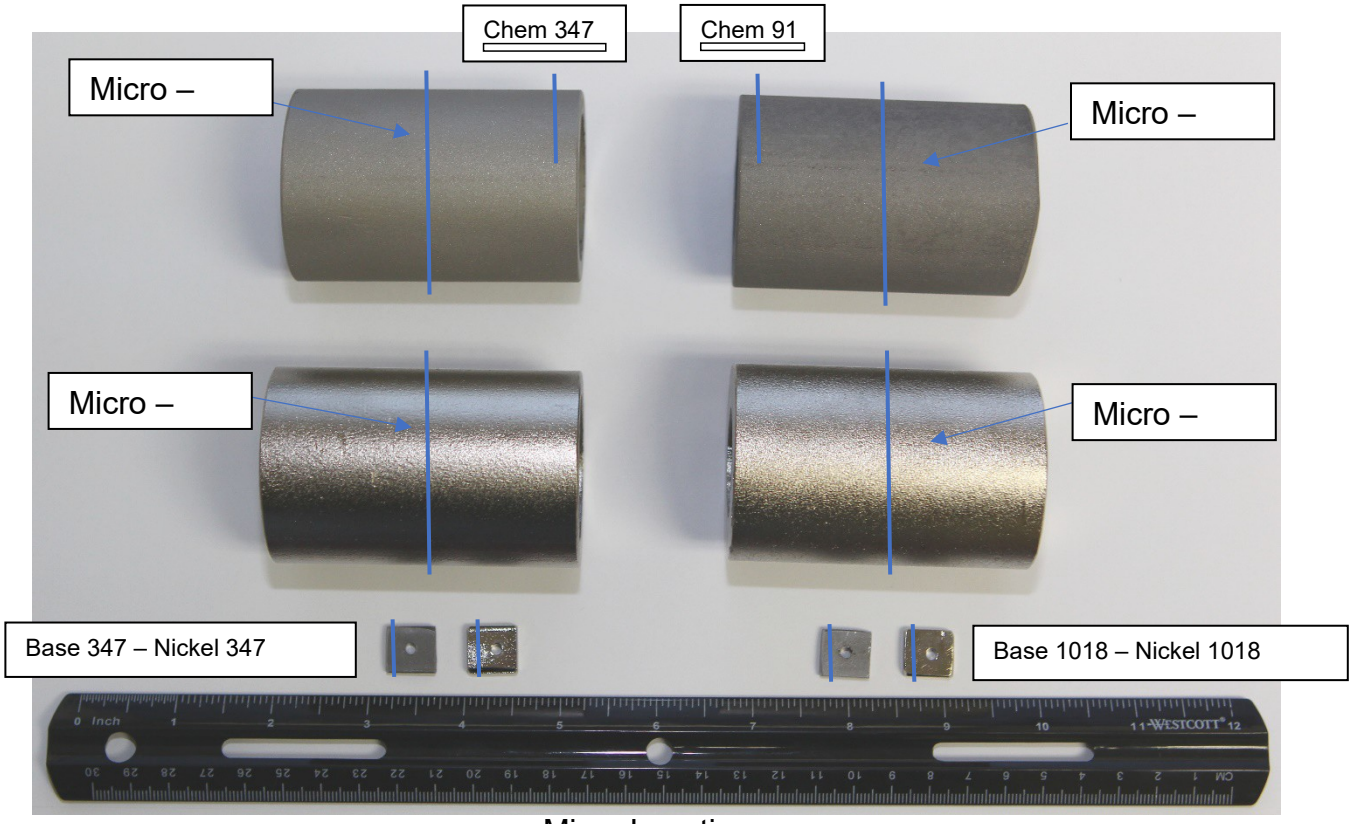

Micro Locations

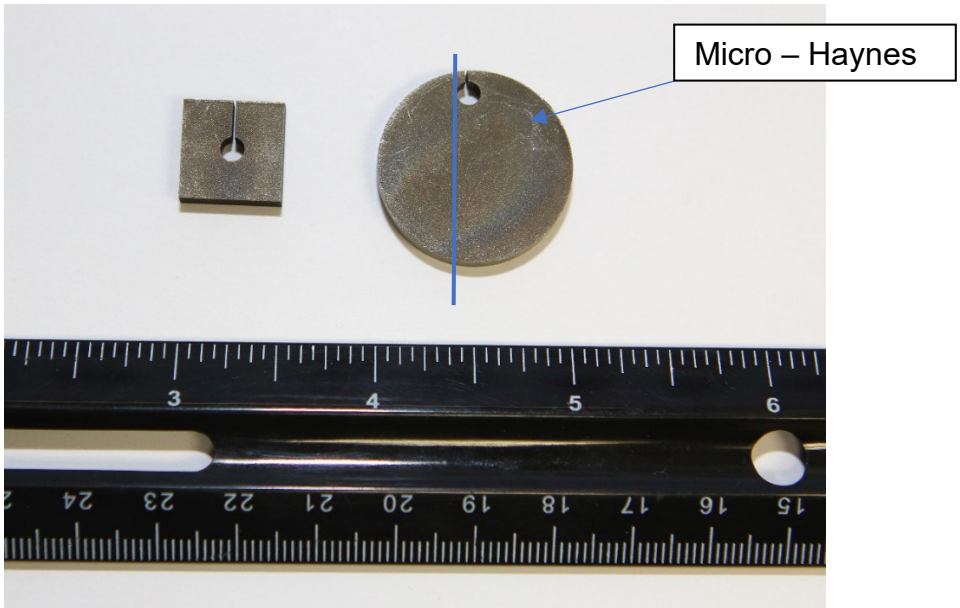

Haynes 230 Coupons

Figure 6. Showing tubular and square coupons for different materials originally evaluated in the as-received condition and after nickel plating, and indicating specimen locations

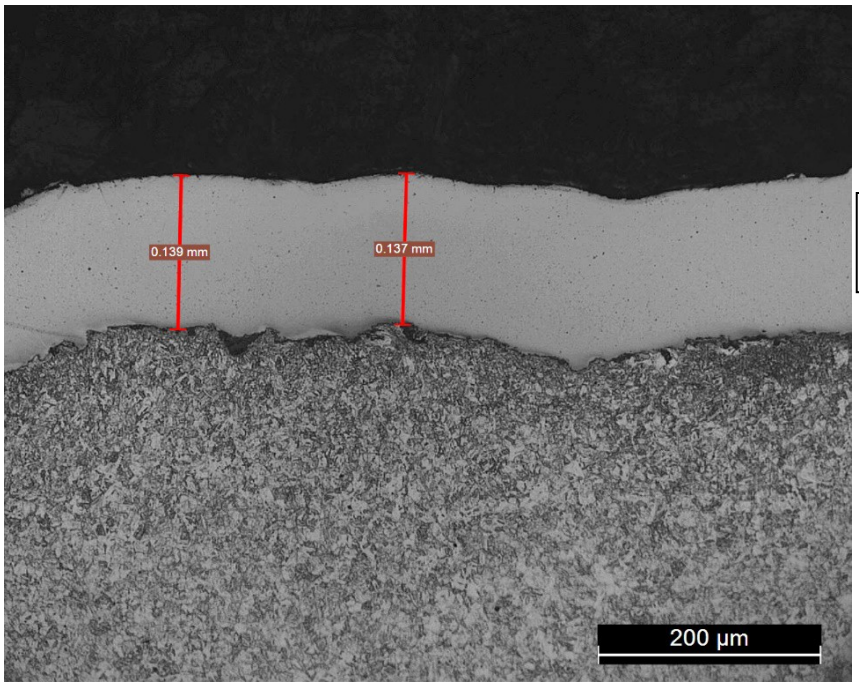

T91 Tube
~5 mils

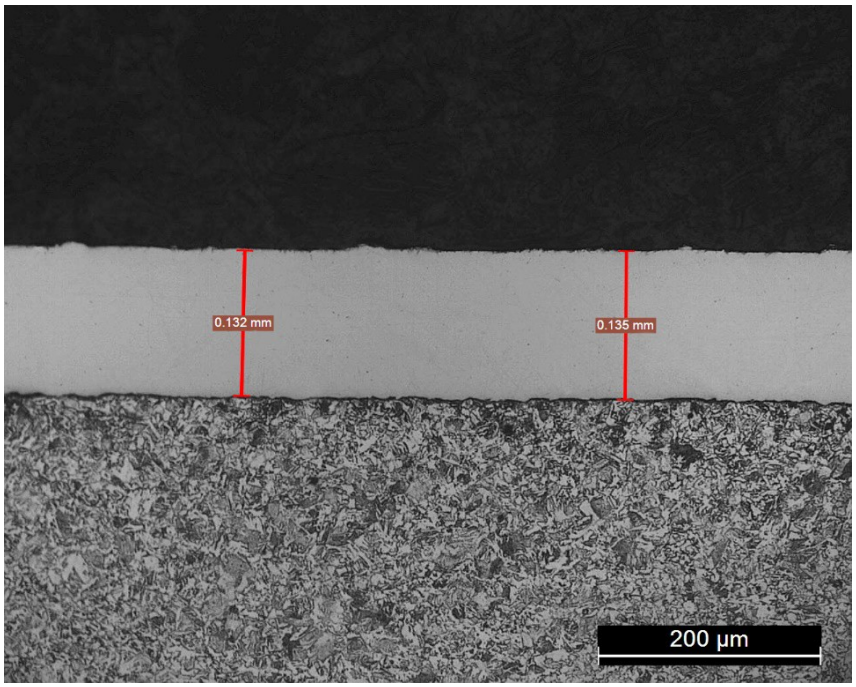

1018
½" Coupon
~5 mils

Figure 7. Showing nickel plating on T91 and 1018 materials

Applied Thermal Coatings
200 Compress Street
Chattanooga, TN 37405
Telephone: 423-267-0647
Fax: 423-267-0637
Email: jhenry@atc-tn.com

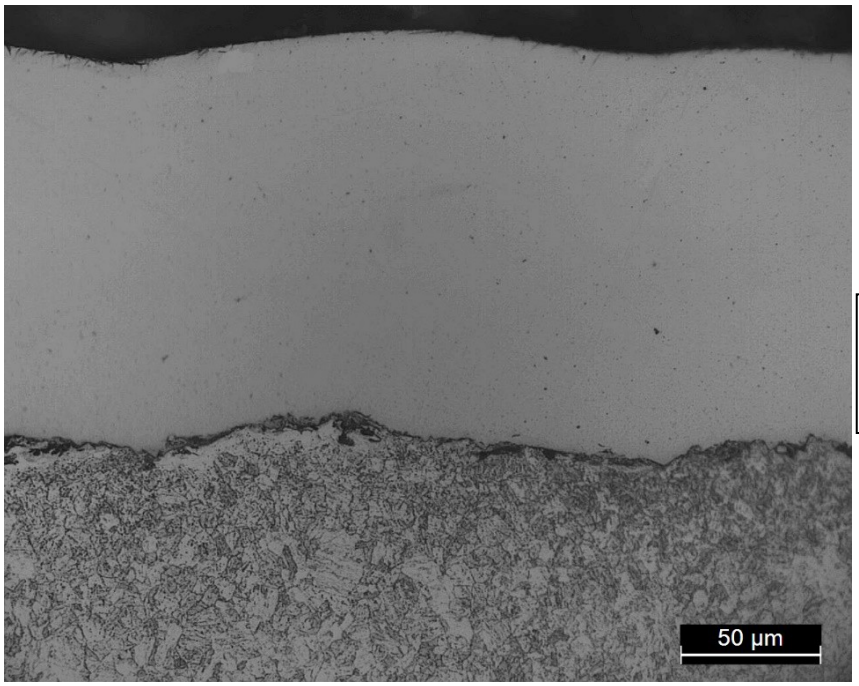

T91 Tube
500x
Interface

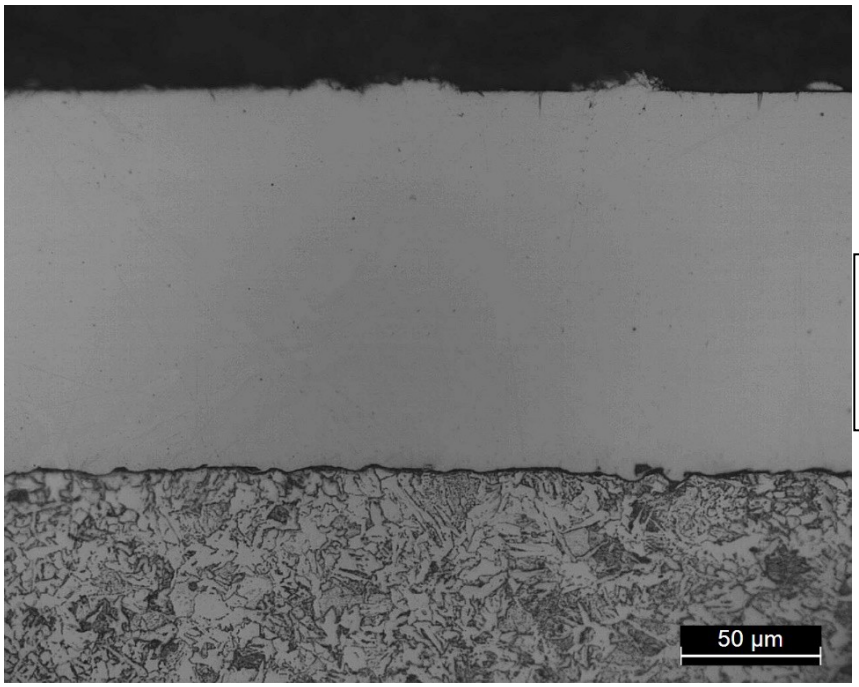

1018
½" Coupon
500x
Interface

Figure 8. Showing the interface between the nickel plating and the substrate at higher magnification

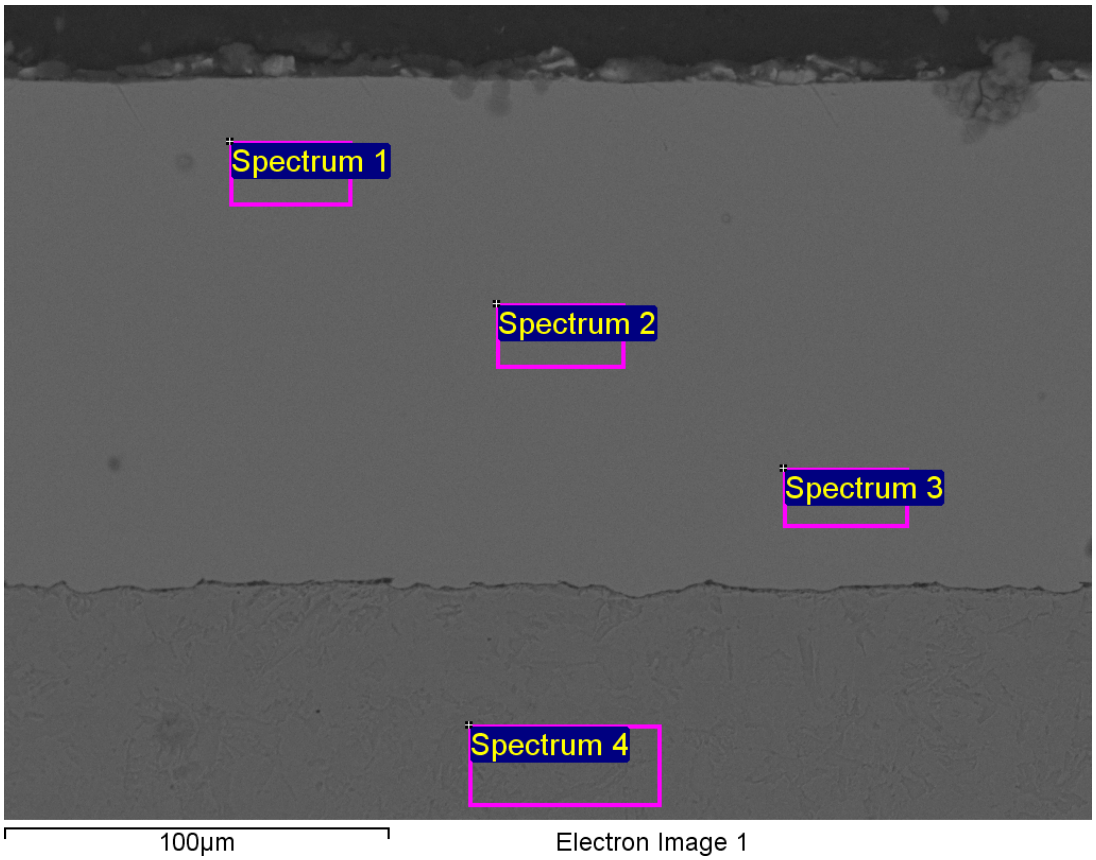

Nickel Plating & Base Metal

Spectrum	In stats.	P	Mn	Fe	Ni	Total
Spectrum 1	Yes	4.44			95.56	100.00
Spectrum 2	Yes	4.69			95.31	100.00
Spectrum 3	Yes	4.39			95.61	100.00
Spectrum 4	Yes		0.68	99.32		100.00
Max.		4.69	0.68	99.32	95.61	
Min.		4.39	0.68	99.32	95.31	

Figure 9. Showing results of an EDS analysis of the nickel plating on 1018 substrate.

Applied Thermal Coatings
200 Compress Street
Chattanooga, TN 37405
Telephone: 423-267-0647
Fax: 423-267-0637
Email: jhenry@atc-tn.com

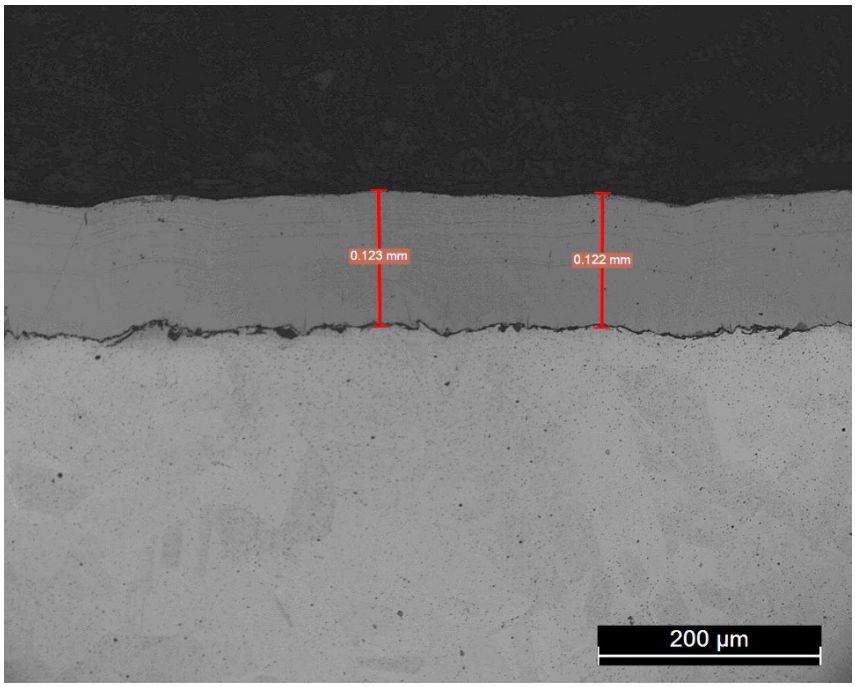

TP347H
Tube
~5 mils

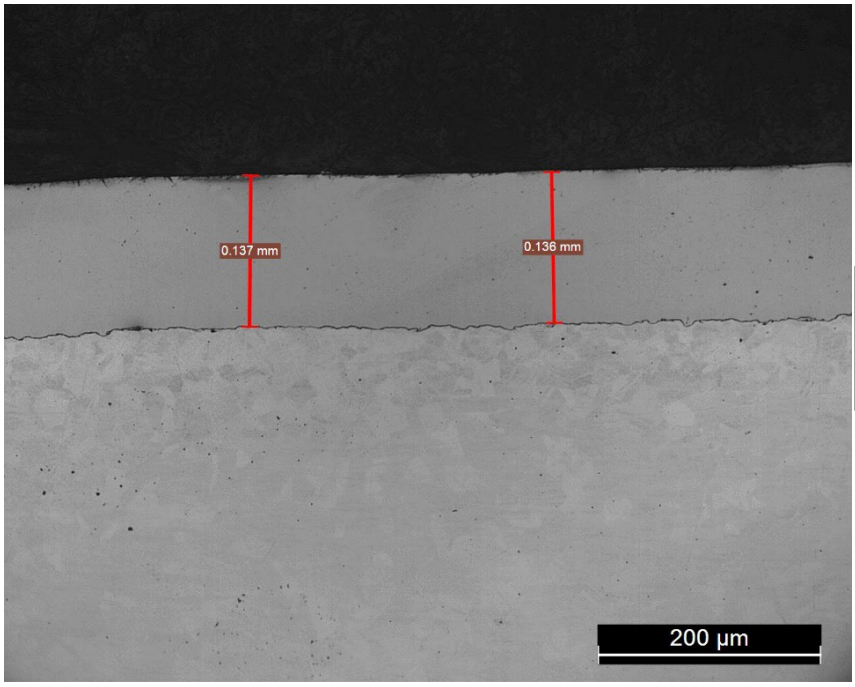

TP347H
½"Coupon
~5 mils

Figure 10. Showing nickel plating on TP347H material, both tubular and square coupons.

Applied Thermal Coatings
200 Compress Street
Chattanooga, TN 37405
Telephone: 423-267-0647
Fax: 423-267-0637
Email: jhenry@atc-tn.com

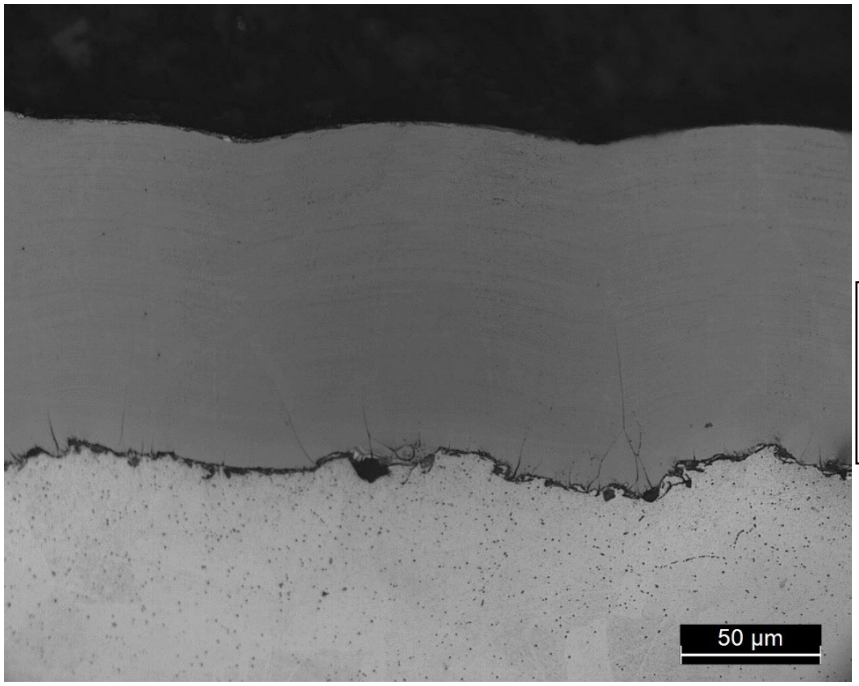

TP347H
Tube
500x
Interface

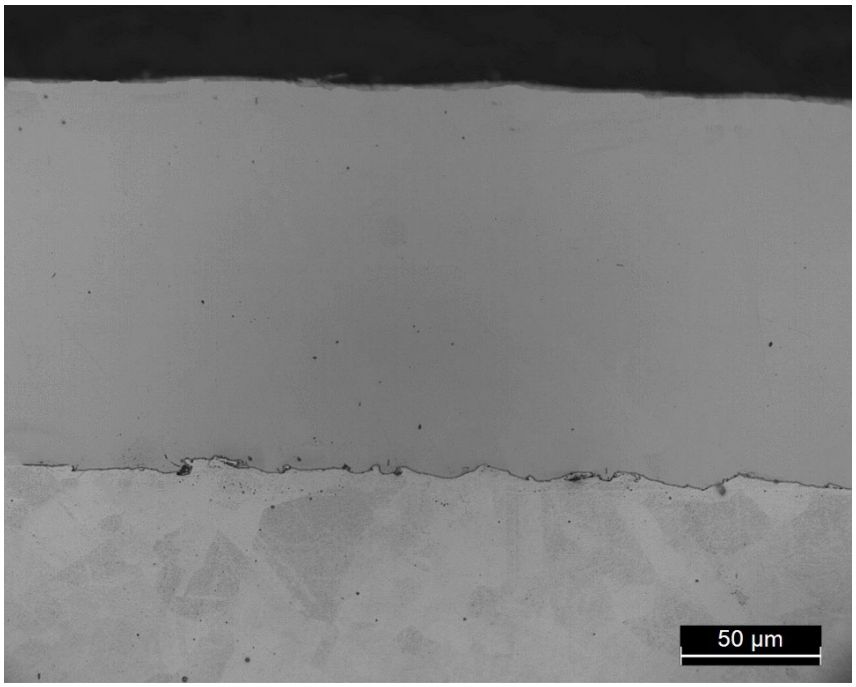

TP347H
½" Coupon
500x
Interface

Figure 11. Showing the interface between the nickel plating and the substrate at higher magnification

Applied Thermal Coatings
200 Compress Street
Chattanooga, TN 37405
Telephone: 423-267-0647
Fax: 423-267-0637
Email: jhenry@atc-tn.com

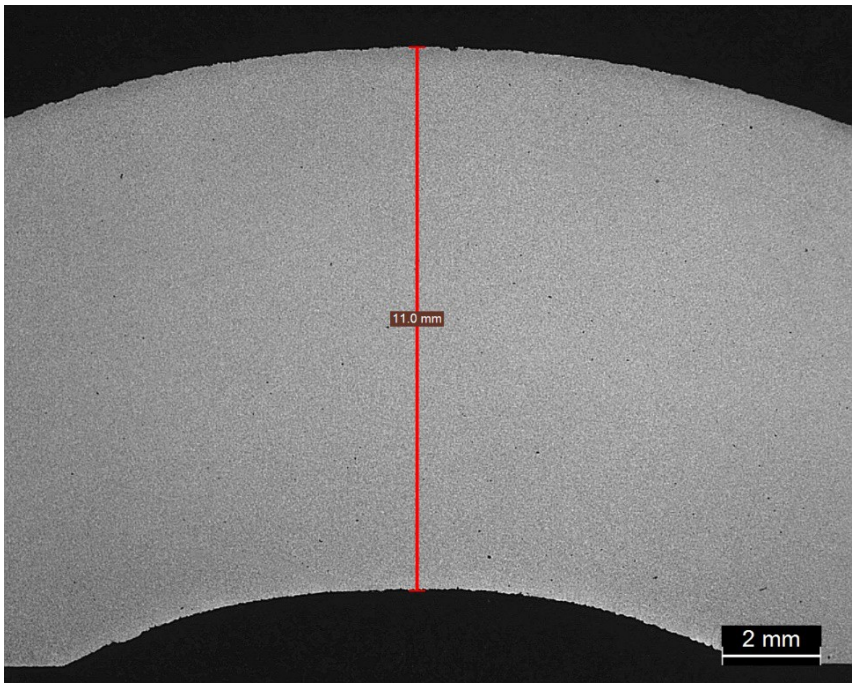

T91 Tube
Base Metal

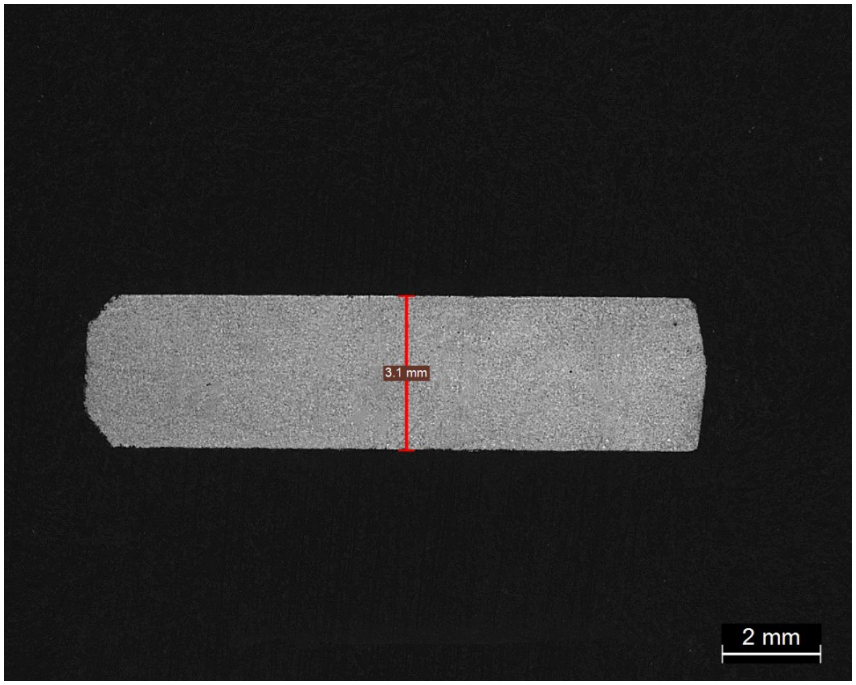

1018 Coupon
Base Metal

Figure 12. Showing transverse sections of a tubular T91 coupon and a 1018 square coupon

Applied Thermal Coatings
200 Compress Street
Chattanooga, TN 37405
Telephone: 423-267-0647
Fax: 423-267-0637
Email: jhenry@atc-tn.com

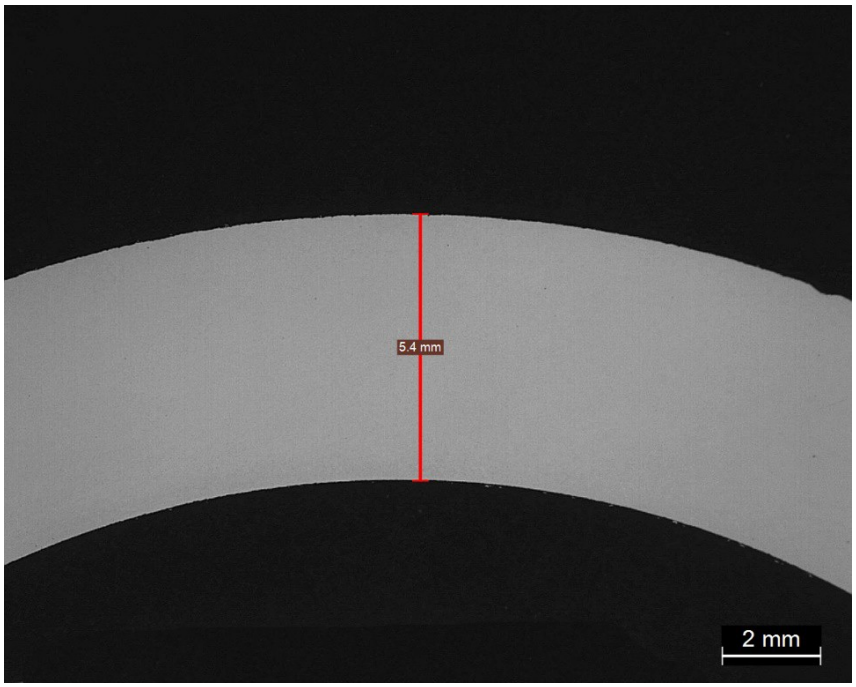

TP347H Tube
Base Metal

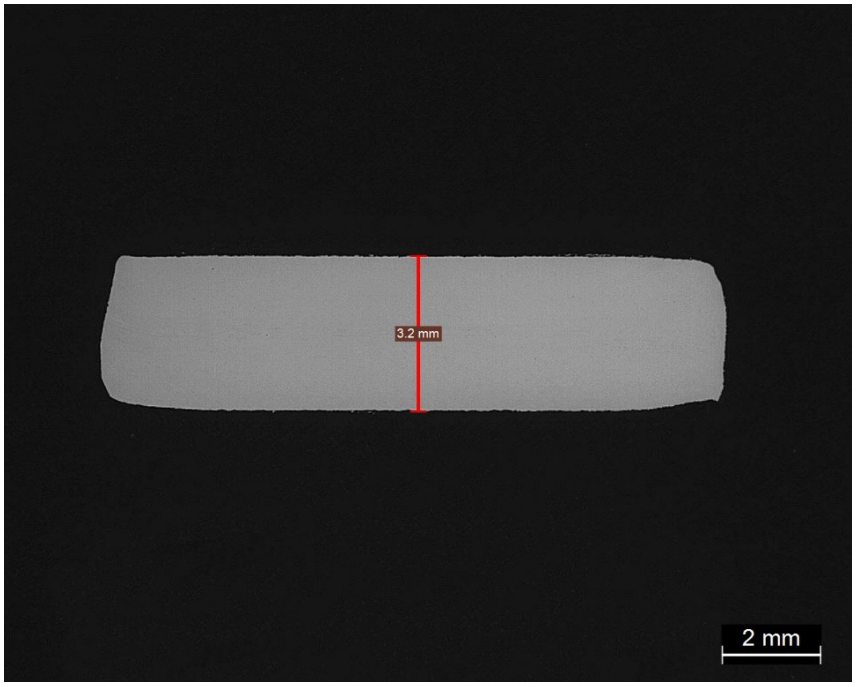

TP347H Coupon
Base Metal

Figure 13. Showing transverse sections of a tubular and square coupons for TP347H material

Applied Thermal Coatings
200 Compress Street
Chattanooga, TN 37405
Telephone: 423-267-0647
Fax: 423-267-0637
Email: jhenry@atc-tn.com

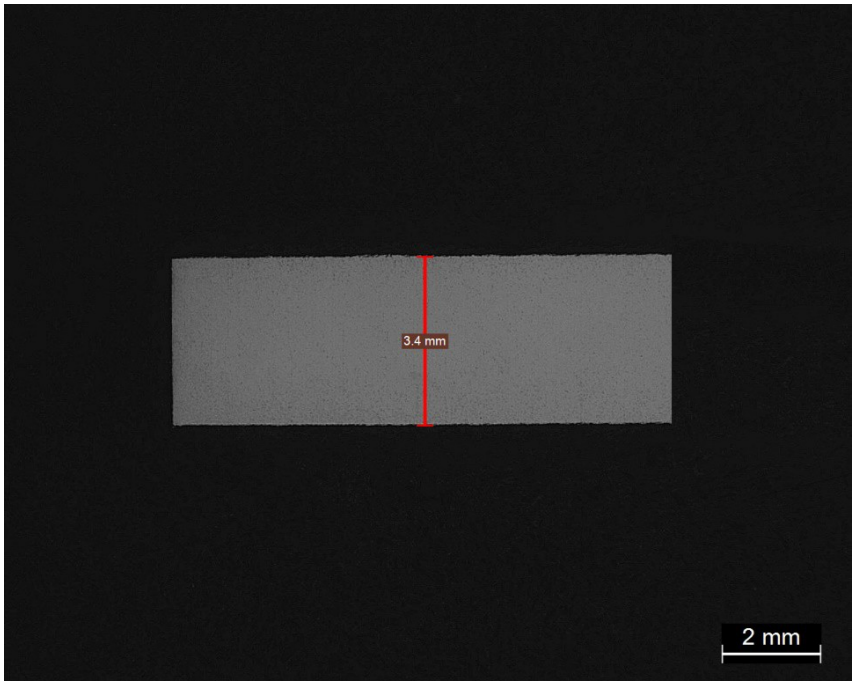

Haynes 230 Coupon
Base Metal

Figure 14. Showing transverse section of a square coupon of Alloy 230

Applied Thermal Coatings
200 Compress Street
Chattanooga, TN 37405
Telephone: 423-267-0647
Fax: 423-267-0637
Email: jhenry@atc-tn.com

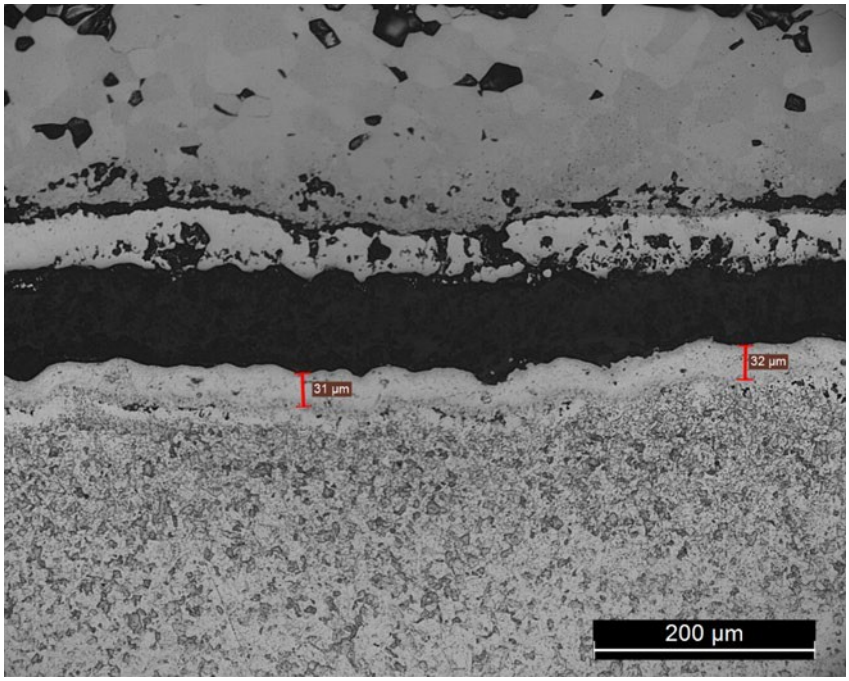

Figure 15. Showing aluminized coating produced on nickel-plated T91 sample with Formulation A at 1472°F for 8 hours

Applied Thermal Coatings
200 Compress Street
Chattanooga, TN 37405
Telephone: 423-267-0647
Fax: 423-267-0637
Email: jhenry@atc-tn.com

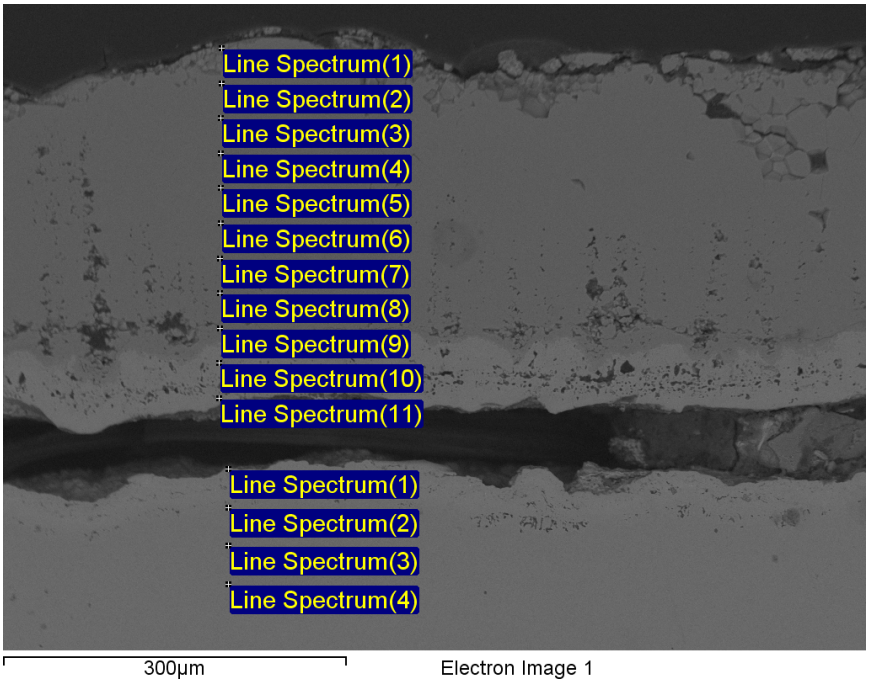

T91 Test Sample Aluminized 1472ºF/8hrs

Spectrum	In stats.	Al	P	Cr	Fe	Ni	Total
Line Spectrum(1)	Yes	40.73			2.23	57.04	100.00
Line Spectrum(2)	Yes	35.29				64.71	100.00
Line Spectrum(3)	Yes	34.49				65.51	100.00
Line Spectrum(4)	Yes	35.39				64.61	100.00
Line Spectrum(5)	Yes	33.54				66.46	100.00
Line Spectrum(6)	Yes	34.30				65.70	100.00
Line Spectrum(7)	Yes	35.20				64.80	100.00
Line Spectrum(8)	Yes	33.49				66.51	100.00
Line Spectrum(9)	Yes	34.02				65.98	100.00
Line Spectrum(10)	Yes		17.58		4.44	77.98	100.00
Line Spectrum(11)	Yes	3.84	14.90		1.89	79.37	100.00
Line Spectrum(1)	Yes	19.49			1.70	78.81	100.00
Line Spectrum(2)	Yes	0.10		7.49	84.70	7.71	100.00
Line Spectrum(3)	Yes			7.83	92.17		100.00
Line Spectrum(4)	Yes			9.88	90.12		100.00
Max.		40.73	17.58	9.88	92.17	79.37	
Min.		0.10	14.90	7.49	1.70	7.71	

Figure 16. Results of EDS analysis of aluminized T91 sample that had been nickel-plated.

Applied Thermal Coatings
200 Compress Street
Chattanooga, TN 37405
Telephone: 423-267-0647
Fax: 423-267-0637
Email: jhenry@atc-tn.com

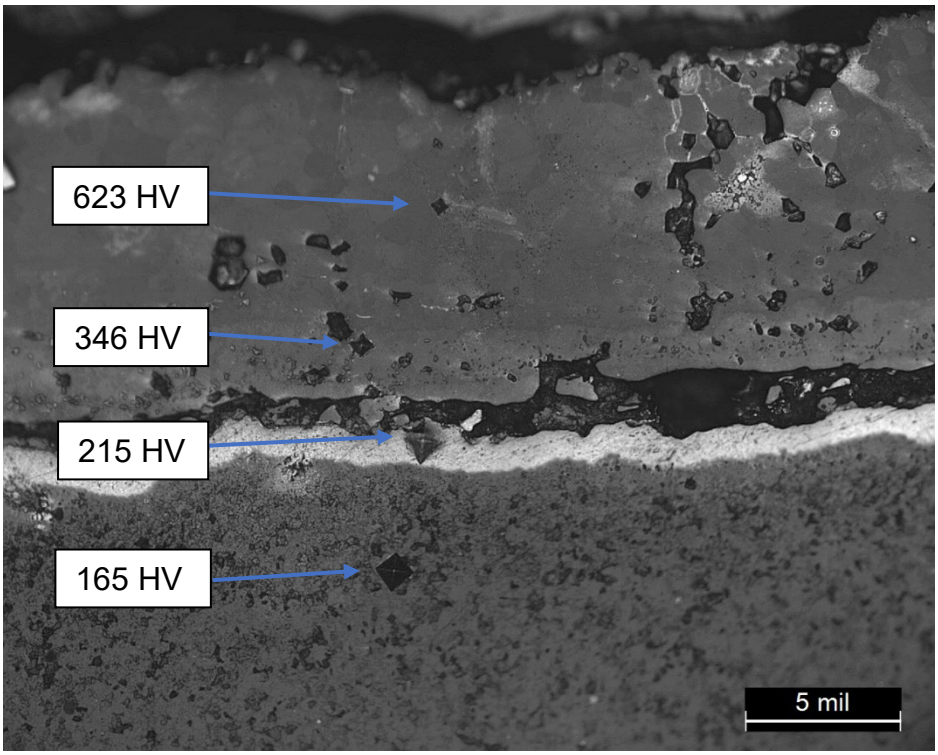

T91 Test Sample Aluminized 1472ºF/8hrs

Figure 17. Results of hardness testing of aluminized T91 sample that had been nickel-plated.

Applied Thermal Coatings
200 Compress Street
Chattanooga, TN 37405
Telephone: 423-267-0647
Fax: 423-267-0637
Email: jhenry@atc-tn.com

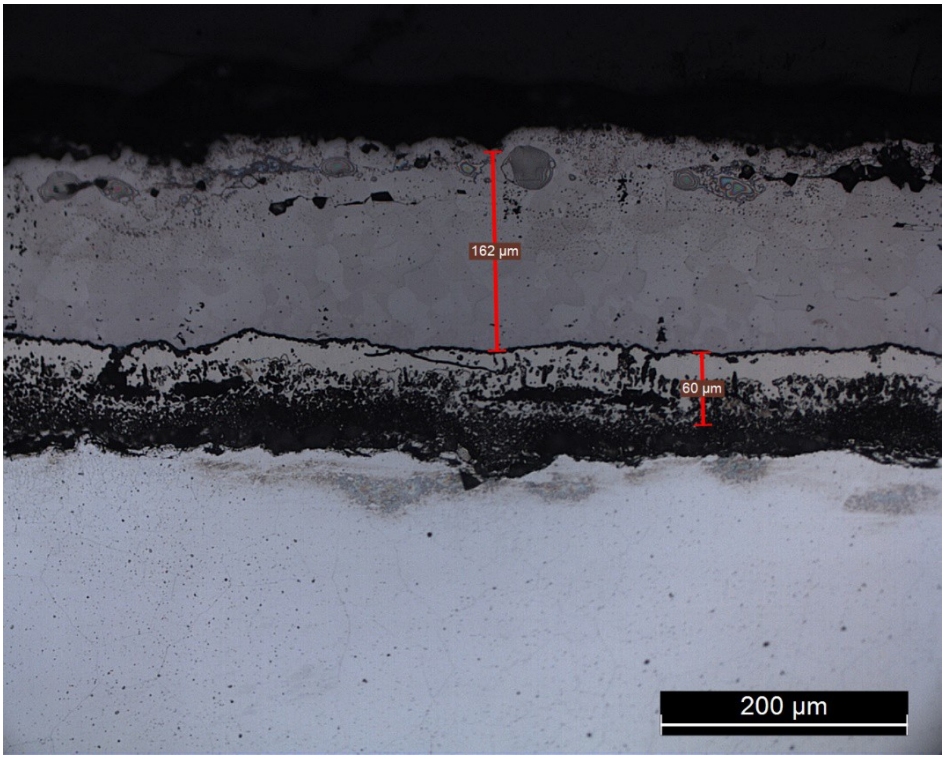

347H Test Sample Aluminized 1472ºF/4hrs

Figure 18. Showing coating produced on nickel-plated TP347H sample with Formulation A at 1472°F for 4 hours

Applied Thermal Coatings
200 Compress Street
Chattanooga, TN 37405
Telephone: 423-267-0647
Fax: 423-267-0637
Email: jhenry@atc-tn.com

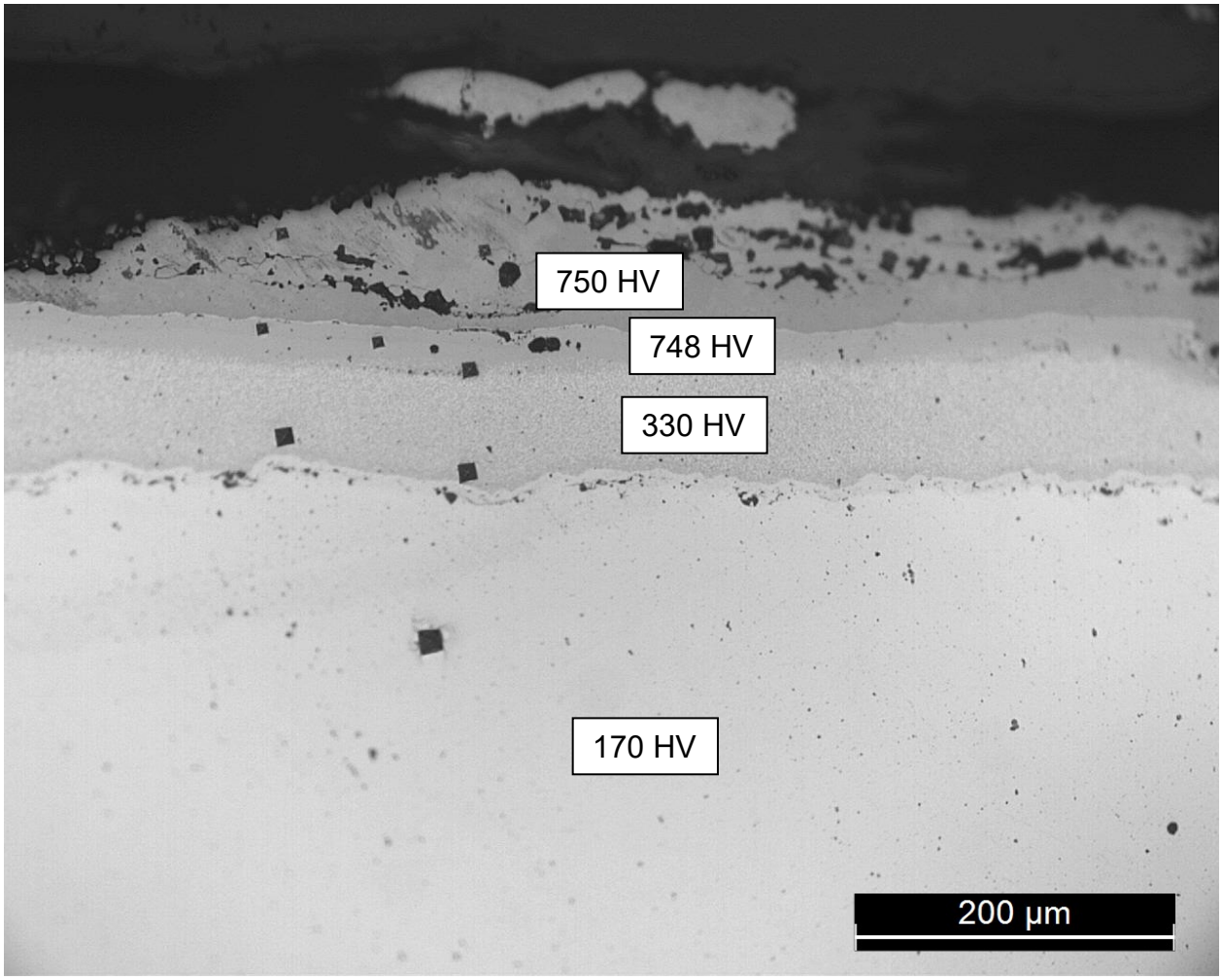

Figure 19. Showing hardness measurement results for coating produced on nickel-plated TP347H sample with Formulation A at 1282°F for 4 hours

Applied Thermal Coatings
200 Compress Street
Chattanooga, TN 37405
Telephone: 423-267-0647
Fax: 423-267-0637
Email: jhenry@atc-tn.com

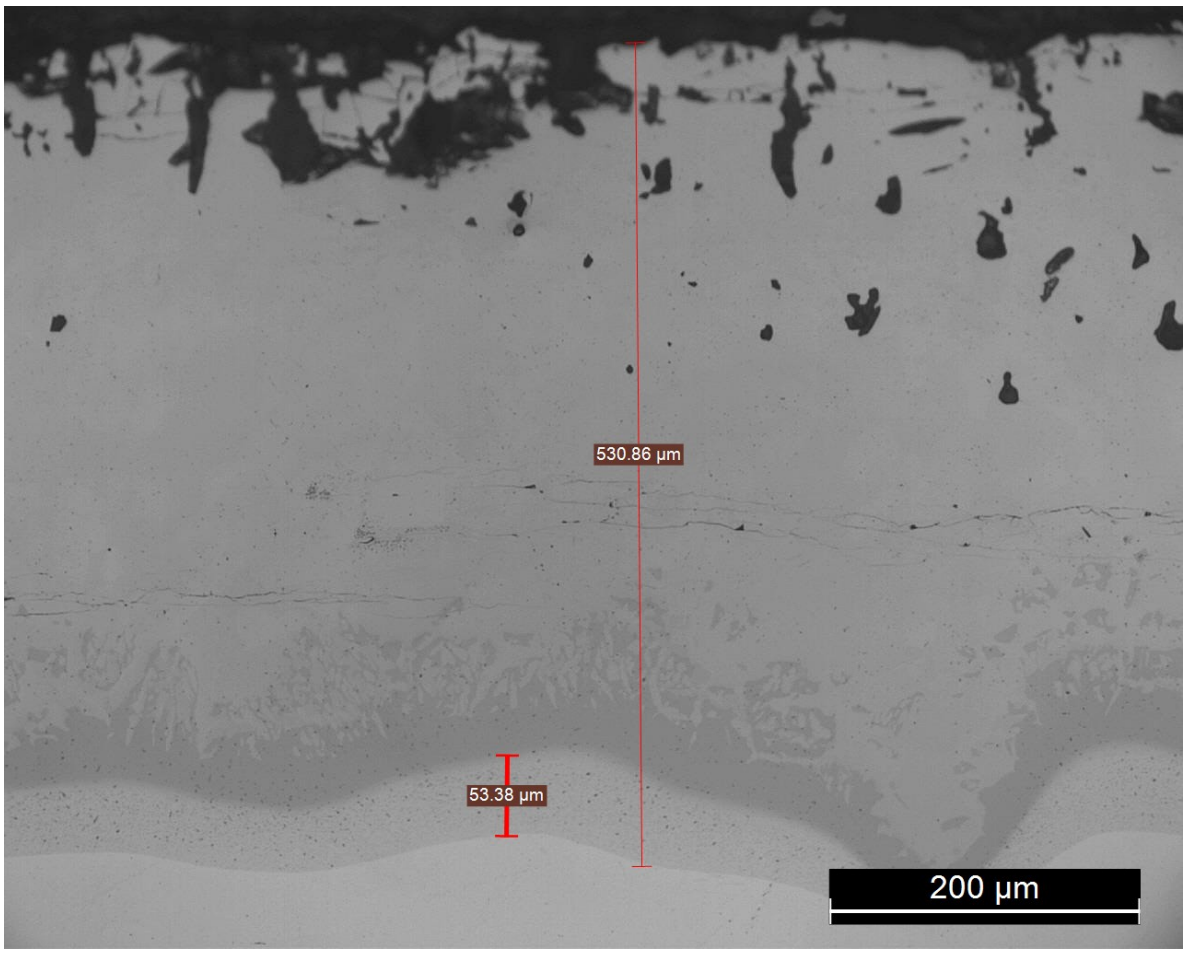

FeAl 700ºC/4hrs - Furnace Cool
“Coupon 2”

Figure 20. Showing iron aluminide coating produced on TP347H sample with Formula A at 1282°F for 4 hours – the coupon had not been nickel-plated.

Applied Thermal Coatings
200 Compress Street
Chattanooga, TN 37405
Telephone: 423-267-0647
Fax: 423-267-0637
Email: jhenry@atc-tn.com

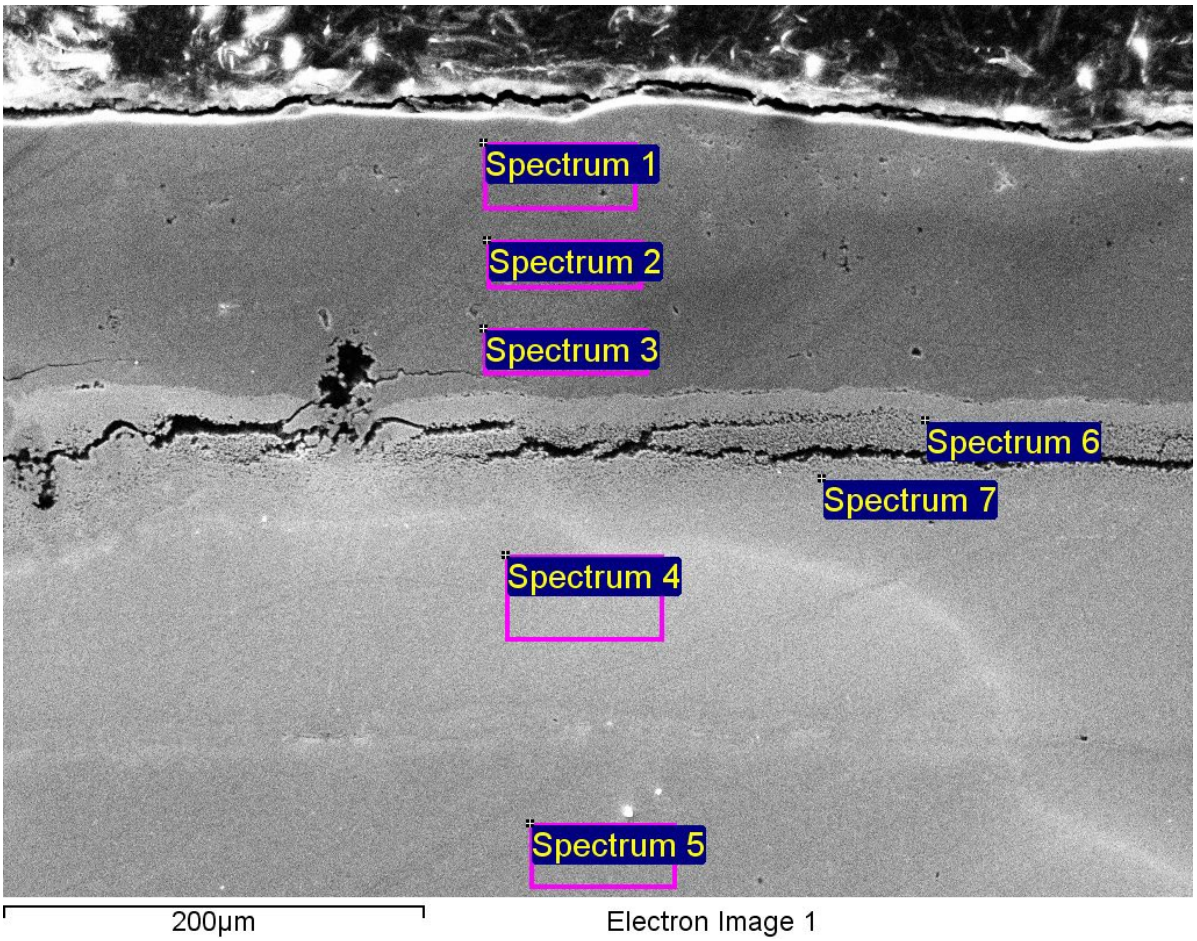

Processing option: All elements analyzed (Normalized)

Spectrum	In stats.	Al	P	Cr	Mn	Fe	Ni	Zr
Spectrum 1	Yes	50.56					47.74	1.70
Spectrum 2	Yes	50.57					49.43	
Spectrum 3	Yes	50.93					49.07	
Spectrum 4	Yes		7.45				92.55	
Spectrum 5	Yes			20.24	2.38	69.40	7.98	
Spectrum 6	Yes		22.32				77.68	
Spectrum 7	Yes	6.51	18.05				75.45	
Max.		50.93	22.32	20.24	2.38	69.40	92.55	1.70
Min.		6.51	7.45	20.24	2.38	69.40	7.98	1.70

All results in atomic%

Figure 21. Showing EDS results from nickel aluminide coating, highlighting the two-layer structure consisting of a top layer of nickel aluminide and a bottom layer of nickel phosphide.

Applied Thermal Coatings
200 Compress Street
Chattanooga, TN 37405
Telephone: 423-267-0647
Fax: 423-267-0637
Email: jhenry@atc-tn.com

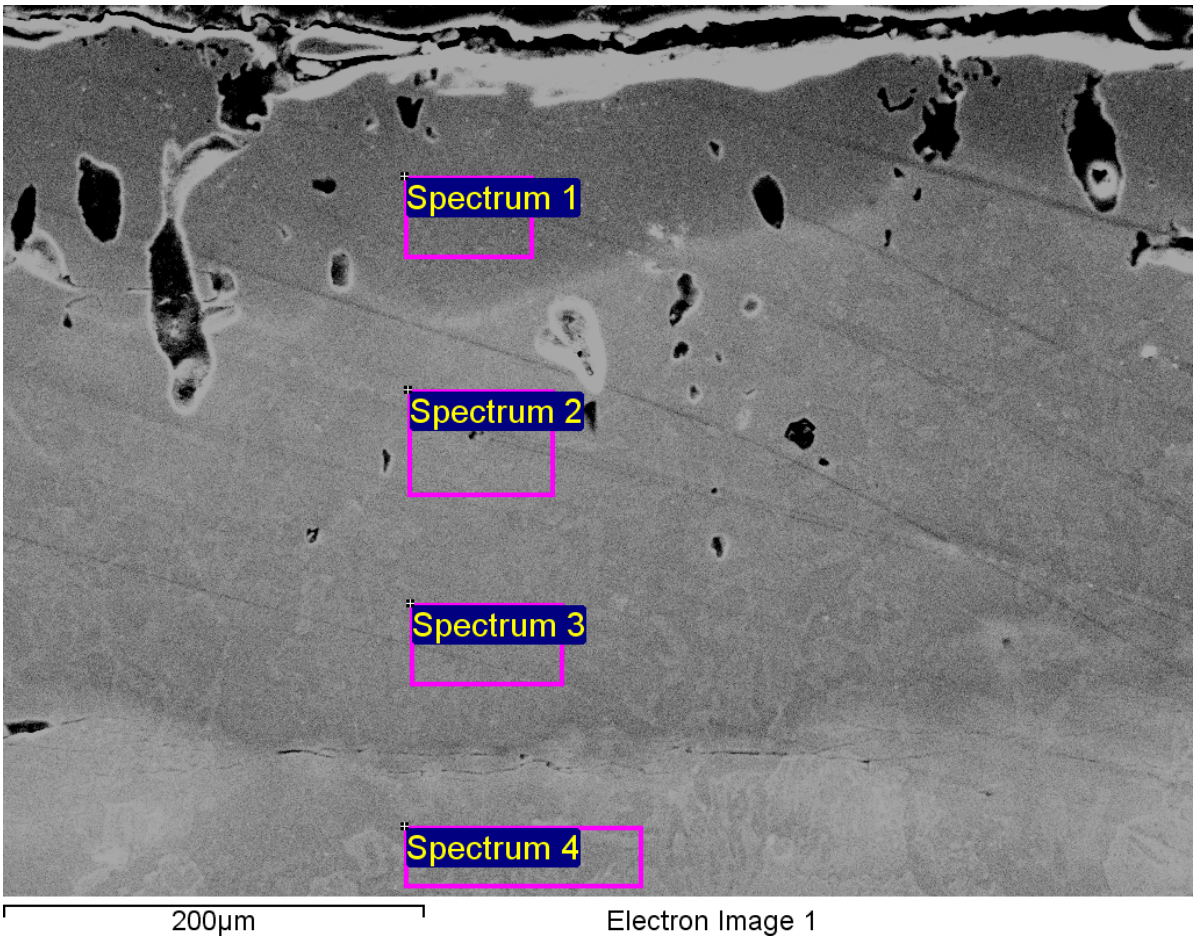

Processing option: All elements analyzed (Normalized)

Spectrum	In stats.	Al	Cr	Mn	Fe	Ni
Spectrum 1	Yes	64.72	7.05	0.20	25.27	2.76
Spectrum 2	Yes	62.71	5.79	0.64	27.81	3.06
Spectrum 3	Yes	61.39	7.09	0.65	26.32	4.55
Spectrum 4	Yes	56.35	9.89	0.95	30.03	2.78
Mean		61.29	7.45	0.61	27.36	3.28
Std. deviation		3.57	1.73	0.31	2.06	0.85
Max.		64.72	9.89	0.95	30.03	4.55
Min.		56.35	5.79	0.20	25.27	2.76

All results in atomic%

Figure 22. Showing EDS results from iron aluminide coating.

Applied Thermal Coatings
200 Compress Street
Chattanooga, TN 37405
Telephone: 423-267-0647
Fax: 423-267-0637
Email: jhenry@atc-tn.com

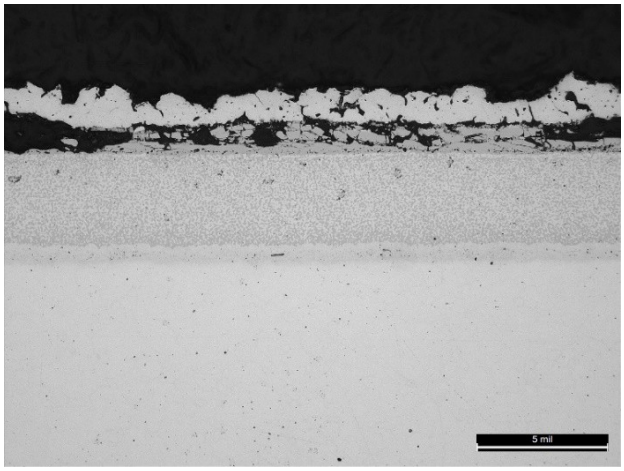

C1-1 200x

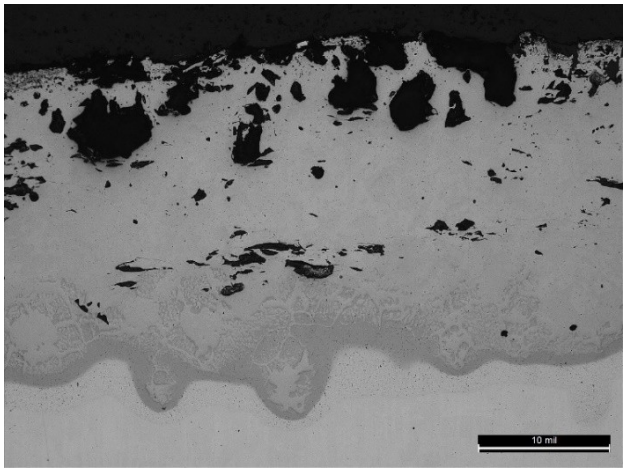

C2-1 100x

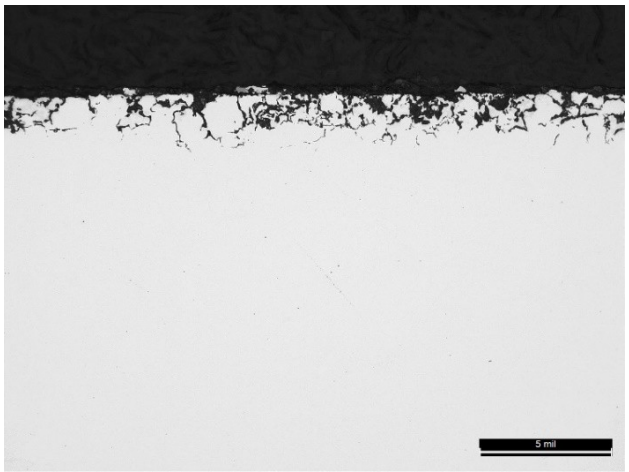

C3-1 200x

Figure 23. Results of electrochemical testing – first Tafel experiment

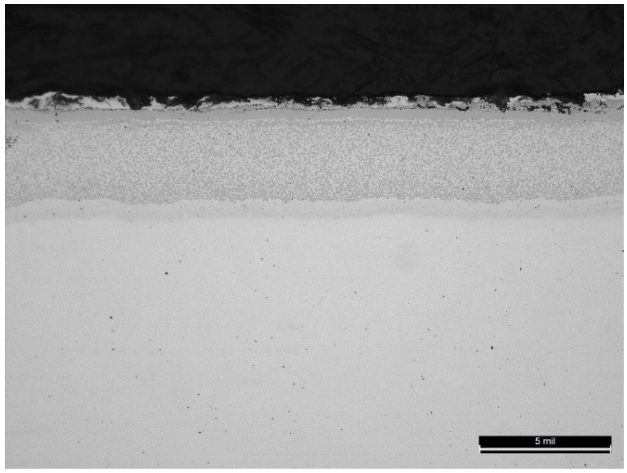

C1-2 200x

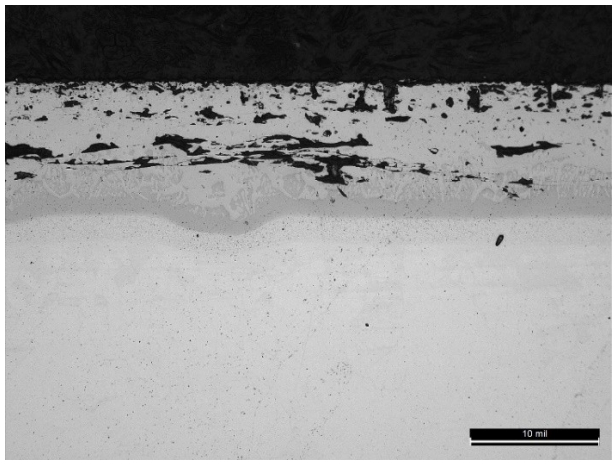

C2-2 100x

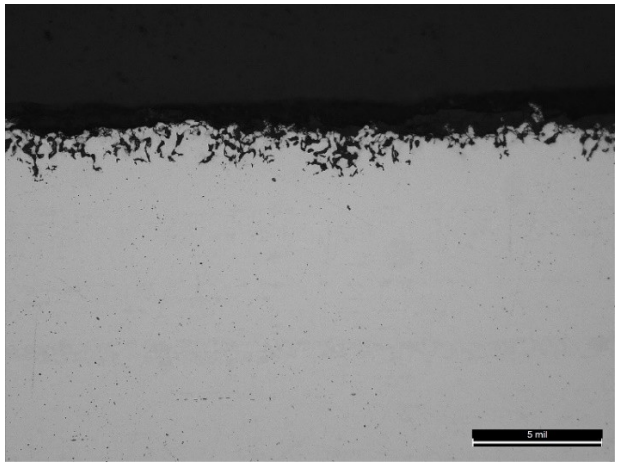

C3-2 200x

Figure 24. Results of electrochemical testing – second Tafel experiment

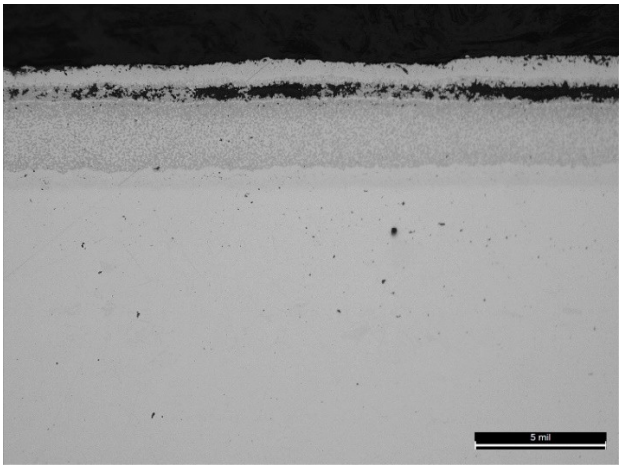

C1-3 200x

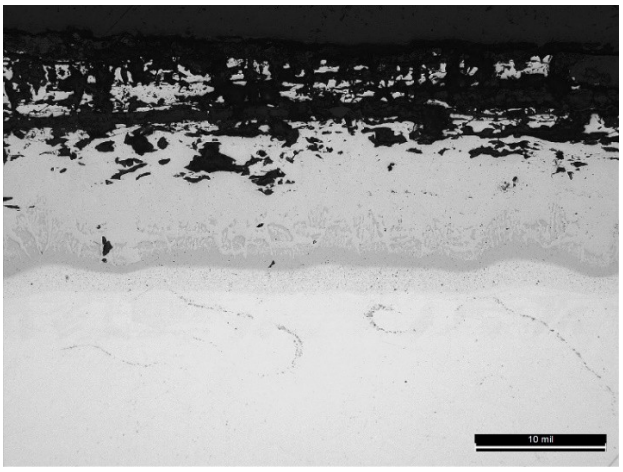

C2-3 100x

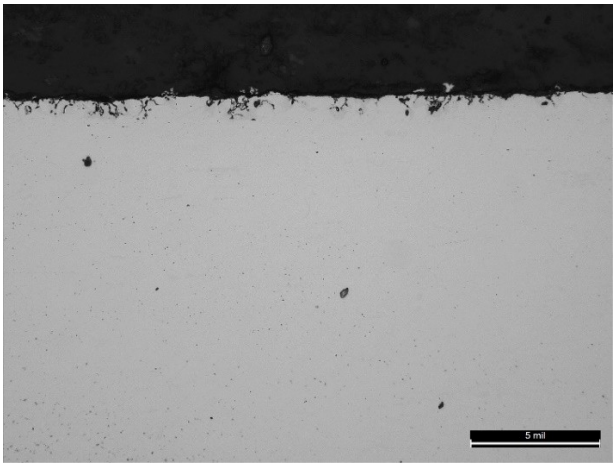

C3-3 200x

Figure 25. Results of electrochemical testing – third Tafel experiment

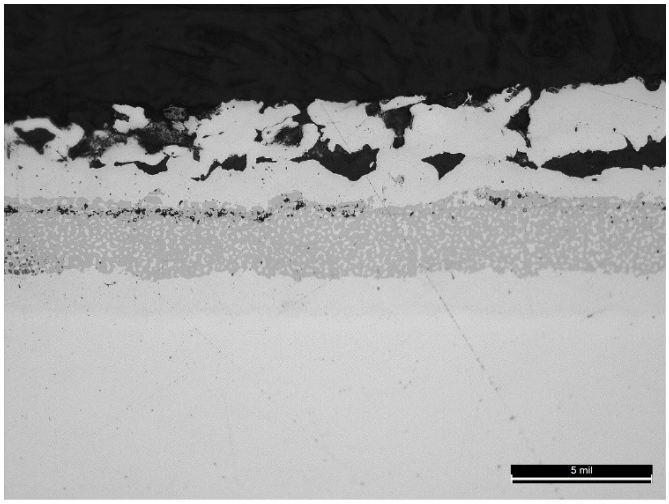

C1-6 200x

Figure 26. Results of immersion corrosion testing – 100 hours at 700°C.

Applied Thermal Coatings
200 Compress Street
Chattanooga, TN 37405
Telephone: 423-267-0647
Fax: 423-267-0637
Email: jhenry@atc-tn.com

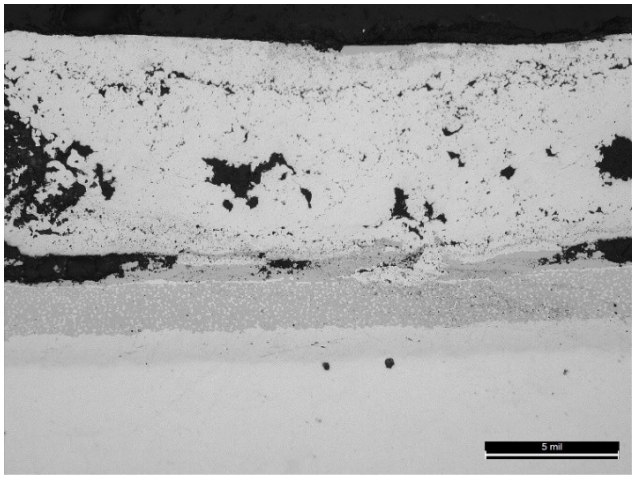

C1-5 200x

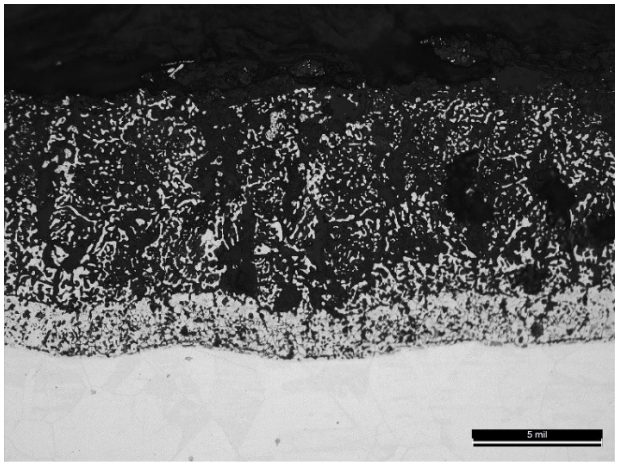

C2-5 100x

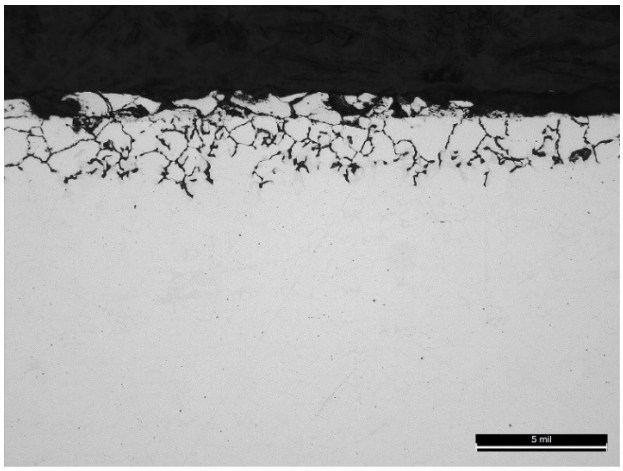

C3-5 200x

Figure 27. Results of immersion corrosion testing – 100 hours at 750°C.

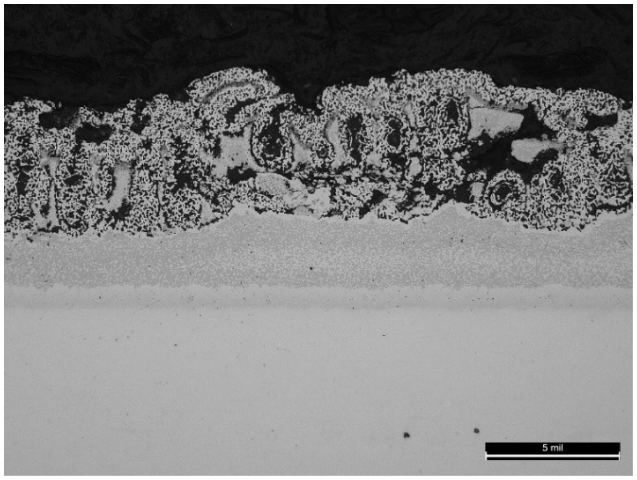

C1-4 200x

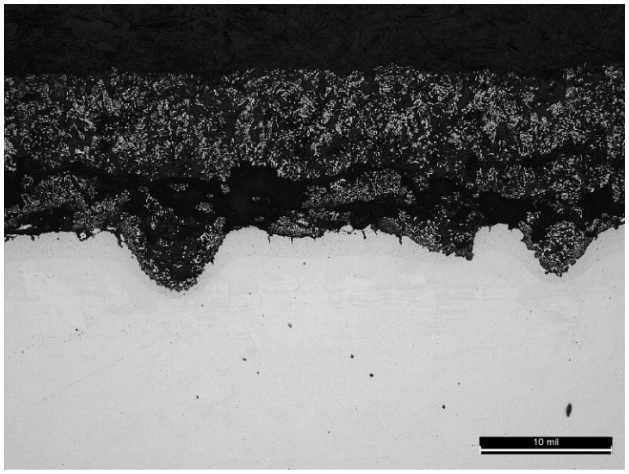

C2-4 100x

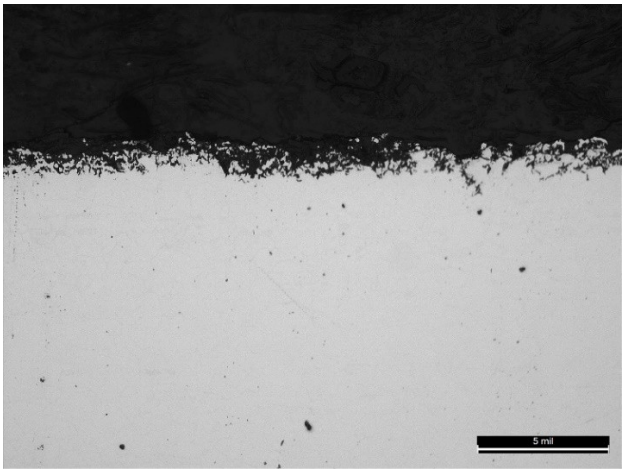

C3-4 200x

Figure 28. Results of immersion corrosion testing – 100 hours at 800°C.

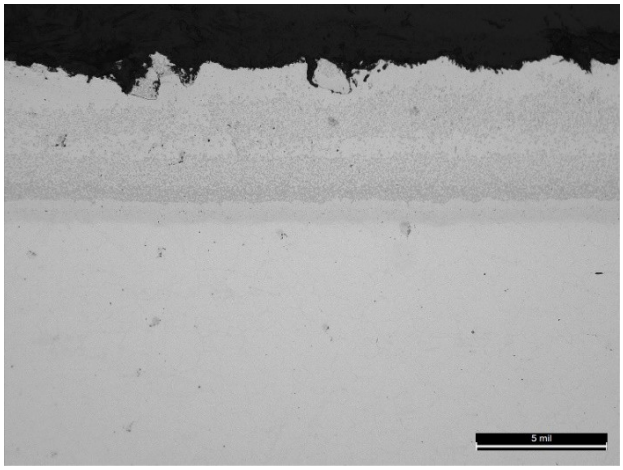

C1-1 200x

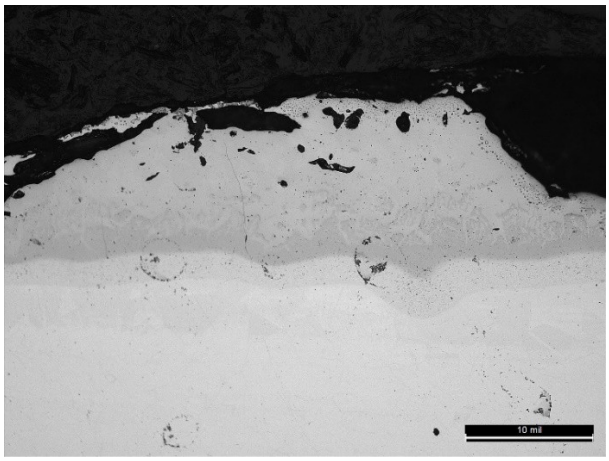

C2-1 100x

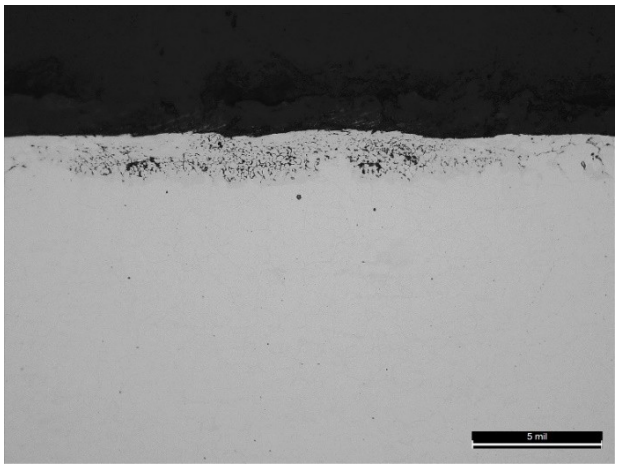

C3-1 200x

Figure 29. Results of immersion corrosion testing – 250 hours at 650°C.

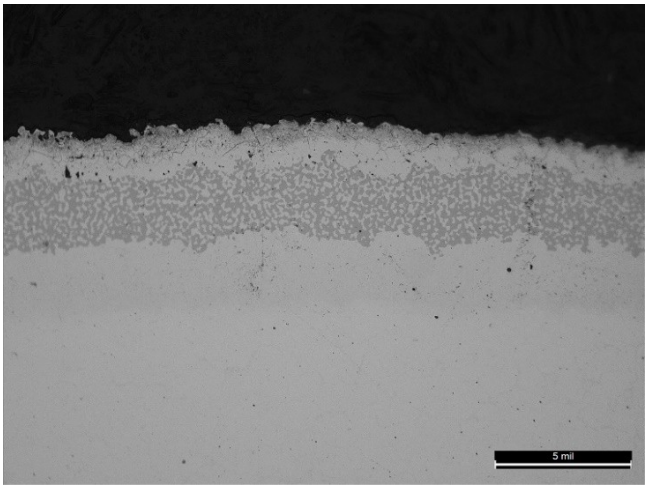

C1-2 200x

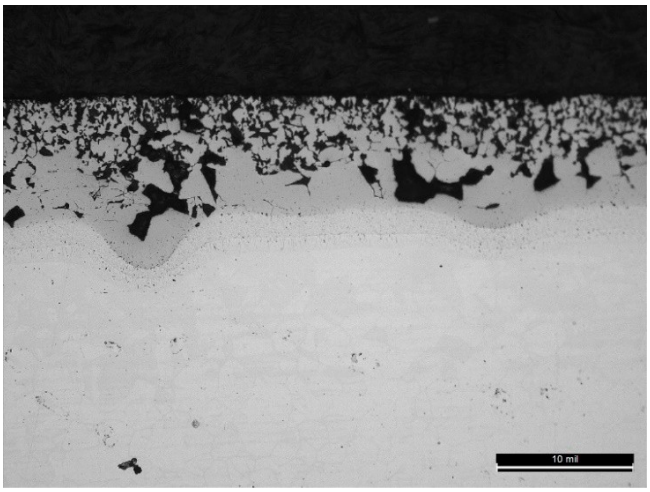

C2-2 100x

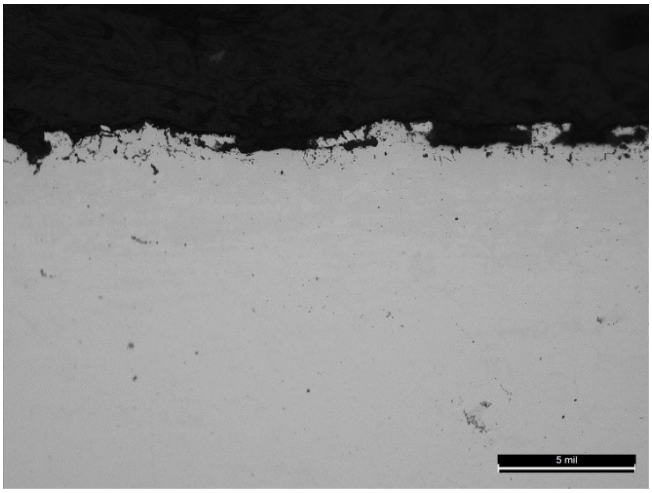

C3-2 200x

Figure 30. Results of immersion corrosion testing – 500 hours at 700°C.

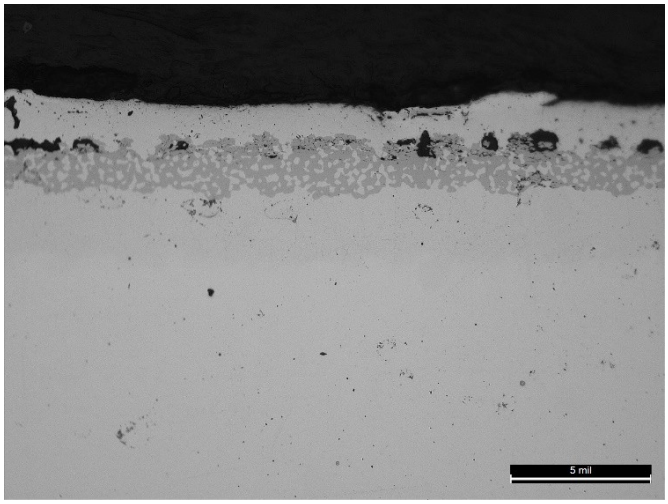

C1-3 200x

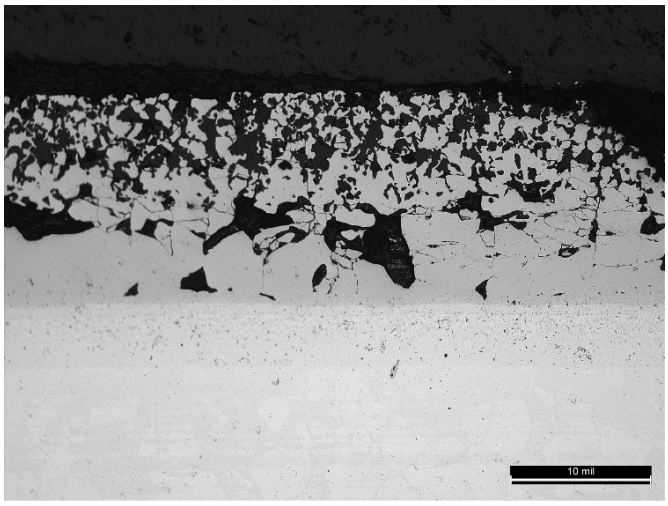

C2-3 100x

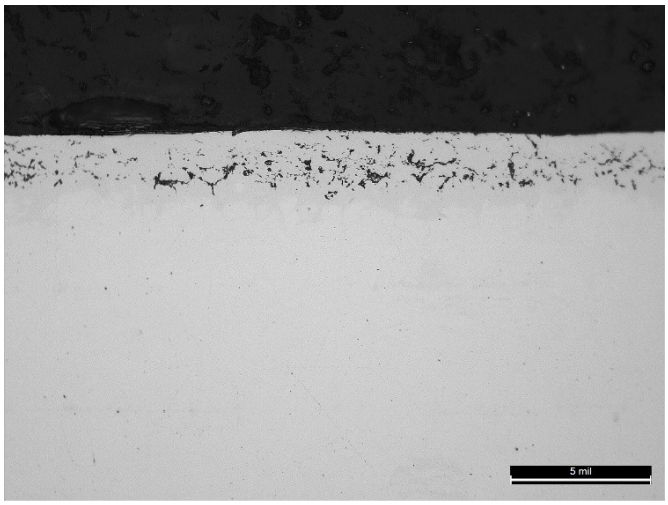

C3-3 200x

Figure 31. Results of immersion corrosion testing – 1000 hours at 750°C.

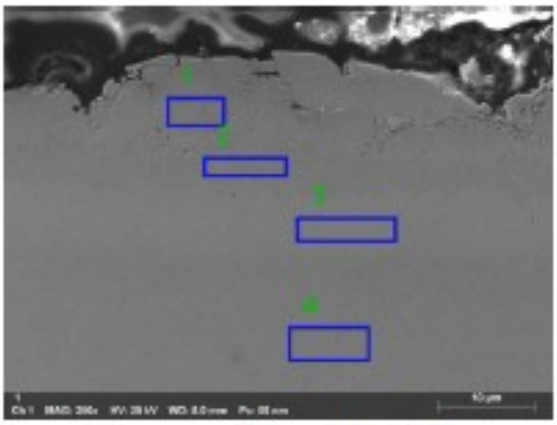

Name	Date	Time	HV [kV]	Mag	WD [mm]
1	9/24/2019	10:58:07 AM	20.0 keV	300x	8.0 mm

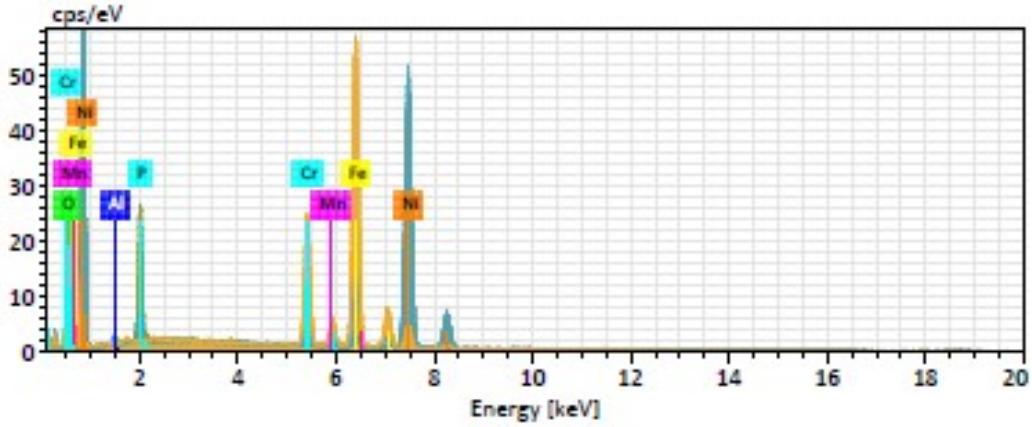

Normalized mass concentration [%]

Spectrum	O	Al	P	Cr	Mn	Fe	Ni
1	2.01	1.12	2.94		0.64	2.82	90.46
2	1.16		12.32				86.52
3				4.06		16.57	79.37
4				19.27	1.66	71.00	8.07
Mean	1.59	1.12	7.63	11.66	1.15	30.13	66.11
Sigma	0.60	0.00	6.63	10.75	0.72	36.05	38.96
SigmaMean	0.30	0.00	3.32	5.38	0.36	18.03	19.48

18G262
C1-2
700C - 500hr

Figure 32. EDS scan of post-exposure coupon C1-2 (nickel aluminide), tested at 700°C for 500 hours.

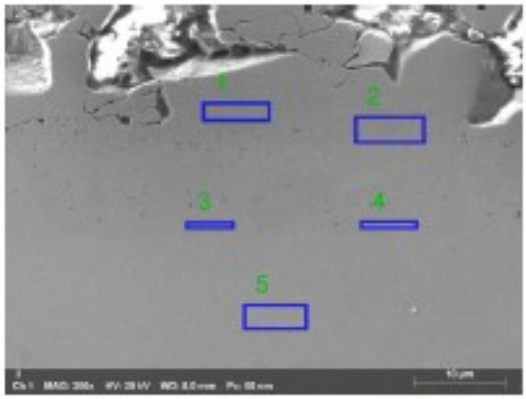

Name	Date	Time	HV [kV]	Mag	WD [mm]
3	9/24/2019	10:45:27 AM	20.0 keV	300x	8.0 mm

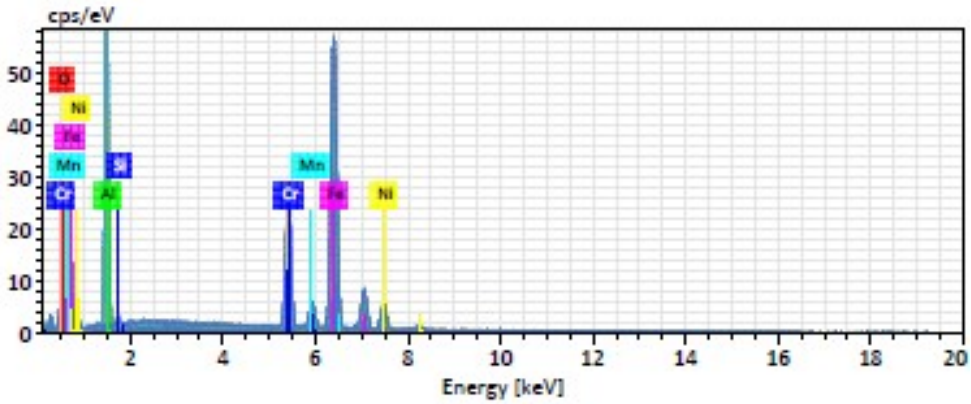

Normalized mass concentration [%]

Spectrum	O	Al	Si	Cr	Mn	Fe	Ni
1	0.31	28.27		10.70	1.13	53.34	6.26
2	0.44	25.27		10.41	0.88	51.76	11.23
3		3.26	0.55	20.65	1.69	67.78	6.06
4		2.76	0.59	20.84	1.64	68.86	5.31
5				19.62	1.70	70.40	8.27
Mean	0.37	14.89	0.57	16.44	1.41	62.43	7.43
Sigma	0.09	13.77	0.03	5.40	0.38	9.08	2.39
SigmaMean	0.04	6.16	0.01	2.41	0.17	4.06	1.07

18G262
C2-2
700C - 500hr

Figure 33. EDS scan of post-exposure coupon C2-2 (iron aluminide), tested at 700°C for 500 hours.

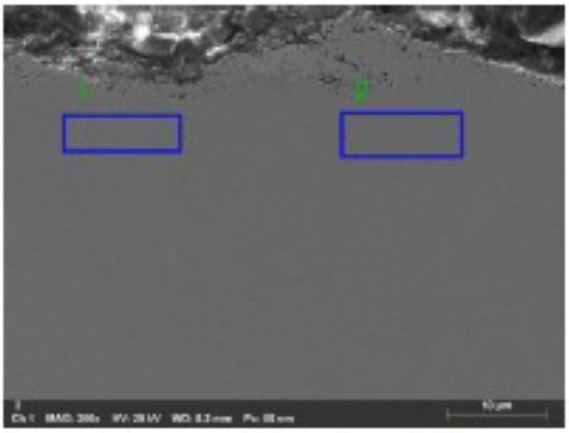

Name	Date	Time	HV [kV]	Mag	WD [mm]
2	9/24/2019	10:28:58 AM	20.0 keV	300x	8.2 mm

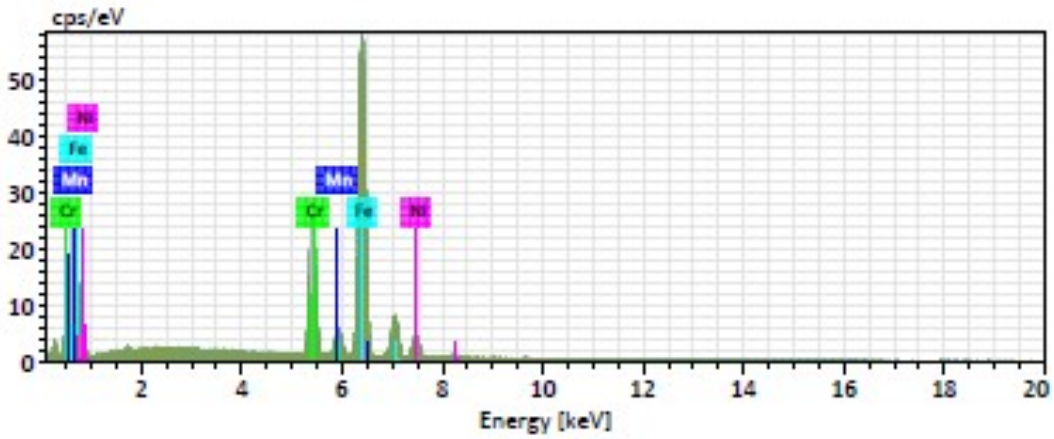

Normalized mass concentration [%]

Spectrum	Cr	Mn	Fe	Ni
1	19.49	1.67	70.82	8.01
2	19.71	1.59	70.71	7.98
Mean	19.60	1.63	70.77	8.00
Sigma	0.16	0.06	0.08	0.02
SigmaMean	0.11	0.04	0.06	0.02

18G262
C3-2
700C-500hr

Figure 34. EDS scan of post-exposure coupon C3-2 (bare), tested at 700°C for 500 hours.

APPENDIX

Applied Thermal Coatings
200 Compress Street
Chattanooga, TN 37405
Telephone: 423-267-0647
Fax: 423-267-0637
Email: jhenry@atc-tn.com

Action item	Ni Plated 1018 (Square)	Ni Plated T91 (Tube Section)	Ni Plated T91 (Square)	Baro 347H (Square) Coupon 8	NON Ni Plated 347H (Square) Coupon 7 FeAl	Ni Plated SS347H (Tube section)	Ni Plated SS347H (Square) Coupon 1 NiAl	Haynes 230 (Edm'ed hole in 0.5" dia disc)	Haynes 230 (1" dia x 1/8" or 1/4" thick disc)	Status
Samples Remaining	---	11	---	unlimited	unlimited	11	3	15	11	---
Total samples made	5	15	10	18	18	15	56	15*	15*	Completed
Pre-Aluminizing Metallography	1	1	1	1	---	1	1	---	1	Completed
Aluminizing Test Recipe B or BB	---	2	---	---	---	2	17	---	2	Completed
Aluminizing Test ATC Recipe	---	2	---	---	18	2	---	---	1	Completed
Post-Aluminizing Metallography (Mounts)	---	3	2	---	1	3	2	---	2	In process
Pre Corrosion Micro-Photos	---	10	8	---	1	19	8	2	3	Completed
Pre Corrosion EDS	1	---	1	---	---	---	1	---	---	Completed
Pre Corrosion Hardness Testing	---	---	---	---	---	1	---	---	---	Completed
Samples Sent to UA for Corrosion Tests	---	---	---	18	18	---	17	---	---	Completed
Post Corrosion Metallography	---	---	---	9	10	---	10	---	---	In process
Post Corrosion Micro-Photos	---	---	---	9	10	---	10	---	---	In process
Aluminizing Test Recipe D or DD		0	0			0	0	0	0	N/A
Aluminizing Test Recipe Y or YY		0	0			0	0	0	0	N/A

Applied Thermal Coatings
200 Compress Street
Chattanooga, TN 37405
Telephone: 423-267-0647
Fax: 423-267-0637
Email: jhenry@atc-tn.com

Appendix A

Applied Thermal Coatings
200 Compress Street
Chattanooga, TN 37405
Telephone: 423-267-0647
Fax: 423-267-0637
Email: jhenry@atc-tn.com

Research Report
May 31, 2018

Corrosion Studies on Intermetallic Coatings for Molten Salt Pump Impellers

SUBMITTED TO:
Mr. Jeff Henry
Principal
Investigator
DOE-SBIR Phase 1
project Applied Thermal
Coatings 200 Compress
Street
Chattanooga, TN. 37405

SUB-CONTRACT TO: THE UNIVERSITY OF ALABAMA
Dr. Ramana G.
Reddy Principal
Investigator
Professor of Metallurgical and Materials
Engineering Department of Metallurgical and
Materials Engineering The University of Alabama
Tuscaloosa, Alabama 35487-0202
Tel: (205) 348 4246
E-mail: rreddy@eng.ua.edu

ABSTRACT

Electrochemical evaluations were performed on alloy coupons in both the bare and the coated conditions, with the testing taking place in molten eutectic KCl-$MgCl_2$ solution at 650ºC, 700ºC, 750ºC, 800ºC using an open circuit potential followed by potentiodynamic polarization. Corrosion potentials and corrosion rates were determined using Tafel slopes. The results confirmed an increase in corrosion resistance for the alloys that had been coated either with nickel aluminide or iron aluminide when compared with bare TP347H material. In addition, the relationship between corrosion rate and temperature was obtained for all coupons tested.

Keywords: SS347, KCl-$MgCl_2$, coating, potentiodynamic polarization, Tafel

Experimental Study

Preparation of the $MgCl_2$-KCl salt

The eutectic mixture of $MgCl_2$-KCl (68 mol% KCl) was prepared using KCl and $MgCl_2$ obtained from VWR (99% purity). The salt was weighed in a proper ratio and mixed for 10 hours using a mixer mill. And the salt mixture was dried in the oven for 24 hours at 150°C in the vacuum atmosphere to avoid moisture absorption.

Preparation of alloy coupons

Coupons 1 and 2 represent coated material (either nickel aluminide for coupon 1 or iron aluminide for coupon 2), while coupon 3 represents bare material. The coupons were polished with 600, 800, 1200 grit SiC abrasive paper progressively to remove surface oxide. To investigate the effect of the oxidized surface on the corrosion rates, corrosion experiments on samples without polishing were also performed. All the samples were cleaned with deionized water and dried in air. The dimensions of the coupon samples are listed in Table 1.

Table 1 Dimensions and weight of samples in the experiment

Samples	Length (cm)	Width (cm)	Thickness (cm)	Diameter of hole (cm)	Weight (g)
Coupon 1	1.39	1.32	0.34	0.30	4.45
Coupon 2	1.46	1.30	0.34	0.30	4.01
Coupon 3	1.29	1.25	0.30	0.30	3.53
Coupon 1 (unpolished)	1.33	1.30	0.35	0.30	4.12
Coupon 2 (unpolished)	1.33	1.32	0.37	0.30	3.71
Coupon 3 (unpolished)	1.23	1.27	0.31	0.30	3.44

Corrosion test set-up

Corrosion experiments were performed at 650°C, 700°C, 750°C, 800°C under argon gas atmosphere. An alumina crucible was used to contain the $MgCl_2$-KCl salt. The platinum wire of 0.5mm diameter was used as the working electrode. Refractory

Applied Thermal Coatings
200 Compress Street
Chattanooga, TN 37405
Telephone: 423-267-0647
Fax: 423-267-0637
Email: jhenry@atc-tn.com

silica-based cement was used to stabilize the alumina tube on the Ni cover. Temperature of the salt was measured using type-K thermocouple. All experiments were conducted in argon gas atmosphere.

Electrochemical corrosion experiments

Prior to the polarization corrosion study, the open circuit potential (OCP) was performed by recording the change of potential vs. time. Once the potential was stabilized, the potentiodynamic polarization sweep (PPS) were performed. In the polarization experiments, a potential polarization of ±250 mV variation was observed with respect of OCP and scanning rate of 2mV/s was applied. Thus, the relationship of current density vs. potential was obtained.

Results and Discussion

The experimental potentiodynamic polarization sweep (PPS) plots for polished coupon 1, coupon 2 and coupon 3 at different temperatures are shown in Fig. A1, A2 and A3. The relative corrosion potential and OCP are presented in Table 2 and the corrosion rates are presented in Table 3.

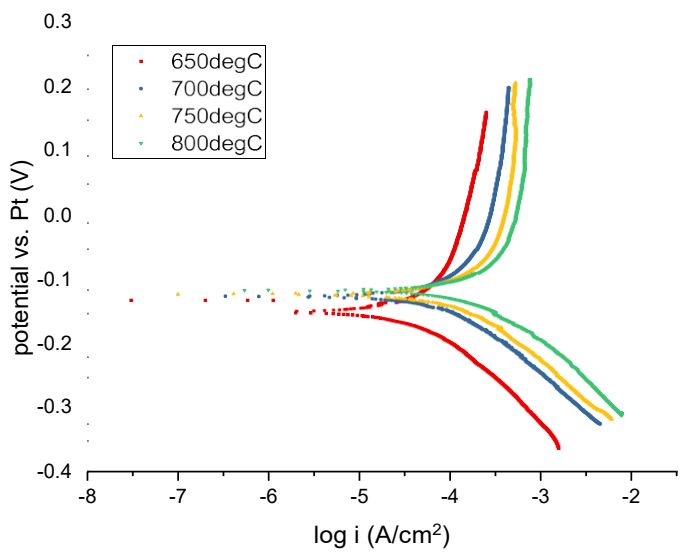

Figure A1. Tafel plots for coupon 1 (nickel aluminide) from PPS corrosion test in $MgCl_2$-KCl at different temperatures

Applied Thermal Coatings
200 Compress Street
Chattanooga, TN 37405
Telephone: 423-267-0647
Fax: 423-267-0637
Email: jhenry@atc-tn.com

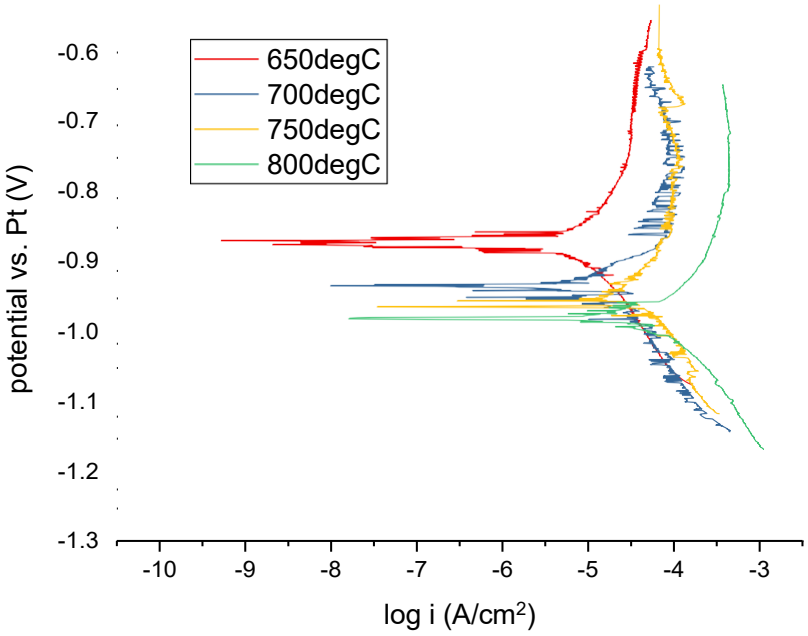

Figure A2. Tafel plots for coupon 2 (iron aluminide) from PPS corrosion test in $MgCl_2$-KCl at different temperatures

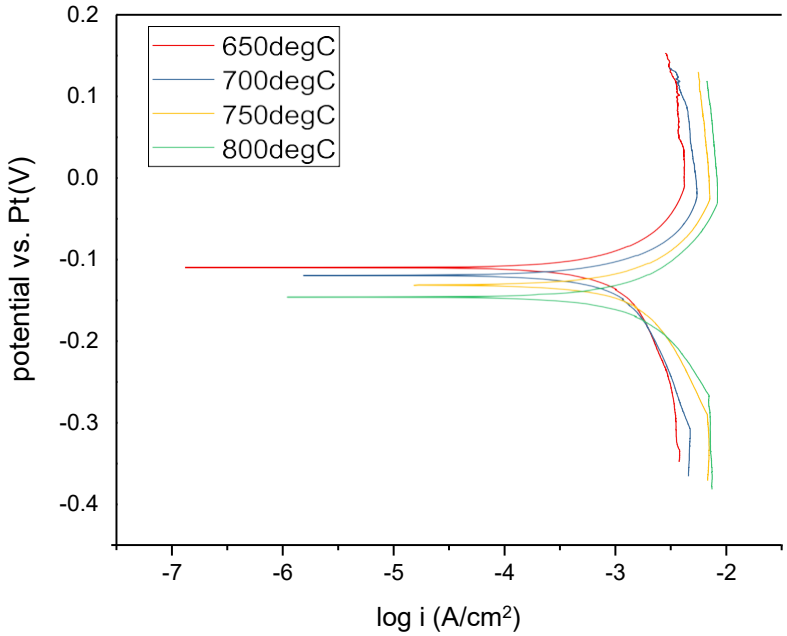

Figure A3. Tafel plots for coupon 3 (bare) from PPS corrosion test in $MgCl_2$-KCl at different temperatures

Applied Thermal Coatings
200 Compress Street
Chattanooga, TN 37405
Telephone: 423-267-0647
Fax: 423-267-0637
Email: jhenry@atc-tn.com

Table 2 OCP and corrosion potential of tested coupons in MgCl2-KCl at different temperatures

Samples	OCP (mV. vs pseudo-Pt)				Ecorr (mV. vs pseudo-Pt)			
Temperature	650°C	700°C	750°C	800°C	650°C	700°C	750°C	800°C
Coupon 1	-136±1	-108±1	-96±1	-90±1	-120	-100	-100	-90
Coupon 2	-835±50	-685±50	-677±70	-700±16	-860	-900	-930	-960
Coupon 3	-113±8	-118±30	-137±30	-143±3	-113	-130	-140	-160

Table 3 Corrosion rate of tested coupons in $MgCl_2$-KCl at different temperatures

Samples	Corrosion rate (A/cm^2)			
Temperature	650°C	700°C	750°C	800°C
Coupon 1	$10^{-4.5}$	$10^{-4.2}$	$10^{-4.0}$	$10^{-3.8}$
Coupon 2	$10^{-5.1}$	$10^{-4.9}$	$10^{-4.6}$	$10^{-4.4}$
Coupon 3	$10^{-3.1}$	$10^{-2.9}$	$10^{-2.7}$	$10^{-2.6}$

The Tafel plots show an active corrosion behavior and the increased temperature leads the decreased corrosion potential and OCP. In addition, the corrosion rates were increased as temperature increased and the relationship for all three coupons is shown in Figure A4, A5 and A6.

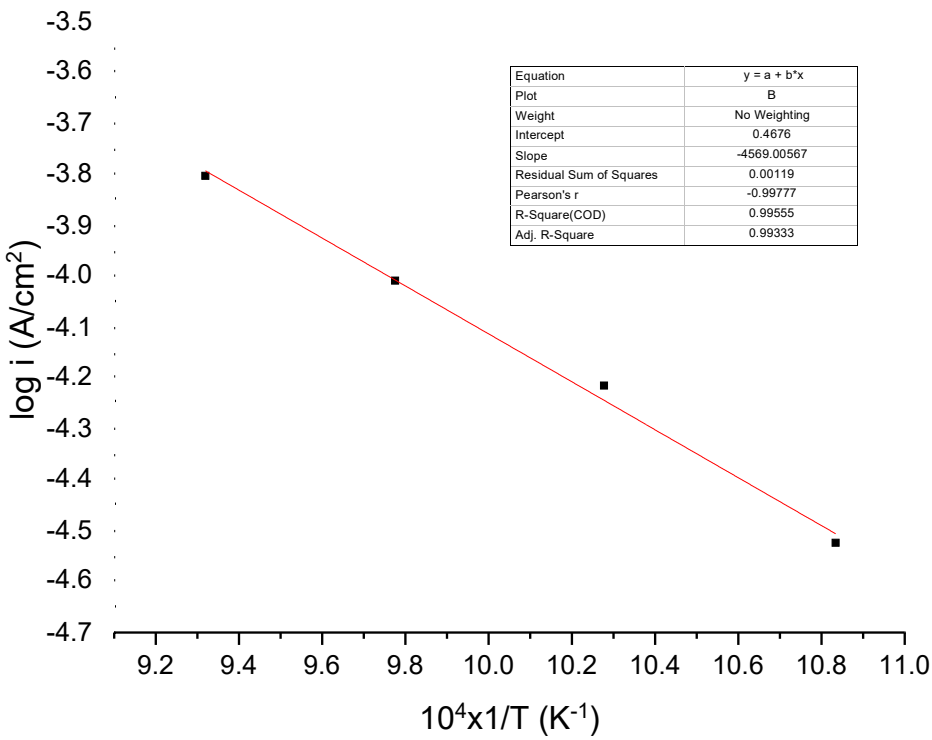

Figure A4. relationship between corrosion rates and temperatures of coupon 1 (nickel aluminide) in $MgCl_2$-KCl

Applied Thermal Coatings
200 Compress Street
Chattanooga, TN 37405
Telephone: 423-267-0647
Fax: 423-267-0637
Email: jhenry@atc-tn.com

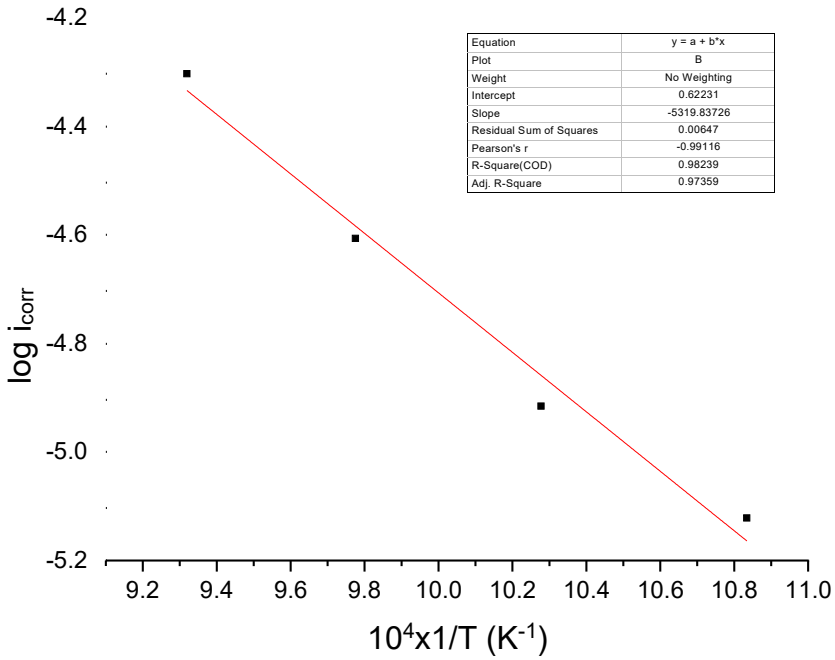

Figure A5. relationship between corrosion rates and temperatures of coupon 2 (iron aluminide) in $MgCl_2$-KCl

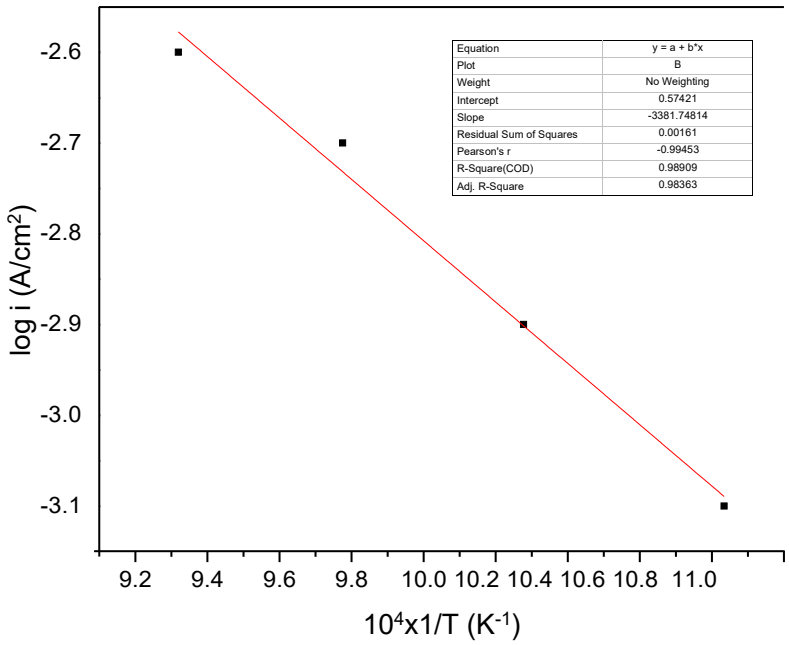

Figure A6. relationship between corrosion rates and temperatures of coupon 3 (bare) in $MgCl_2$-KCl

An Arrhenius type equation relationship between corrosion rates and temperatures was obtained and is presented in Table 4. The activation energy for corrosion was calculated and also presented in the Table 4.

Table 4 relationship between corrosion rates and temperatures of coupon 1, 2, 3 in $MgCl_2$-KCl

Samples	Relation between i_{corr} and T	Activation energy (kJ)
Coupon 1	Log i=-4569.01/T+0.47	37.99
Coupon 2	Log i=-5319.84/T+0.62	44.23
Coupon 3	Log i=-3381.75/T+0.57	28.12

To investigate effect of pre-test surface preparation on the corrosion rate, coupon 1 and 2 were tested in the as-received condition by linear polarization at different temperatures, and coupon 3 was tested in the as-received condition by PPS. The results are shown in Figure A7, A8 and A9, respectively.

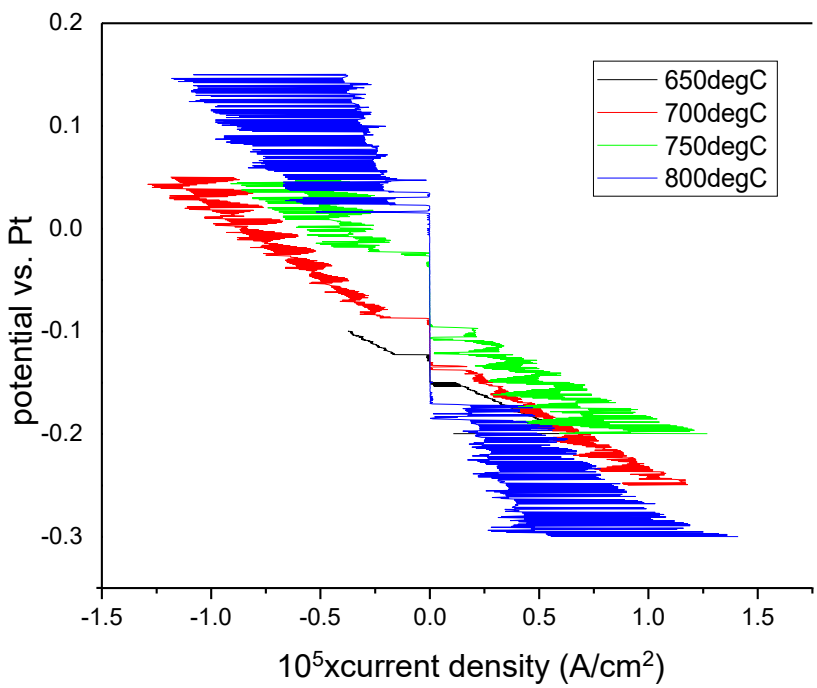

Figure A7. Linear polarization of coupon 1 (nickel aluminide) without polishing at different temperatures in $MgCl_2$-KCl

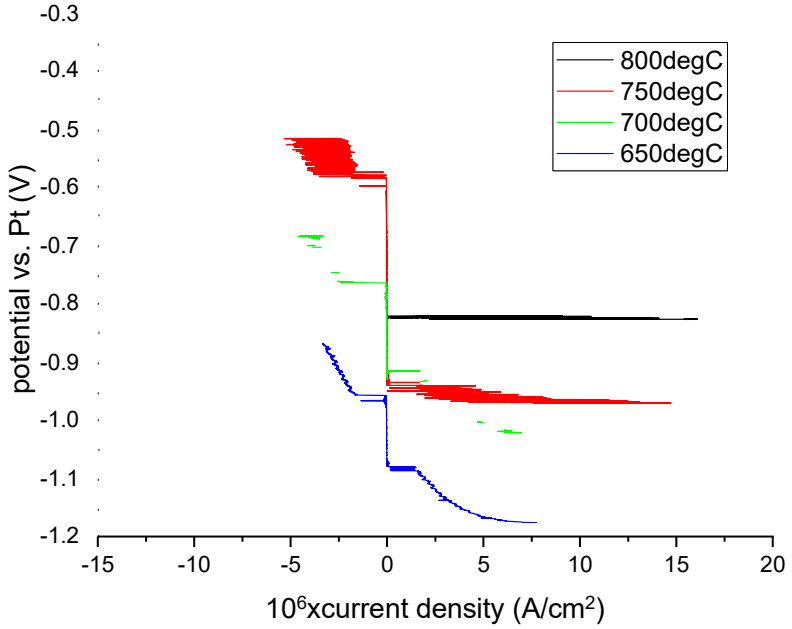

Figure A8. Linear polarization of coupon 2 (iron aluminide) without polishing at different temperatures in $MgCl_2$-KCl

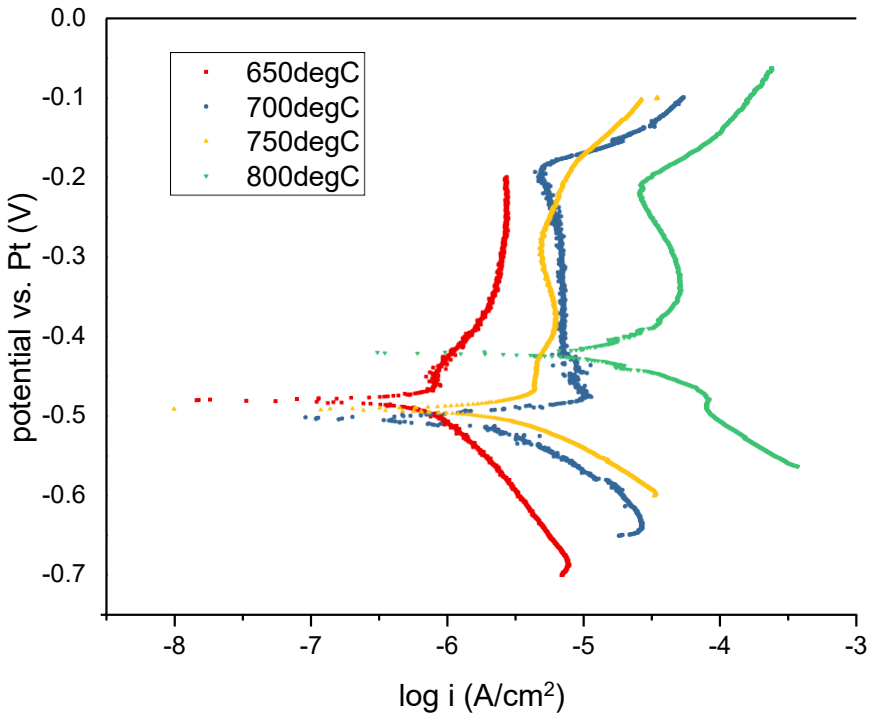

Figure A9. Tafel plots for coupon 3 (bare) without polishing at different temperatures in $MgCl_2$-KCl

Applied Thermal Coatings
200 Compress Street
Chattanooga, TN 37405
Telephone: 423-267-0647
Fax: 423-267-0637
Email: jhenry@atc-tn.com

As shown in Figure A7 and A8, for coupons 1 and coupon 2, during some specific potential range, the current density is zero. This can be due to the presence of an intact oxidized layer on the surface of the coupon in that potential range, which inhibited the diffusion of elements and the transferring of electrons. For coupon 3, a passivation zone was observed, as shown in Figure 9.

The passivation zone was increased as the temperature decreased. In comparing these results with those obtained from the polished coupon 3, the corrosion rates are smaller as the oxidized surface increases the corrosion resistance. The corrosion potentials and corrosion rates of unpolished coupon 3 are presented in Table 5.

Table 5 Corrosion potentials and corrosion rates of unpolished coupon 3 at different temperatures

Temperature (°C)	E_{corr} (V vs. pseudo-Pt)	i_{corr} (A/cm^2)
650	-0.48	$10^{-6.2}$
700	-0.51	$10^{-5.7}$
750	-0.51	$10^{-5.5}$
800	-0.40	$10^{-4.7}$

Conclusions

1) The coatings increase the corrosion resistance when compared to the bare alloy (coupon 3), with coupon 2 (iron aluminide) showing higher corrosion resistance and greater stability in $MgCl_2$-KCl salt
2) The relationship between the corrosion rate and temperatures follows the trend reflected in the Arrhenius equation, and the activation energy of each sample was calculated.
3) The unpolished coupons showed a higher level of stability in the $MgCl_2$-KCl salt due to the presence of an oxide layer.

Applied Thermal Coatings
200 Compress Street
Chattanooga, TN 37405
Telephone: 423-267-0647
Fax: 423-267-0637
Email: jhenry@atc-tn.com

Appendix B

Applied Thermal Coatings
200 Compress Street
Chattanooga, TN 37405
Telephone: 423-267-0647
Fax: 423-267-0637
Email: jhenry@atc-tn.com

Report 2: Summary of experiments

ABSTRACT

Electrochemical evaluations have been completed on coupons 1, 2 and 3 in the molten eutectic KCl-$MgCl_2$ at 650°C, 700°C, 750°C, 800°C using an open circuit potential followed by a potentiodynamic polarization. Coupon 1 represented a substrate material coated with nickel aluminide, coupon represented a substrate material coated with iron aluminide and coupon 3 represented the bare substrate material (Tp347H). From these evaluations, corrosion potential and corrosion rates were determined by using Tafel slopes and Faraday's law. Weight loss was also determined and the results were comparable to the corrosion rate obtained from Tafel experiment. In addition, the relation between corrosion rate and temperature was predicted in this study by using Arrhenius equation. The results indicated that the coatings increase the corrosion resistance of the coupon and protect it from further corrosion.

Following the electrochemical evaluations, long-term dipping experiments were performed at 700°C, 750°C, 800°C for 100 hours in molten $MgCl_2$-KCl salt. The results of the long-term dipping corrosion tests were not consistent with the results of the electrochemical evaluations. Corrosion of coupon 2 (iron aluminide) was severe and the coating was loosely bonded after corrosion.

Introduction

Experimental

Preparation of $MgCl_2$-KCl salt

The eutectic mixture of $MgCl_2$-KCl (68 mol% KCl) was prepared using KCl and $MgCl_2$ from VWR (99% purity). The single salt was weighed in a proper ratio and mixed for 10 hours with a jar mixing machine. The mixture then was dried in the oven for 24 hours at 150°C in the vacuum atmosphere to avoid moisture absorption.

Preparation of alloys

Coupon 1 and 2 are coated with nickel aluminide (coupon 1) and iron aluminide (coupon 2), which are stable in $MgCl_2$-KCl molten salt; coupon 3 is bare alloy. The coupons were progressively ground with 600, 800, 1200 grit SiC abrasive papers progressively to remove surface oxide. To investigate the effect of the oxidized surface on the corrosion, coupons that had not been ground also were tested. All the coupons were cleaned with deionized water and dried with air. The dimensions of coupons are listed in Table 1.

Table 1 Dimensions and weight of coupons in the polarization experiment

Coupons	Length (cm)	Width (cm)	Thickness (cm)	Diameter of hole (cm)	Weight (g)
Coupon 1 (C1-1)	1.39	1.32	0.34	0.30	4.45
Coupon 1 (C1-2)	1.33	1.31	0.35	0.30	4.23
Coupon 2 (C2-1)	1.46	1.30	0.34	0.30	4.01
Coupon 2 (C2-2)	1.33	1.34	0.37	0.30	3.74

Coupon 3 (C3-1)	1.29	1.25	0.30	0.30	3.53
Coupon 3 (C3-2)	1.31	1.26	0.31	0.30	3.62
Coupon 1 (C1-3) (unpolished)	1.33	1.30	0.35	0.30	4.12
Coupon 2 (C2-3) (unpolished)	1.33	1.32	0.37	0.30	3.71
Coupon 3 (C3-3) (unpolished)	1.23	1.27	0.31	0.30	3.44

Dimensions of long-term tested coupons are listed in Table 2.

Table 2 Dimensions and weight of coupons in the long-term dipping experiment

800°C	L(mm)	W(mm)	T(mm)	weight (g)
C1-4	13.44	13.04	3.42	4.158
C2-4	13.20	13.41	3.43	3.724
C3-4	13.32	12.54	3.08	3.853
750°C				
C1-5	13.08	12.14	3.38	3.761
C2-5	13.08	13.20	3.47	3.727
C3-5	12.55	12.50	3.04	3.608
700°C				
C1-6	13.42	12.96	3.40	4.08
C2-6	13.53	13.10	3.46	3.795
C3-6	12.77	12.50	3.02	3.611

Corrosion test set-up

Corrosion experiments were performed at 650°C, 700°C, 750°C, 800°C under argon gas atmosphere. The crucible was made of Al_2O_3 which is proved to be stable in the $MgCl_2$-KCl salt. The working electrode was tested coupons which is tied by a 0.5 mm platinum wire. Reference electrode and counter electrode were made from the same Pt wire (0.5 mm). The electrodes were passed through the holes on the Ni cover and protected by alumina tube. Refractory silica-based cement was used to stabilize the alumina tube on the Ni cover. Temperature was calibrated prior to the experiment with two type-K thermocouples. Argon UHP was used as the cover gas.

Electrochemical corrosion experiments

Prior to the polarization corrosion study, the open circuit potential (OCP) was performed by recording the change of potential vs. time. Once the potential was stable and the system reached equilibrium, the potentiodynamic polarization sweep (PPS) were started. In the polarization experiments, a potential polarization of ±250mV with respect of OCP and scanning rate of 2mV/s was applied. Thus, the relationship of current density vs. potential was obtained.

Long-term dipping corrosion experiments

The furnace used in this experiment was vertical tube furnace. Before the experiment, temperatures at different height were calibrated. Once the relationship between temperature and height was obtained, the Al_2O_3 crucibles with coupons inside were stacked together and put in the Al_2O_3 tube. The furnace was evacuated using a vacuum pump and flushed with UHP Argon gas at least two times to eliminate the possible air or moisture inside the system. After that, the furnace was heated and kept at 673 K for 1 hour to remove any moisture attached to the salt or hydrated water inside the salt. The furnace was again evacuated and flushed with Argon gas and later kept at a consistent pressure which was a little higher than the atmospheric pressure. Eventually, the furnace was heated to 1073 K and kept for 100 hours.

Results

Weight loss, corrosion rates and corrosion potentials of different coupons are listed in Table 3 and Table 4.

Table 3 Corrosion rate of C1, C2 and C3 in $MgCl_2$-KCl at different temperatures for 100 hours

800degC	weight (g)	after corrosion weight (g)	area (cm^2)	corrosion rate ($mg/cm^2/day$)	corrosion rate (A/cm^2)
C1-4	4.158	4.103	5.32	2.483	$10^{-3.79}$
C2-4	3.724	3.384	5.37	15.208	$10^{-3.01}$
C3-4	3.853	3.52	4.93	16.199	$10^{-2.98}$
750degC					
C1-5	3.761	3.73	4.88	1.524	$10^{-4.01}$
C2-5	3.727	3.418	5.28	14.054	$10^{-3.04}$
C3-5	3.608	3.372	4.66	12.153	$10^{-3.10}$
700degC					
C1-6	4.08	4.056	5.27	1.093	$10^{-4.15}$
C2-6	3.795	3.513	5.39	12.562	$10^{-3.09}$
C3-6	3.611	3.44	4.72	8.697	$10^{-3.25}$

Calculation of corrosion rate conversion from weight loss to current density was carried out using the equation (1).

$$1(gg)(ccmm)^{-2}(ddddyy)^{-1} = 1.12\,^{nn}\text{?}_{MM}\,(AA)(ccmm^{-2}) \qquad (1)$$

where “n” is transferred electrons, “d” is density of the alloys and “M” is atomic weight of the dissolved element. In the present work, “n” was assumed to be 3 and “M” was assumed to be atomic weight of Cr for the calculations.

Table 4 Corrosion rates of C1, C2 and C3 in $MgCl_2$-KCl at different temperatures (Tafel)

Coupons	Corrosion rate (A/cm^2)			
Temperature	650°C	700°C	750°C	800°C
C1 (average)	$10^{-4.47\pm0.03}$	$10^{-4.20\pm0.01}$	$10^{-3.97\pm0.03}$	$10^{-3.75\pm0.05}$
C2 (average)	$10^{-5.20\pm0.10}$	$10^{-4.95\pm0.05}$	$10^{-4.65\pm0.05}$	$10^{-4.45\pm0.05}$

Applied Thermal Coatings
200 Compress Street
Chattanooga, TN 37405
Telephone: 423-267-0647
Fax: 423-267-0637
Email: jhenry@atc-tn.com

C3 (average)	$10^{-3.15\pm0.05}$	$10^{-2.95\pm0.05}$	$10^{-2.75\pm0.05}$	$10^{-2.63\pm0.02}$

Table 5 Corrosion potentials of C1, C2 and C3 in $MgCl_2$-KCl at different temperatures (Tafel)

Coupons	Corrosion potential (V vs. pseudo-Pt)			
Temperature	650°C	700°C	750°C	800°C
C1-1	-120	-100	-100	-90
C1-2	-680	-630	-590	-530
C2 (average)	-840±20	-900±5	-930±5	-950±10
C3 (average)	-560±40	-523±12	-487±8	-442±3

The corrosion rate for C1 (nickel aluminide) as predicted by the Tafel calculations and as measured in the long-term experiment were in reasonably good agreement. However, for C2 (iron aluminide) the superior corrosion resistance predicted by the Tafel experiment was not reproduced in the long-term experiment, where the C2 coupon showed a high weight loss. The discrepancy appears to be related to the fact that the coating was not coherent after corrosion. Coating was cleaned with water even it was not dissolved into the salt. The C3 (bare) coupon showed a higher corrosion rate, which was consistent both in Tafel and in long-term experiment. There was a little difference between the corrosion rates of C3 in both experiments.

Applied Thermal Coatings
200 Compress Street
Chattanooga, TN 37405
Telephone: 423-267-0647
Fax: 423-267-0637
Email: jhenry@atc-tn.com

Appendix C

Applied Thermal Coatings
200 Compress Street
Chattanooga, TN 37405
Telephone: 423-267-0647
Fax: 423-267-0637
Email: jhenry@atc-tn.com

Research Report

Corrosion Studies on Intermetallic Coatings for Molten Salt Pump Impellers

SUBMITTED TO:
Mr. Jeff Henry
Principal
Investigator
DOE-SBIR Phase 1
project Applied Thermal
Coatings 200 Compress
Street
Chattanooga, TN. 37405

SUB-CONTRACT TO: THE UNIVERSITY OF ALABAMA
Dr. Ramana G.
Reddy Principal
Investigator
Professor of Metallurgical and Materials
Engineering Department of Metallurgical and
Materials Engineering The University of Alabama
Tuscaloosa, Alabama 35487-0202
Tel: (205) 348 4246
E-mail: rreddy@eng.ua.edu

March 25, 2019

ABSTRACT

The long-term dipping corrosion experiments were performed at different temperatures for each of the different coupons in molten $MgCl_2$-KCl salt. The corrosion rates were calculated in terms of weight loss. Coupons 1 (nickel aluminide) and 2 (iron aluminide) showed good corrosion resistances in the molten salt and the coatings were still intact on the surface after corrosion experiment. The compositions of the surfaces were further confirmed by SEM/EDS. Therefore, the tests confirm that the presence of the coatings increases the corrosion resistance of the material and acts to protect it from further corrosion.

Introduction

Experiment

Preparation of $MgCl_2$-KCl salt

The eutectic mixture of $MgCl_2$-KCl (68 mol% KCl) was prepared using KCl and $MgCl_2$ from VWR (99% purity). The single salt was weighed in a proper ratio and mixed for 10 hours with a jar mixing machine. The mixture then was dried in the oven for 24 hours at 150°C in the vacuum atmosphere to avoid moisture absorption.

Preparation of alloys

Coupons 1 and 2 are coated with either nickel aluminide (coupon 1) or iron aluminide (coupon 2), which are stable in $MgCl_2$-KCl molten salt; coupon 3 is bare TP347H material. All the samples were cleaned with deionized water and dried with air. The dimensions of samples are listed in Table 1 and Table 2.

Table 1. Dimensions and weight of samples in the long-term dipping experiment

Samples	Length (cm)	Width (cm)	Thickness (cm)	Diameter of hole (cm)	Weight (g)
650°C (250 hours)					
Coupon 1 (C1-1)	1.35	1.32	0.34	0.30	4.191
Coupon 2 (C2-1)	1.29	1.34	0.36	0.30	4.189
Coupon 3 (C3-1)	1.37	1.26	0.30	0.30	4.133
700°C (500 hours)					
Coupon 1 (C1-2)	1.35	1.32	0.34	0.30	4.208
Coupon 2 (C2-2)	1.28	1.31	0.35	0.30	3.598
Coupon 3 (C3-2)	1.36	1.27	0.30	0.30	4.140
750°C (1000 hours)					
Coupon 1 (C1-3)	1.35	1.30	0.34	0.30	4.180
Coupon 2 (C2-3)	1.42	1.33	0.35	0.30	4.240
Coupon 3 (C3-3)	1.37	1.28	0.30	0.30	4.283

Applied Thermal Coatings
200 Compress Street
Chattanooga, TN 37405
Telephone: 423-267-0647
Fax: 423-267-0637
Email: jhenry@atc-tn.com

Table 2. Dimensions and weight of samples in the long-term dipping experiment

	L(mm)	W(mm)	T(mm)	weight (g)
800°C				
C1-4	13.44	13.04	3.42	4.158
C2-4	13.20	13.41	3.43	3.724
C3-4	13.32	12.54	3.08	3.853
750 ^{o}C				
C1-5	13.08	12.14	3.38	3.761
C2-5	13.08	13.20	3.47	3.727
C3-5	12.55	12.50	3.04	3.608
700 ^{o}C				
C1-6	13.42	12.96	3.40	4.08
C2-6	13.53	13.10	3.46	3.795
C3-6	12.77	12.50	3.02	3.611

Corrosion test set-up

Corrosion experiments were performed at different temperatures (650, 700, 750, and 800°C) under an argon gas atmosphere for periods of 100h, 250h, 500h, and 1000h. The crucible was made of Al_2O_3 which has been demonstrated to be stable in the $MgCl_2$-KCl salt. Temperature was calibrated prior to the experiment with two type-K thermocouples. Argon UHP was used as the cover gas.

The furnace used in this experiment was a vertical tube furnace. Before the experiments were initiated, temperatures at different heights in the furnace were calibrated. Once the relationship between temperature and furnace height was established, the Al_2O_3 crucibles with the samples inside were stacked together and put in the Al_2O_3 tube. The furnace was evacuated using a vacuum pump and flushed with UHP Argon gas at least two times to eliminate the possible air or moisture inside the system. After that, the furnace was heated and kept at 673 K for 1 hour to remove any moisture attached to the salt or hydrated water inside the salt. The furnace was again evacuated and flushed with Argon gas and later kept at a consistent pressure which was a little higher than the atmospheric pressure. Eventually, the furnace was heated to the specified temperature.

Results and discussion

Weight loss of different coupons corrosion for a longer time are listed in Table 3.

Applied Thermal Coatings
200 Compress Street
Chattanooga, TN 37405
Telephone: 423-267-0647
Fax: 423-267-0637
Email: jhenry@atc-tn.com

Table 3. Corrosion rate of C1, C2 and C3 in $MgCl_2$-KCl at different temperatures

	weight (g)	after corrosion weight (g)	area (cm^2)	Weight loss (g)	corrosion rate ($mg/cm^2/day$)
650°C (250h)					
C1-1	4.191	4.145	5.24	0.046	0.843
C2-1	4.189	3.602	5.16	0.587	10.912
C3-1	4.133	3.746	4.91	0.388	7.594
700°C (500h)					
C1-2	4.208	4.105	5.26	0.103	0.941
C2-2	3.598	3.218	5.03	0.38	3.626
C3-2	4.140	3.612	4.89	0.528	5.184
750°C (1000h)					
C1-3	4.180	4.05	5.21	0.13	0.599
C2-3	4.240	3.754	5.58	0.486	2.091
C3-3	4.283	3.664	4.90	0.619	3.031

The weight loss and corrosion rate of different coupons are also shown in Figure 1 and2.

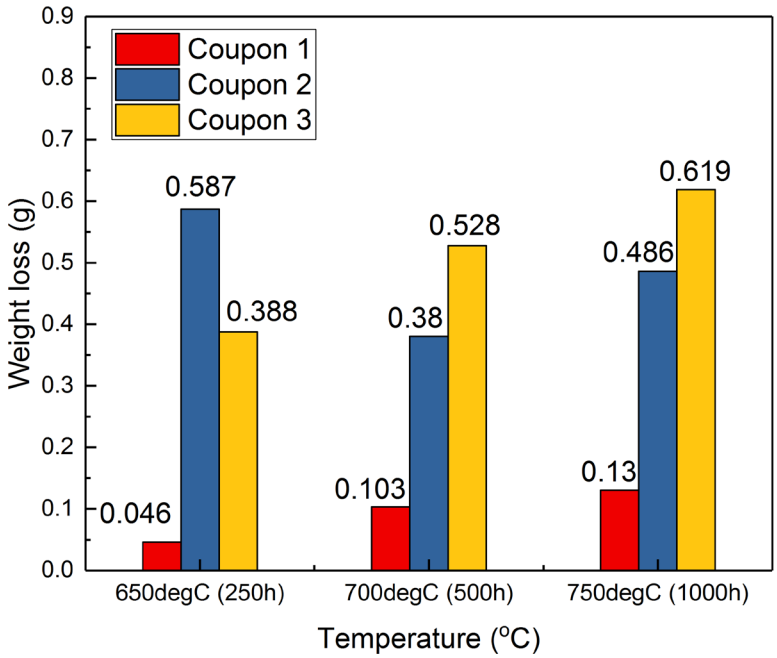

Figure C1. Weight loss of different alloys at different temperatures.

Applied Thermal Coatings
200 Compress Street
Chattanooga, TN 37405
Telephone: 423-267-0647
Fax: 423-267-0637
Email: jhenry@atc-tn.com

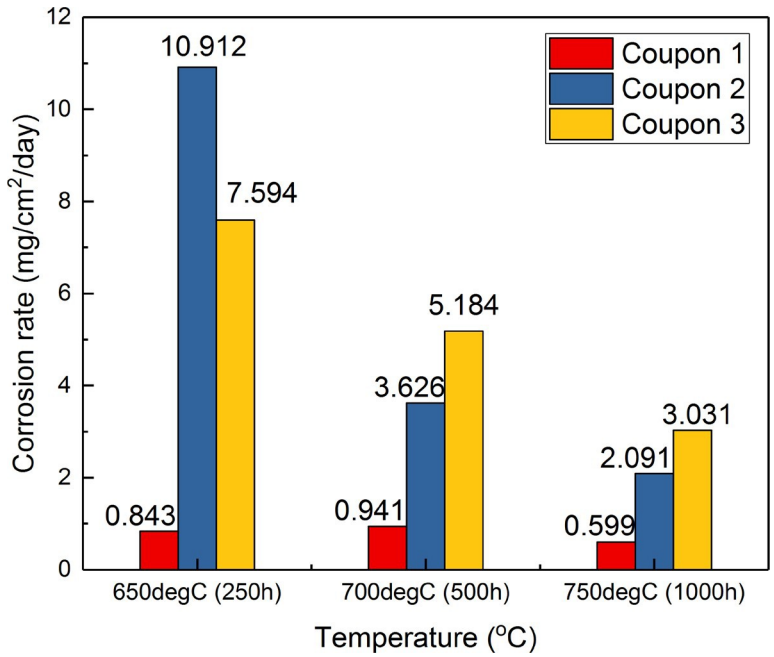

Figure C2. Corrosion rate of different alloys at different temperatures.

As shown in Figures C1 and C2, coupon 1 consistently exhibited the lowest corrosion rate among the three conditions tested. This would indicate, of course, that the nickel aluminide has the best corrosion resistance in the $MgCl_2$-KCl molten salt of the three material options tested. In addition, weight loss of all the samples was shown to increase with increasing temperature and time, except for the coupon 2 at 650°C. Because a portion of the coating on coupon 2 (650°C) was broken during the cleaning process, the weight loss of this sample is larger than the others. The coating and coupon 2 at 650°C are shown in Figure C3.

Applied Thermal Coatings
200 Compress Street
Chattanooga, TN 37405
Telephone: 423-267-0647
Fax: 423-267-0637
Email: jhenry@atc-tn.com

Figure C3. Coating of coupon 2 (650°C) is broken at the edge after corrosion.

Applied Thermal Coatings
200 Compress Street
Chattanooga, TN 37405
Telephone: 423-267-0647
Fax: 423-267-0637
Email: jhenry@atc-tn.com

Moreover, the corrosion rate was seen to decrease as the temperature and time increased for coupons 2 and coupon 3. The reason for this is that there is saturation of the elements dissolved into the salt, so that the driving force for corrosion is reduced when large number of elements are depleted from the alloy. Therefore, the corrosion rate is lower for the longer time experiments.

As reported previously, the 100-hour corrosion experiments were also performed on these three alloys, and the weight loss of sample are listed in Table 4.

Table 4. Corrosion rate of C1, C2 and C3 in $MgCl_2$-KCl at different temperatures for 100 hours

	weight (g)	after corrosion weight (g)	area (cm^2)	Weight loss (g)	corrosion rate ($mg/cm^2/day$)
800^oC (100h)					
C1-4	4.158	4.103	5.32	0.055	2.483
C2-4	3.724	3.384	5.37	0.34	15.208
C3-4	3.853	3.52	4.93	0.333	16.199
750^oC (100h)					
C1-5	3.761	3.73	4.88	0.031	1.524
C2-5	3.727	3.418	5.28	0.309	14.054
C3-5	3.608	3.372	4.66	0.236	12.153
700^oC (100h)					
C1-6	4.08	4.056	5.27	0.024	1.093
C2-6	3.795	3.513	5.39	0.282	12.562
C3-6	3.611	3.44	4.72	0.171	8.697

To have a good understanding of the corrosion of these alloys, the result is compared with the longer-term experiments (250h, 500h, and 1000h). And the result is shown in Figure C4.

Applied Thermal Coatings
200 Compress Street
Chattanooga, TN 37405
Telephone: 423-267-0647
Fax: 423-267-0637
Email: jhenry@atc-tn.com

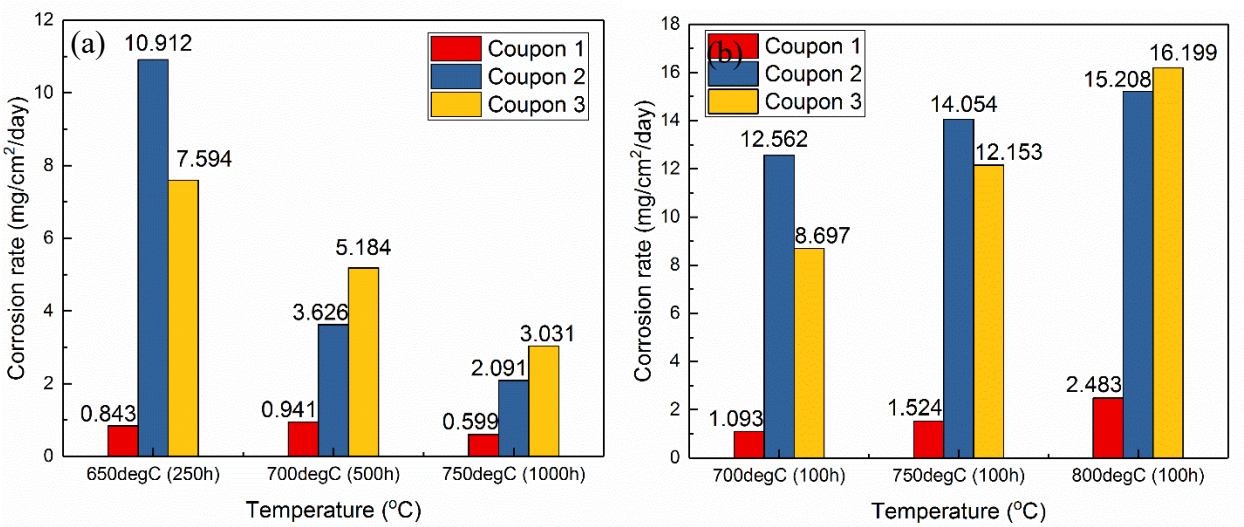

Figure C4. Corrosion rate of different alloys at different temperature ((a)-this study for longer time at 650, 700, and 750°C and (b)-last study for 100-hour experiment at 700, 750, and 800°C)

Applied Thermal Coatings
200 Compress Street
Chattanooga, TN 37405
Telephone: 423-267-0647
Fax: 423-267-0637
Email: jhenry@atc-tn.com

As shown in Figure 4, even where the time range is different, the corrosion rate of coupon 1 is comparable in both experiments at 700ºC. For the other two coupons, the longer time causes the lower corrosion rate.

During the 100-hour dipping experiment, the weight loss of coupon 2 (iron aluminide) was found to be larger than that of coupon 3 (bare). This is believed to be the case because the coating of coupon 2 is incoherent after corrosion and it is flushed by the water during the cleaning process. Some of the coating might be corroded by the hydrated water in the salt and the un-corroded coating is not coherent to the matrix material. The hydrated water is from $MgCl_2$ and $MgCl_2$ salt is easy to absorb the H_2O in the air and forms as $MgCl_2*4H_2O$. The XRD of impure $MgCl_2$ is shown in Figure C5.

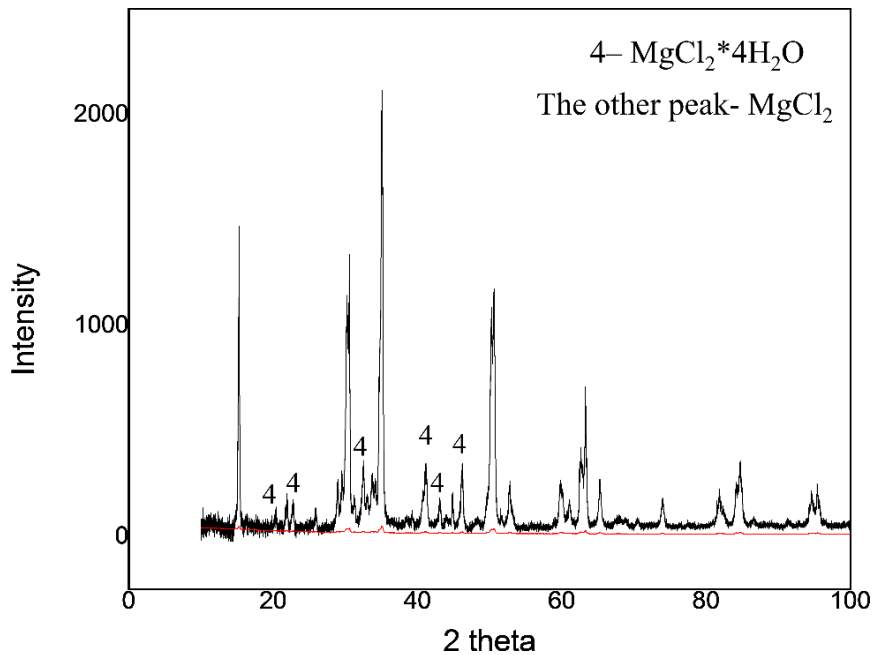

Figure C5. XRD of impure $MgCl_2$ salt before corrosion.

The hydrated water will remain in the salt even at the high temperature, and $MgCl_2*4H_2O$ will finally form as Mg(OH)Cl. The reaction is shown in equation (1)

$$MgCl_2 * 4HH_2OO \xrightarrow{\text{above } 230^{o}CC} Mg(OO\text{H})CCCC + HHCCCC(g) + 3HH_2OO(g) \qquad \Delta GG \leq 0 \qquad (1)$$

The remaining Mg(OH)Cl salt will easily react with Fe at higher temperature and the reaction is shown in equation (2).

$$2MMg(OOHH)CCCC + Fe \xrightarrow{800^{o}CC} FFeCCCC_2 + HH_2(g) + 2MMgOO \qquad \Delta GG = -64kkj/mmol \qquad (2)$$

Therefore, the coating Fe-Al alloy on the coupon 2 will be corroded easily by taking the reaction shown in equation (2). Thus, even there is some Fe-Al alloy not corroded, the coating is not coherent to the matrix material.

Applied Thermal Coatings
200 Compress Street
Chattanooga, TN 37405
Telephone: 423-267-0647
Fax: 423-267-0637
Email: jhenry@atc-tn.com

However, the hydrated water was controlled in this study (longer-time corrosion experiment). The coating remained intact on the surface for all the coupon 2 samples, which will be confirmed by EDS data later. And the corrosion rate of coupon 2 is lower than coupon 3 (bare alloy).
Therefore, the coating on coupon 2 still can be considered to be protective the matrix alloy from further corrosion if the hydrated water is controlled in the salt.

Prior to the SEM and EDS experiment of the samples after corrosion, SEM and EDS has been performed on the cross-section of the initial coupon 1 before corrosion. And the result is shown in Figure C6.

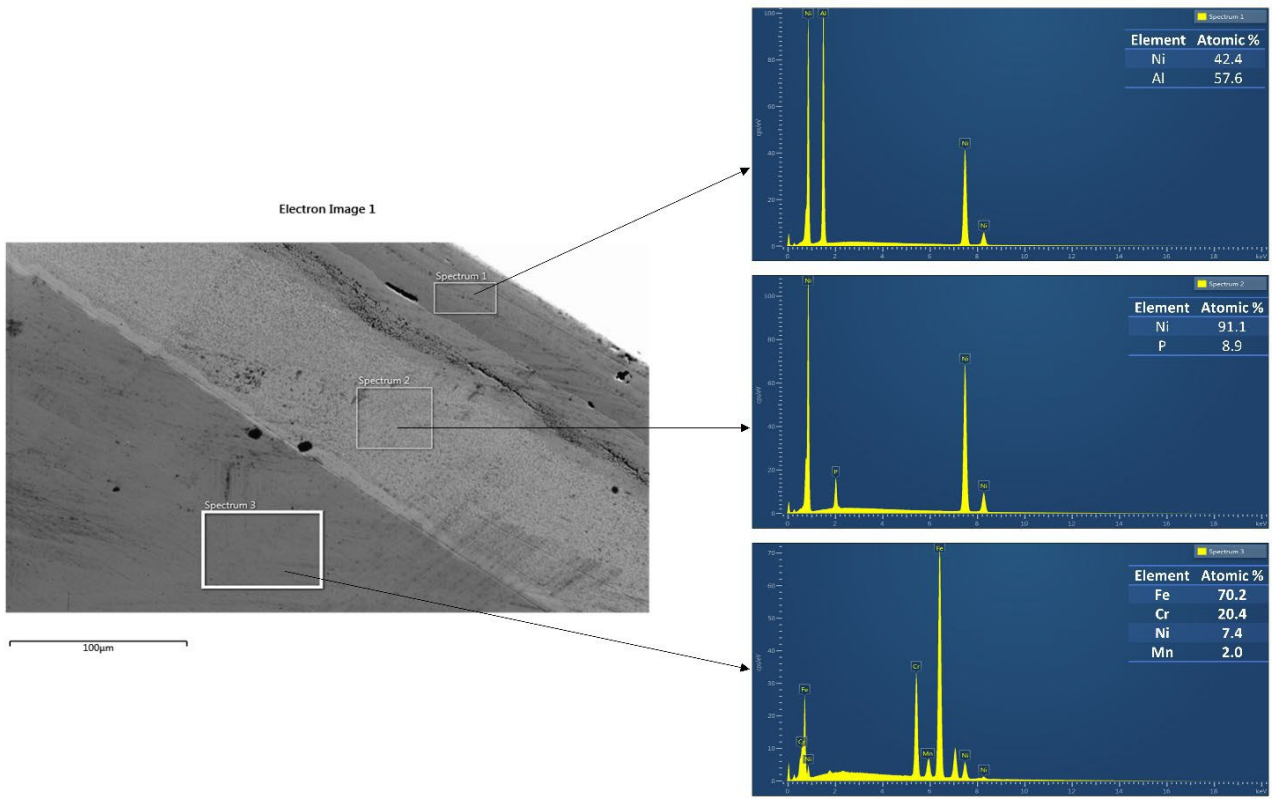

Figure C6. SEM and EDS of cross-section of coupon 1 before corrosion

As shown in Figure C6, there are two different layers of the coating on coupon 1, the outer layer being a Ni-Al alloy and the inner layer being a Ni-P alloy. These two coatings are not strongly bonded due to the presence of a high density of voids at the interface. The details are shown in Figure C7.

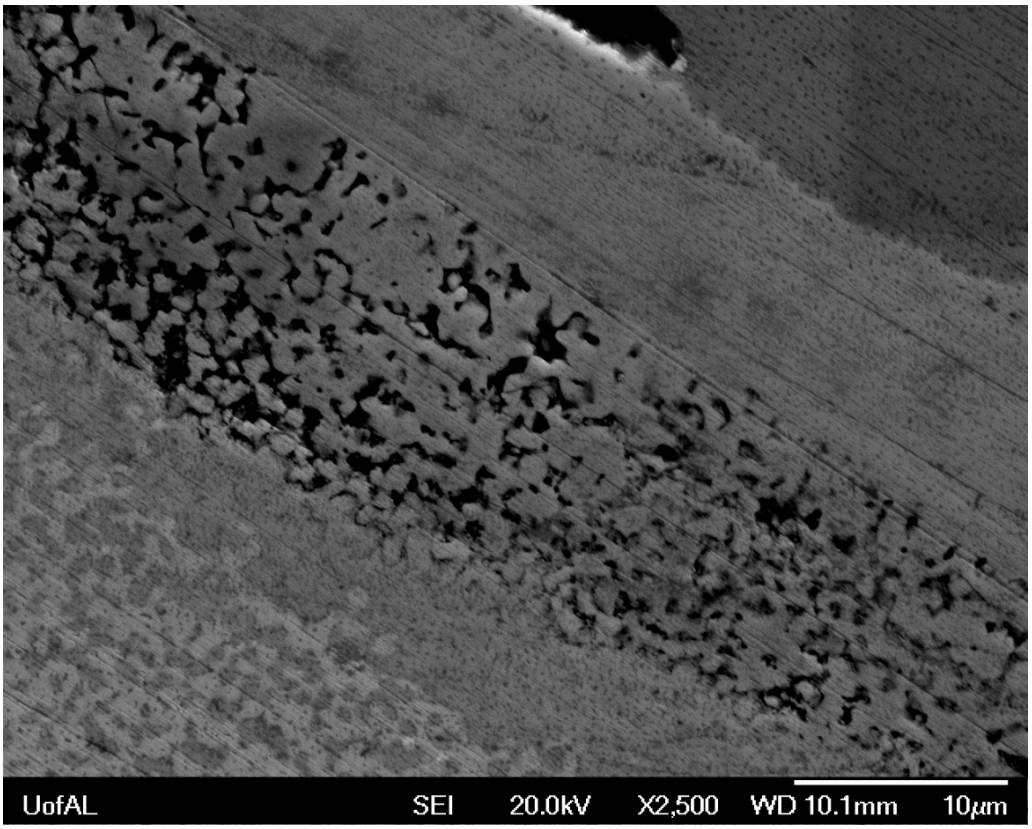

Figure C7. SEM of the interface between two coatings of coupon 1 before corrosion

The SEM and EDS experiments were also performed on the coupons after corrosion. As the corrosion mechanisms are similar at different temperatures, the results only show the SEM and EDS result of the coupons at 700°C, which is shown in Figure C8.

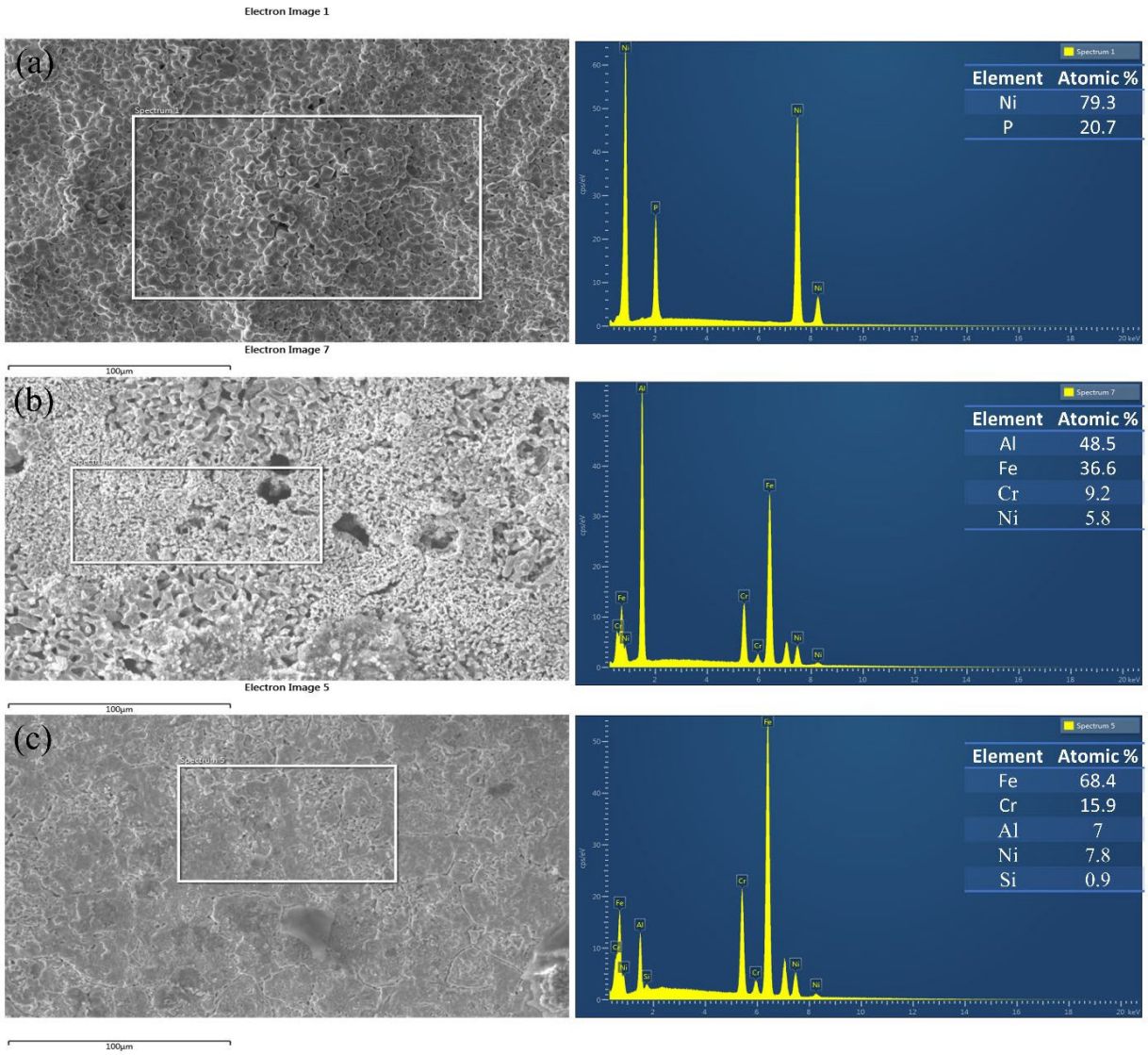

Figure C8. SEM and EDS for the coupons after corrosion at 700°C for 500h ((a)- coupon 1, (b)- coupon 2, and (c)-coupon 3).

As shown in Figure 8 (a), the layer on the surface is predominantly Ni-P after corrosion. Compared with Figure 6, the top layer of Ni-Al alloy has been dissolved into the salt and the concentration of Ni is decreased in the second layer (Ni-P alloy). Because the first layer and second layer are not coherent, and thermal expansion differential likely causes stress in the Ni-Al alloy at higher temperature, the surface of coupon 1 is cracked after corrosion, as shown in Figure C9.

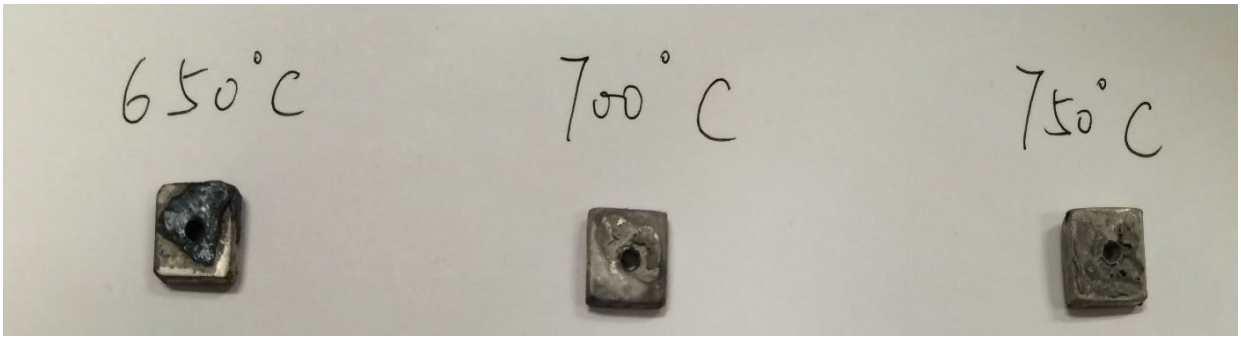

Figure C9. Coupon 1 after corrosion at different temperatures.

The cracked surface layer proved to be Ni-Al alloy (the initial coating on the surface) and the result is shown in Figure C10.

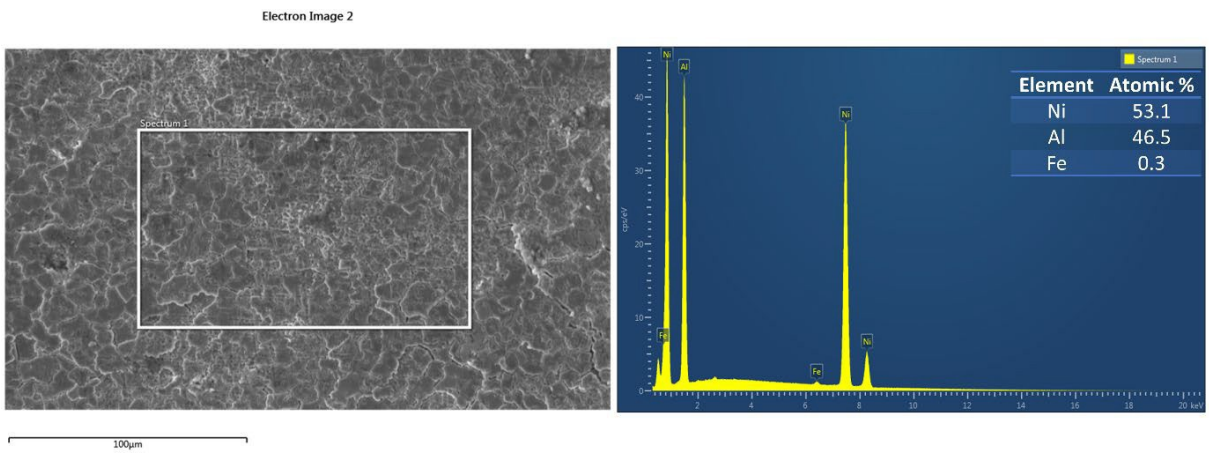

Figure C10. EDS result of the cracked surface of coupon 1 after corrosion at 650°C.

As shown in Figure 8 (b), the EDS results show that the surface of coupon 2 is Al-Fe alloy, which is also the initial layer observed on coupon 2 prior to the corrosion test. This demonstrates that the coating remained intact following the corrosion test, which means that the matrix alloy was protected. For the coupon 3 (Figure 8 (c)), the major element is Fe and the concentration of Cr is only 15.9 %, which is diminished compared with the initial composition.

Summary

The long-term dipping corrosion tests carried out in $MgCl_2$-KCl molten salt for coupons 1, 2 and 3 were performed at 650°C, 700°C and 750°C for 250h, 500h and 1000h, respectively. Coupon 1 (nickel aluminide) exhibited the lowest corrosion rate and it has the best corrosion resistance in the $MgCl_2$-KCl molten salt. The coating on coupon 2 (iron aluminide) also can protect the matrix alloy as the corrosion rate is lower than coupon 3

and the coating is still existed after corrosion. However, in the 100-hour corrosion experiment, the coating on coupon 2 is not coherent after corrosion, which is due to the hydrated water in the salt. The hydrated water needs to be controlled, otherwise, it will react with Fe and the coating (Fe-Al) of coupon 2 will be corroded. In the longer-time corrosion experiment, the coatings remained on the surface after corrosion and the EDS results also confirmed that. For the coupon 1 material, the outer coating and inner coating are not coherent. The outer coating (Ni-Al) is cracked at higher temperature due to the thermal expansion or dissolved into the salt. However, the inner coating (Ni-P) can still protect the matrix alloy from further corrosion and coupon 1 exhibited the best corrosion resistance among these three coupons.

Applied Thermal Coatings
200 Compress Street
Chattanooga, TN 37405
Telephone: 423-267-0647
Fax: 423-267-0637
Email: jhenry@atc-tn.com